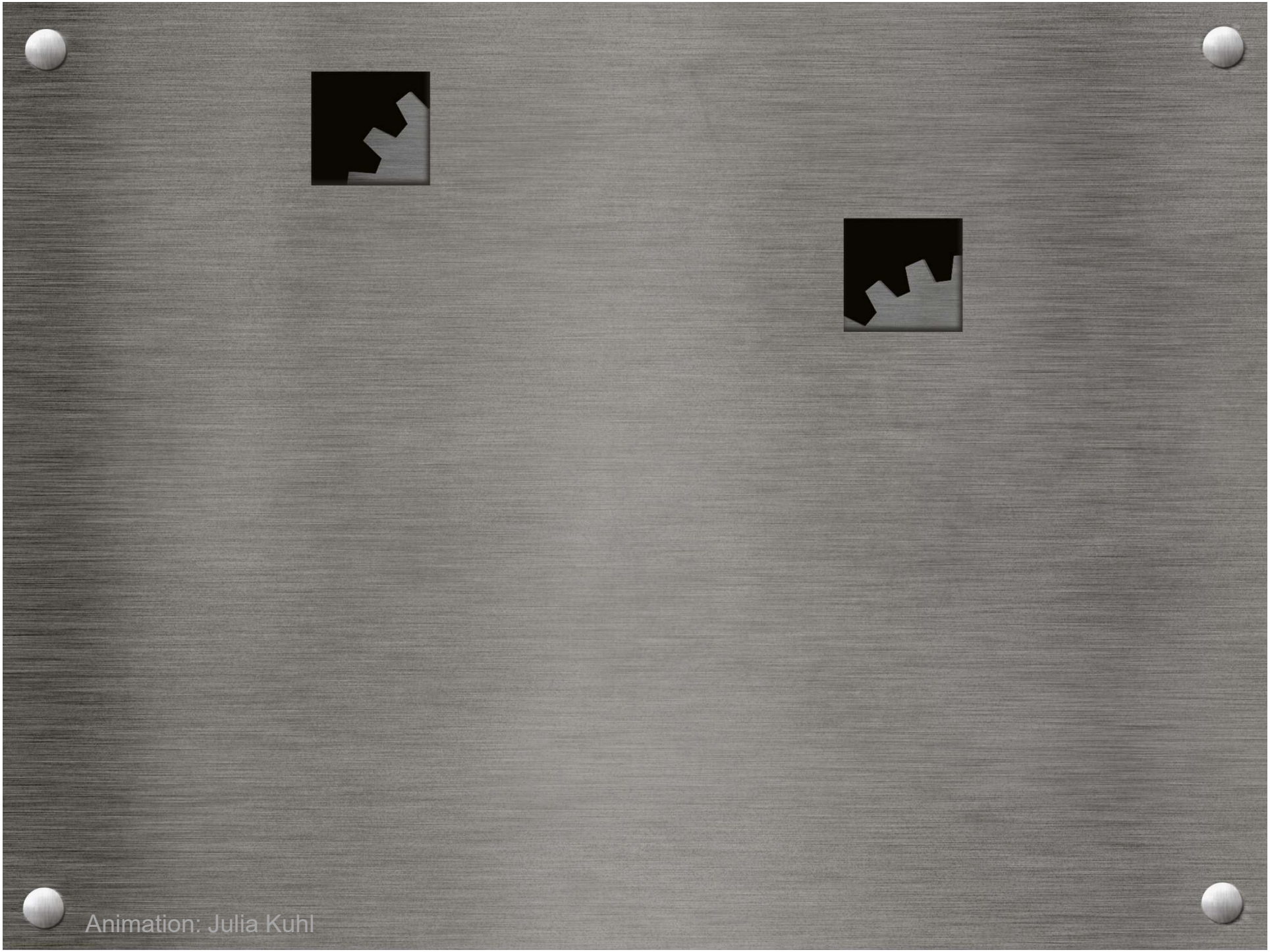
Animation: Julia Kuhl

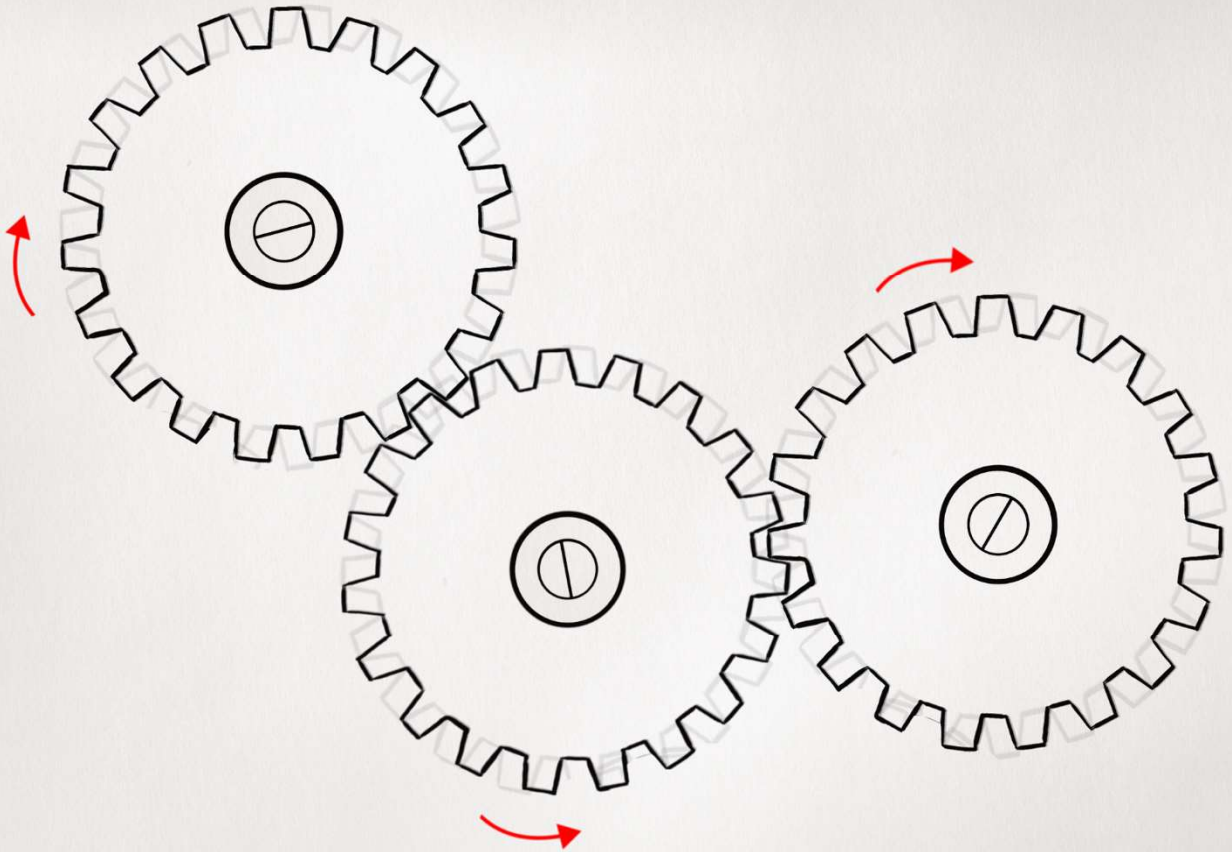

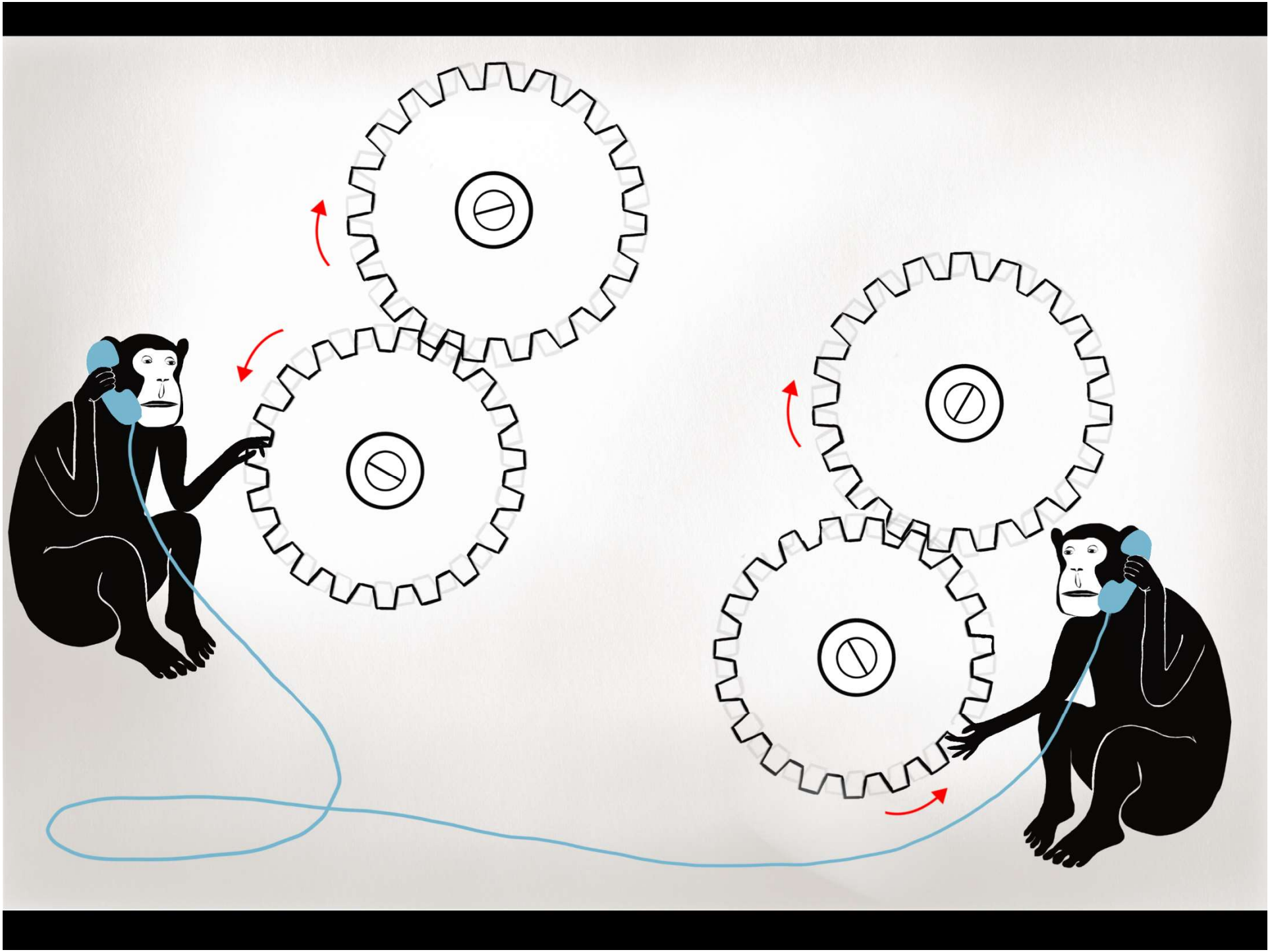


visual
input
1: flight
0: approach

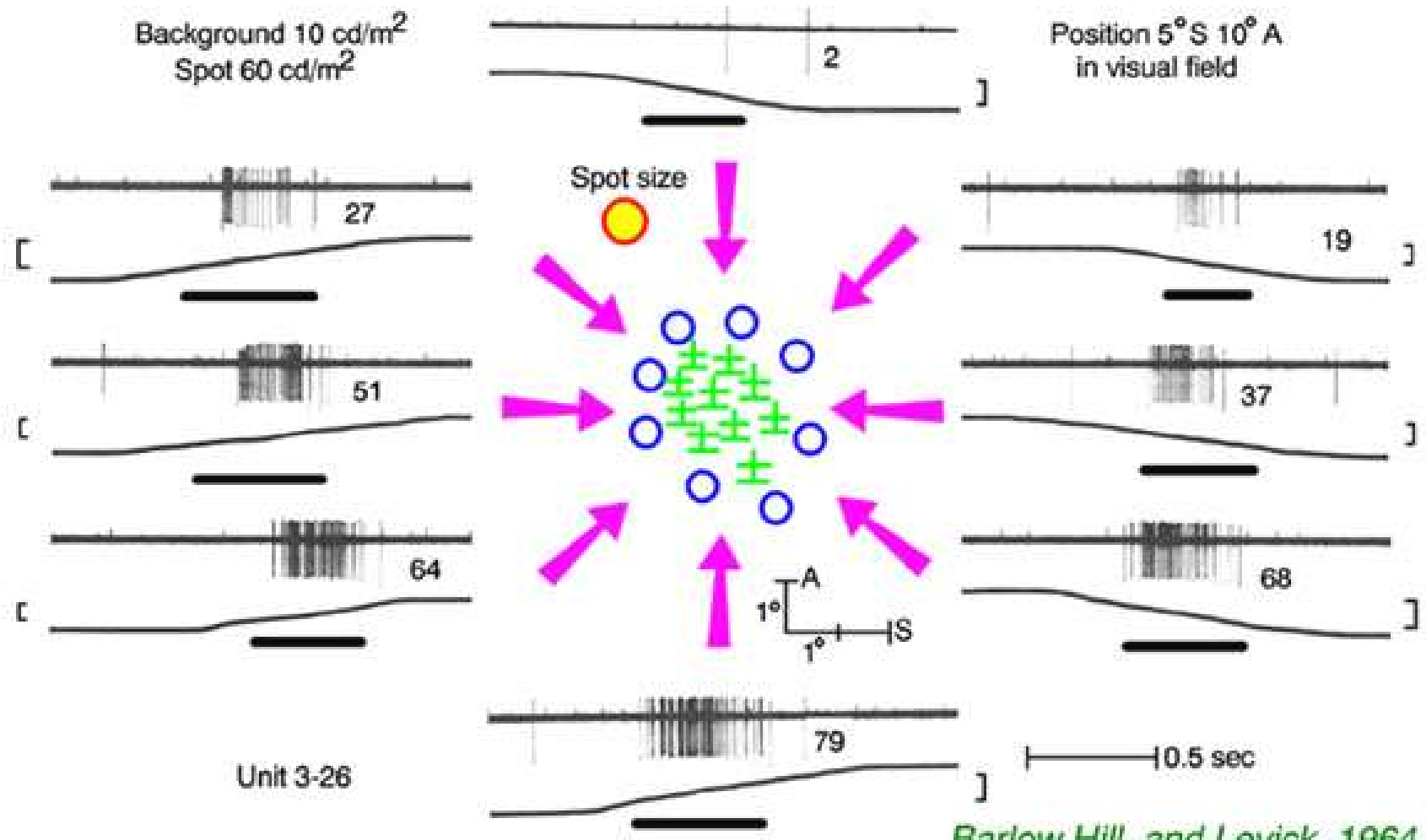
Background 10 cd/m2
Spot 60 cd/m2
Position 5° S 10° A
in visual field
Spot size
2
27
19
51
37
64
68
79
A
1°
S
1°
Unit 3-26
0.5 sec
Barlow,Hill, and Levick, 1964

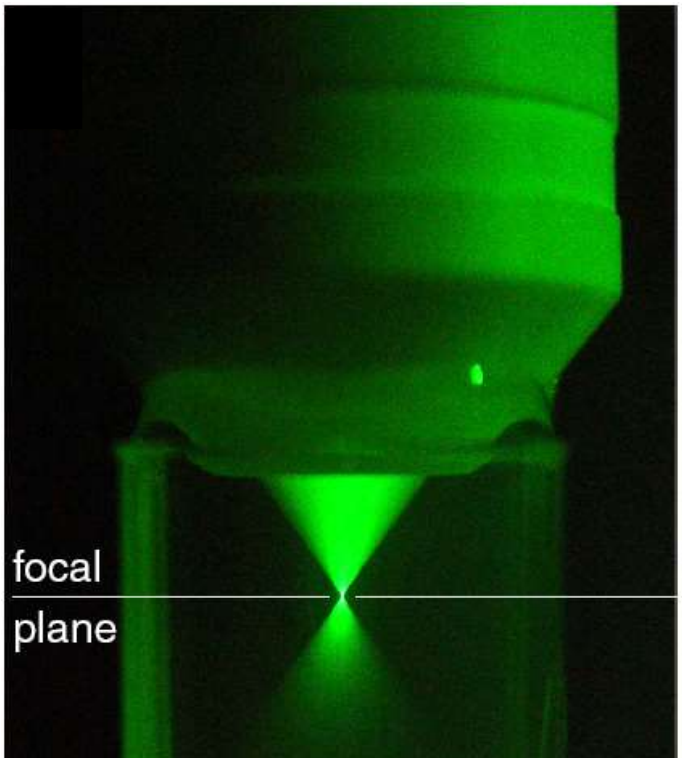
focal
plane

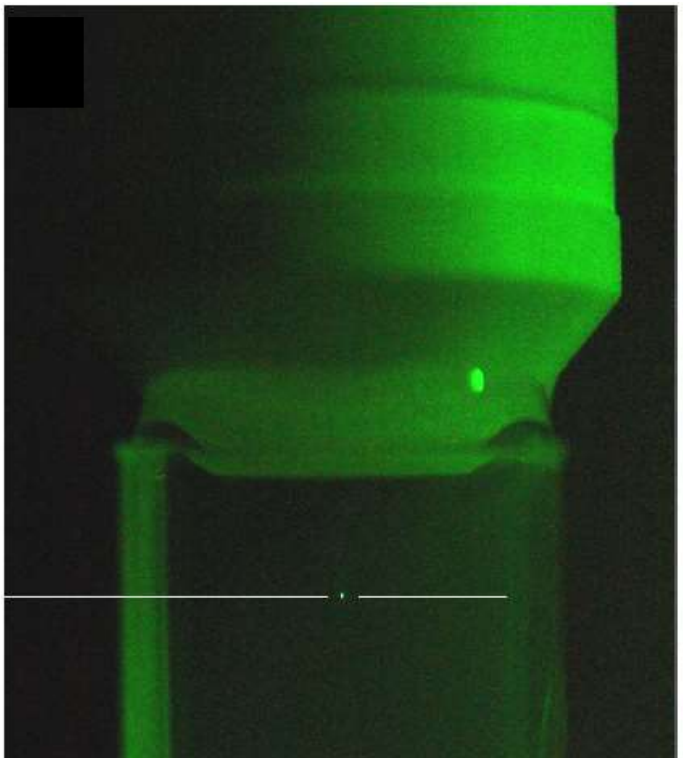

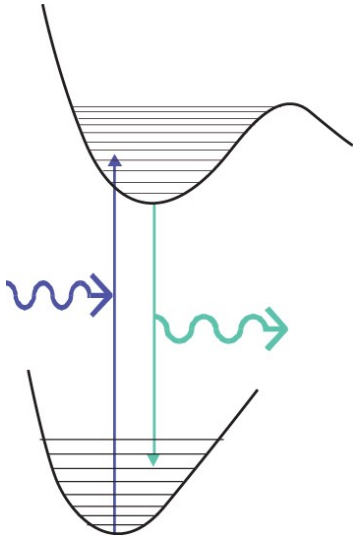

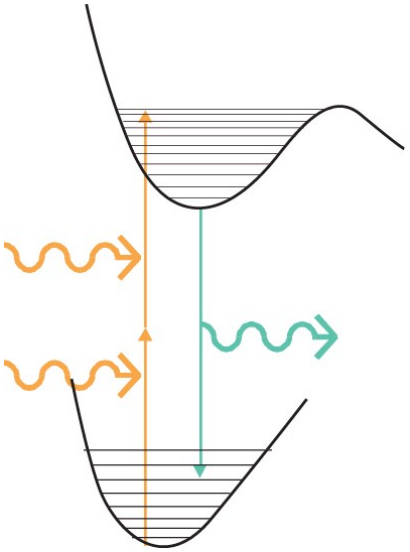

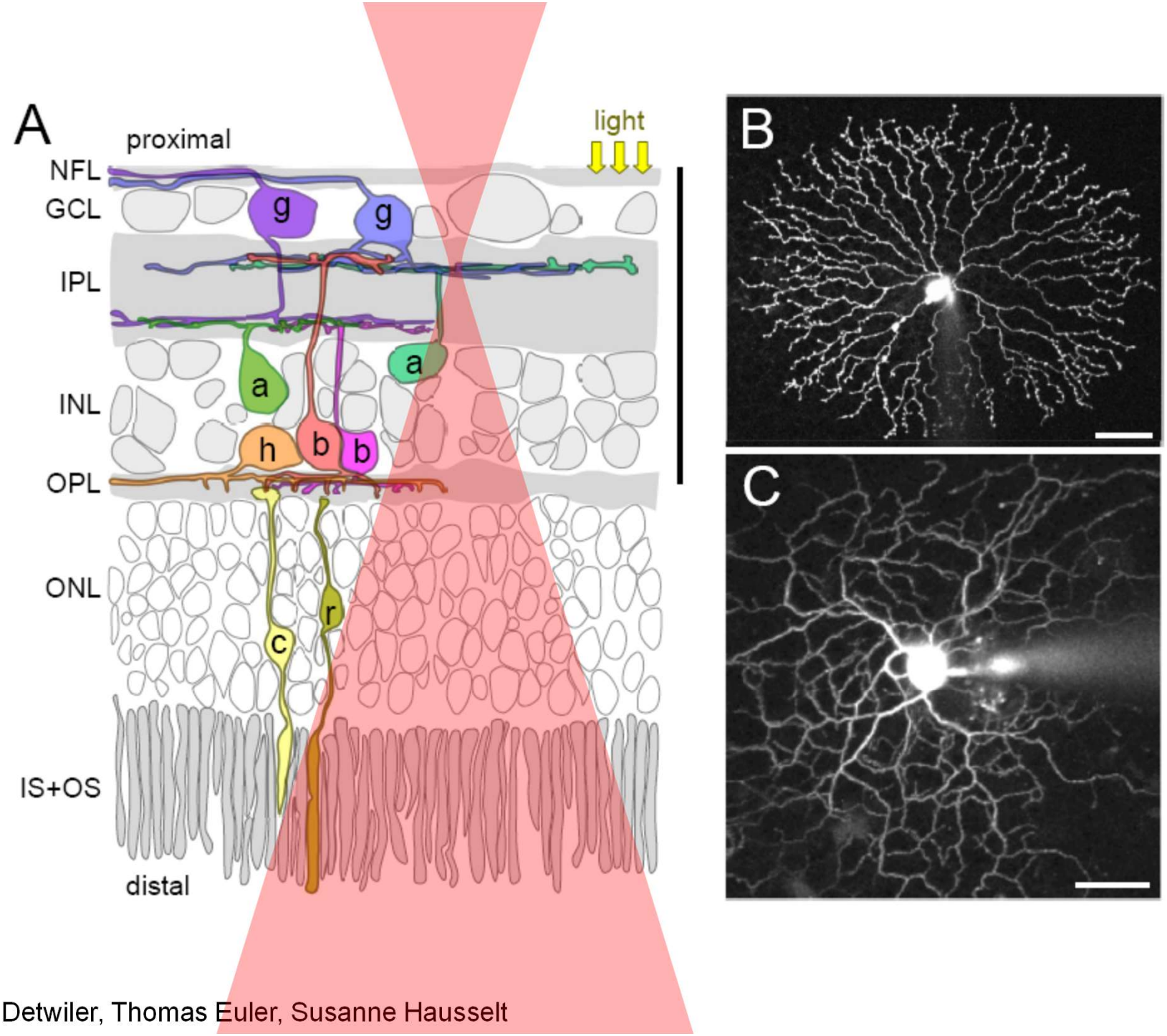

Peter Detwiler, Thomas Euler, Susanne Hausselt

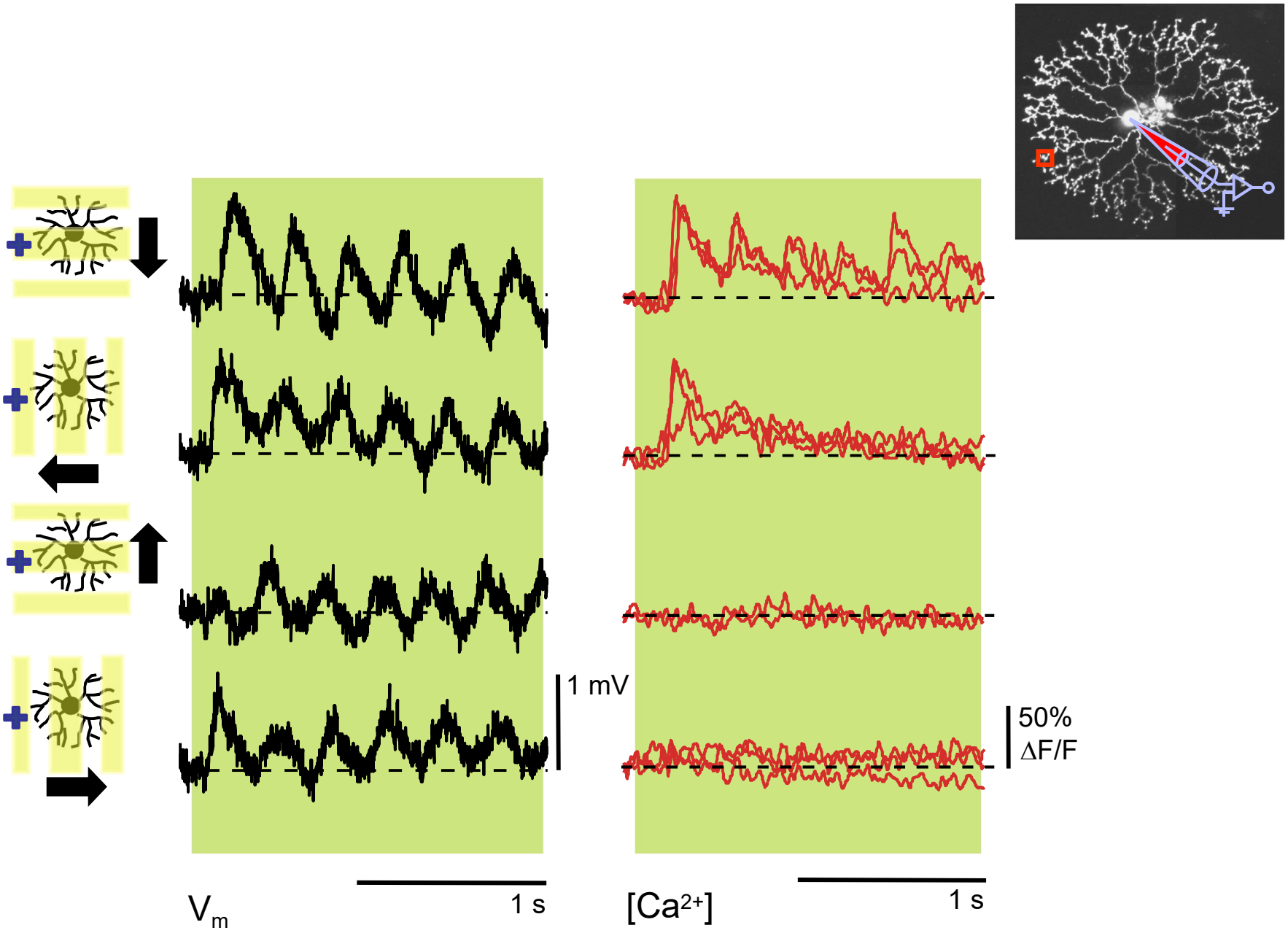

Euler, Detwiler, …, 2002

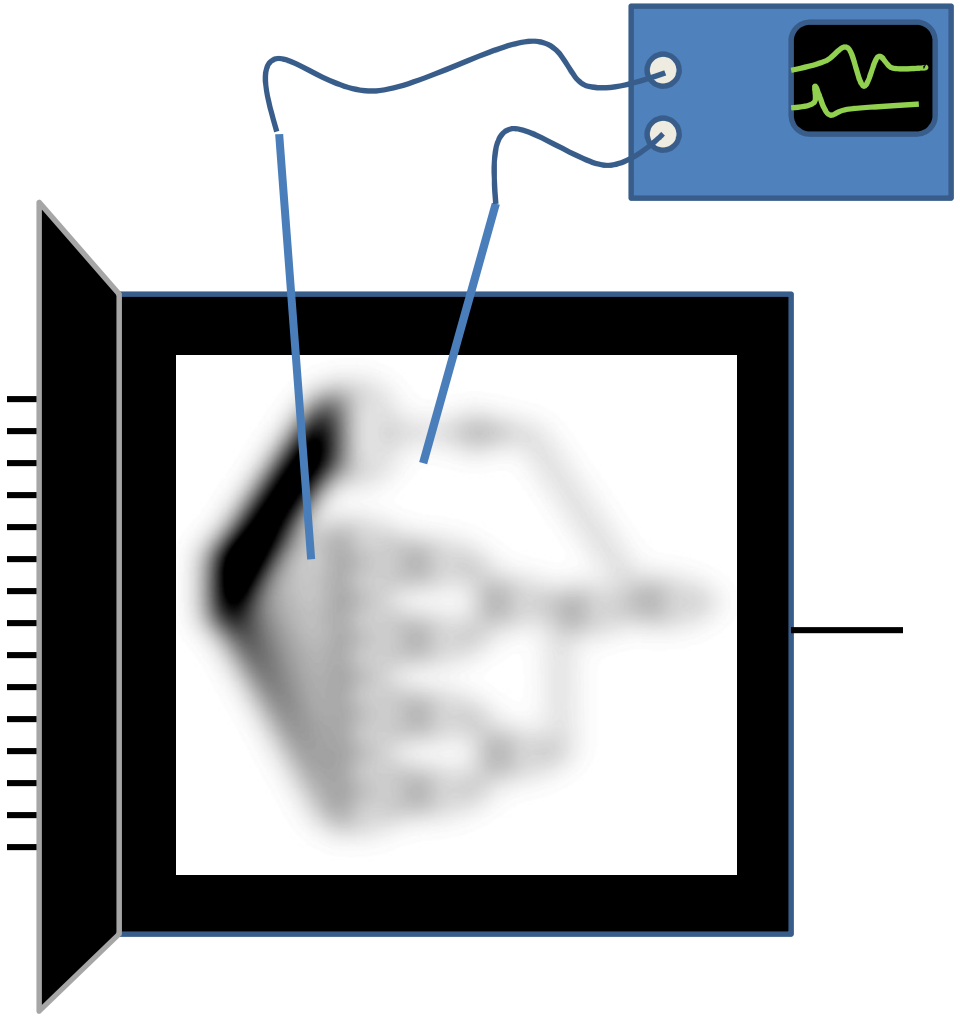

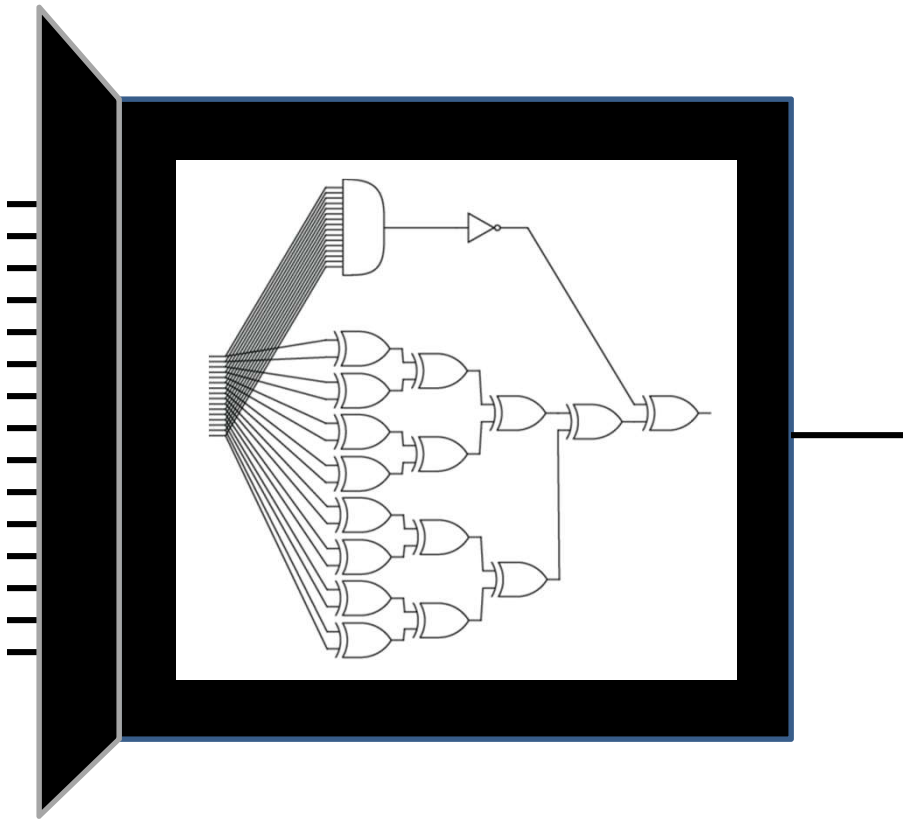

"Santiago Ramon y Cajal - arguably the most accomplished **anatomist** in the history of neuroscience - became recognized as such not only because of his incredible anatomical skills and his indefatigable working habits, but also because of his uncanny sense of the **functional implications** of his work, a sense that made him a true genius in the field of biology."

Llinas, R. R. (2003). "The contribution of Santiago Ramon y Cajal to functional neuroscience." Nat. Rev. Neurosci., **4**(1): 77-80.

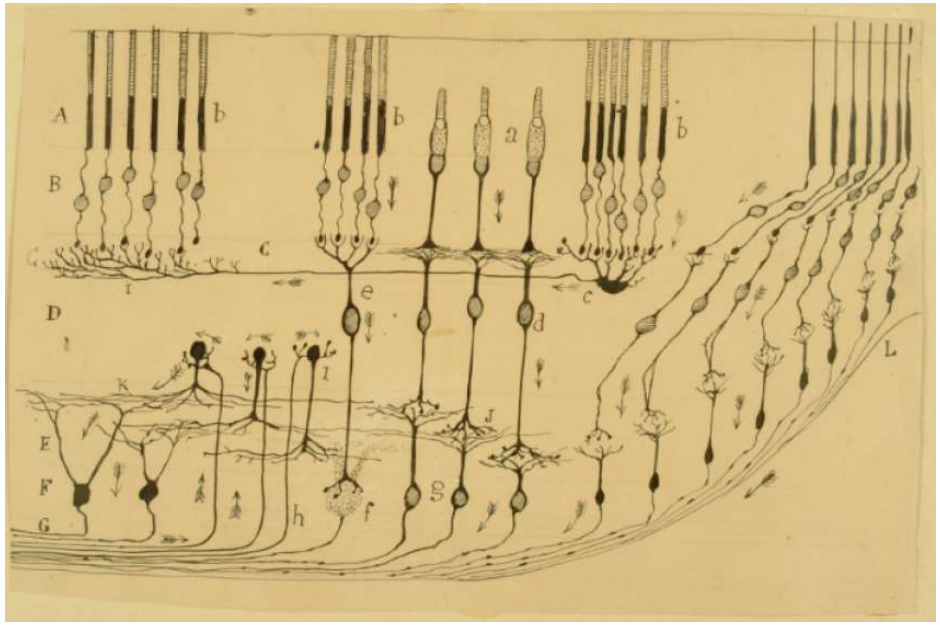

Quad II circuit diagram

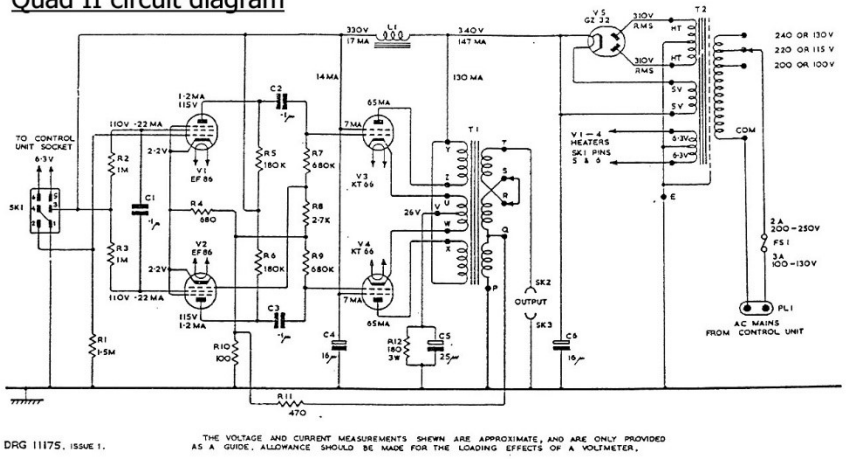

http://www.geocities.com/ResearchTriangle/Lab/6722/quadiicirb.html

Component properties are essential

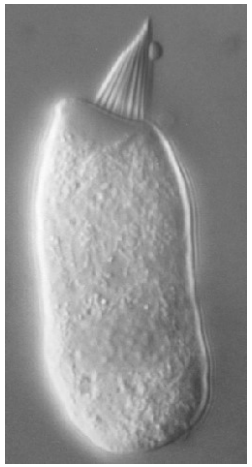

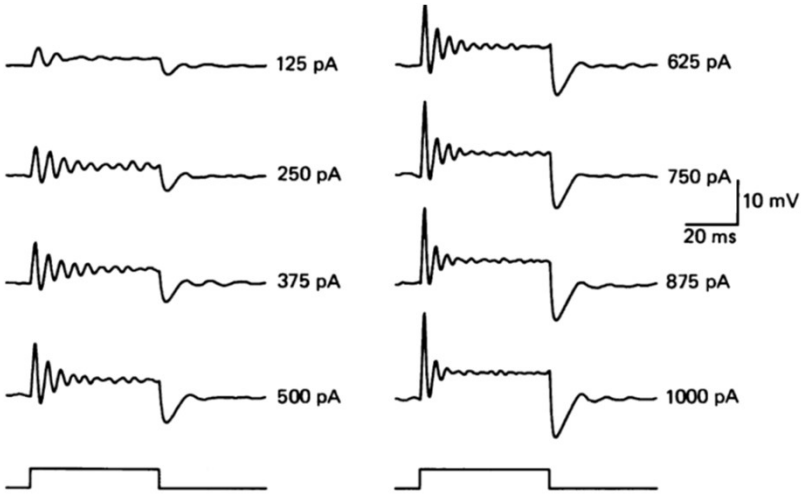

Hudspeth and Lewis 1988

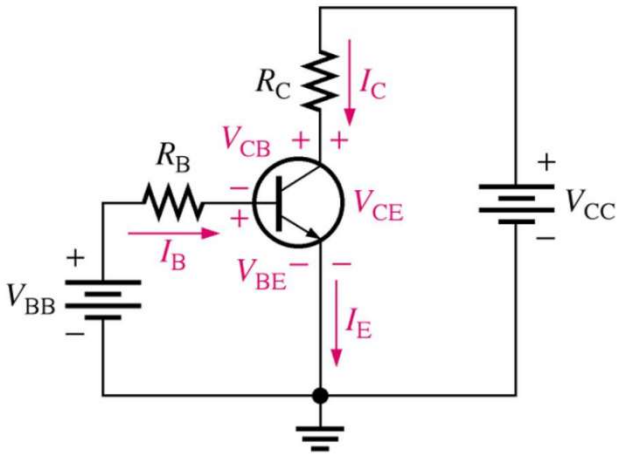

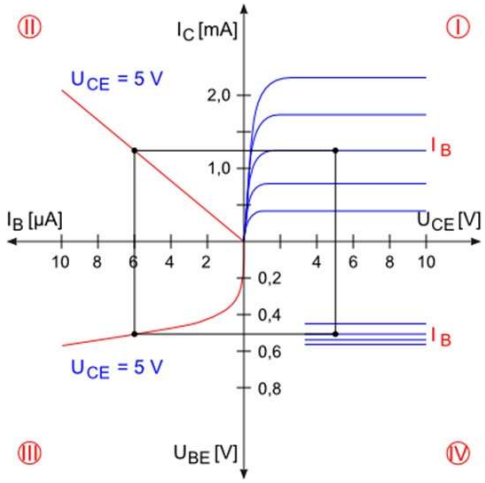

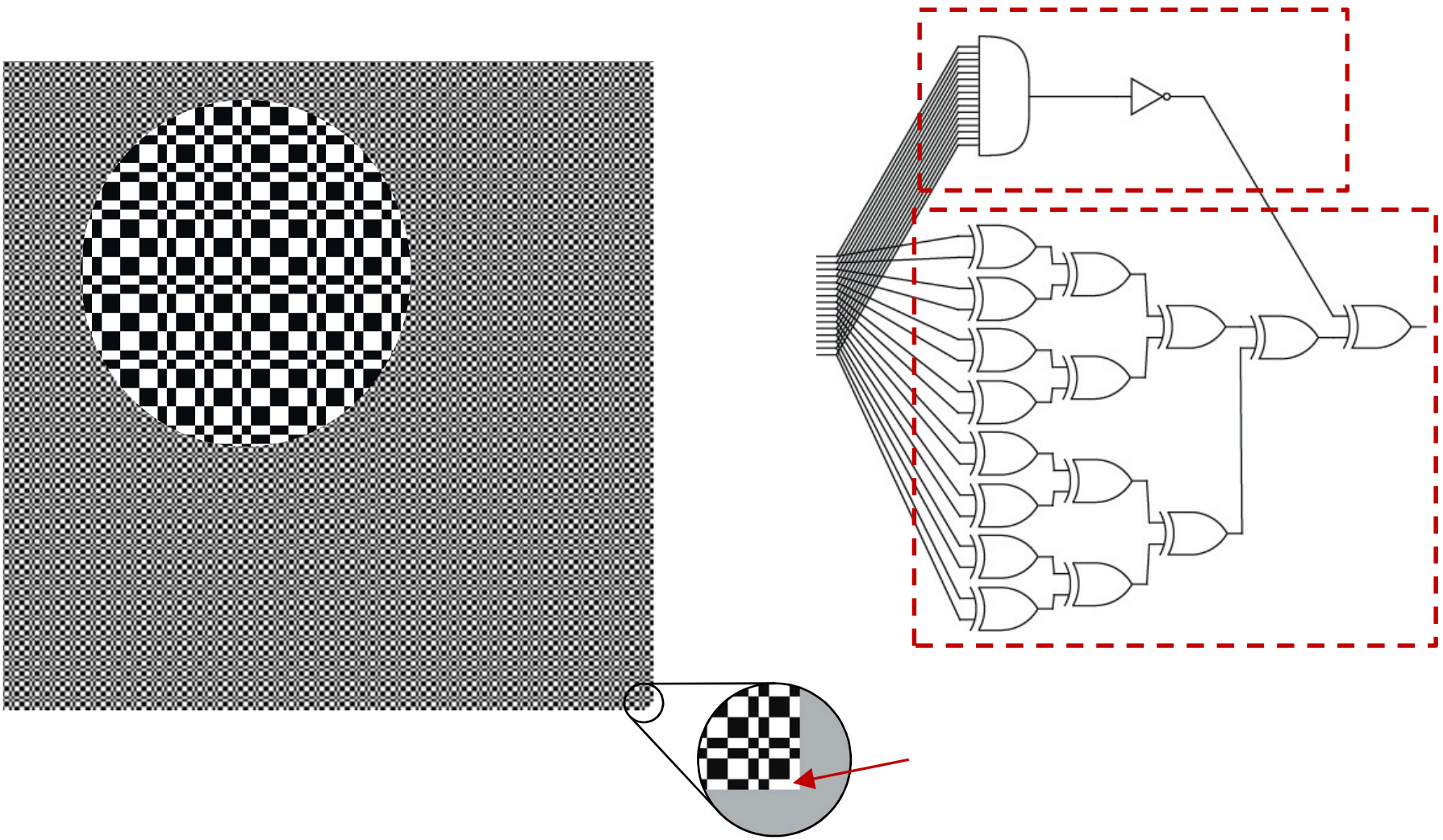

Phil. Trans. R. Soc. Lond. B 314, 1–340 (1986)
Printed in Great Britain

[1]

THE STRUCTURE OF THE NERVOUS SYSTEM OF THE NEMATODE *CAENORHABDITIS ELEGANS*

By J. G. WHITE, E. SOUTHGATE, J. N. THOMSON AND S. BRENNER, F.R.S.

Laboratory of Molecular Biology, Medical Research Council Centre, Hills Road, Cambridge CB2 2QH, U.K.

(*Received 9 August 1984 – Revised 12 November 1984*)

1984

1979

THREE-DIMENSIONAL COMPUTER RECONSTRUCTION OF NEURONS AND NEURONAL ASSEMBLIES

9136

E. R. Macagno, C. Levinthal, and I. Sobel
Department of Biological Sciences, Columbia University, New York, New York 10027

1975

Three-Dimensional Reconstruction from Serial Sections

RANDLE W. WARE
California Institute of Technology
Pasadena, California

AND

VINCENT LOPRESTI
Columbia University, New York, New York

Three Dimensional Reconstruction from Serial Sections

CYRUS LEVINTHAL & RANDLE WARE*
Department of Biological Sciences, Columbia University, New York, NY 10027

1972

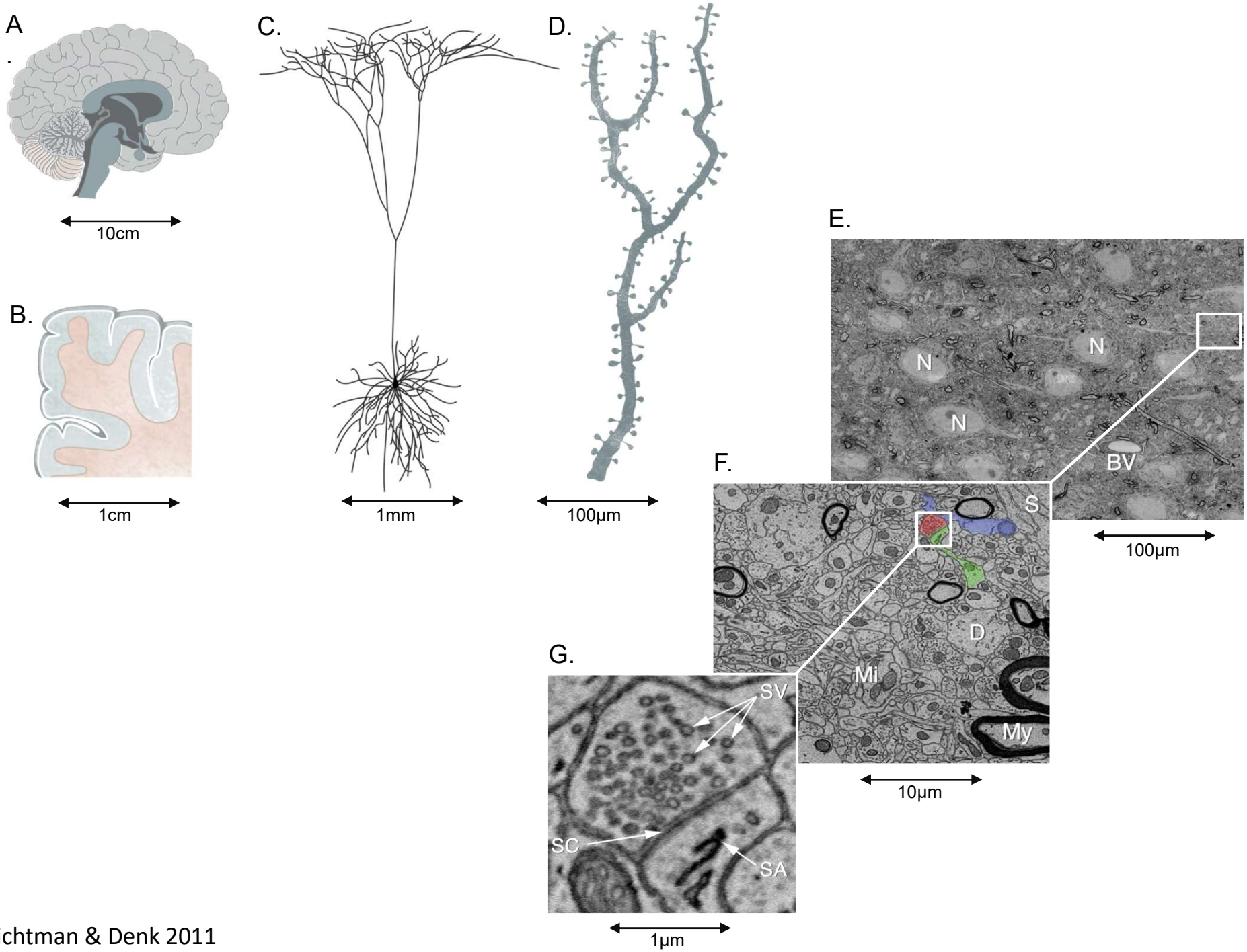

Lichtman & Denk 2011

ssTEM

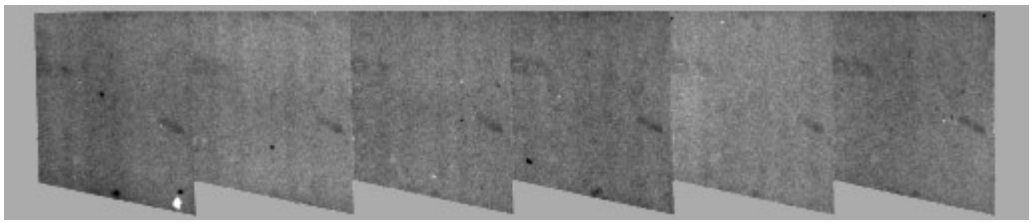

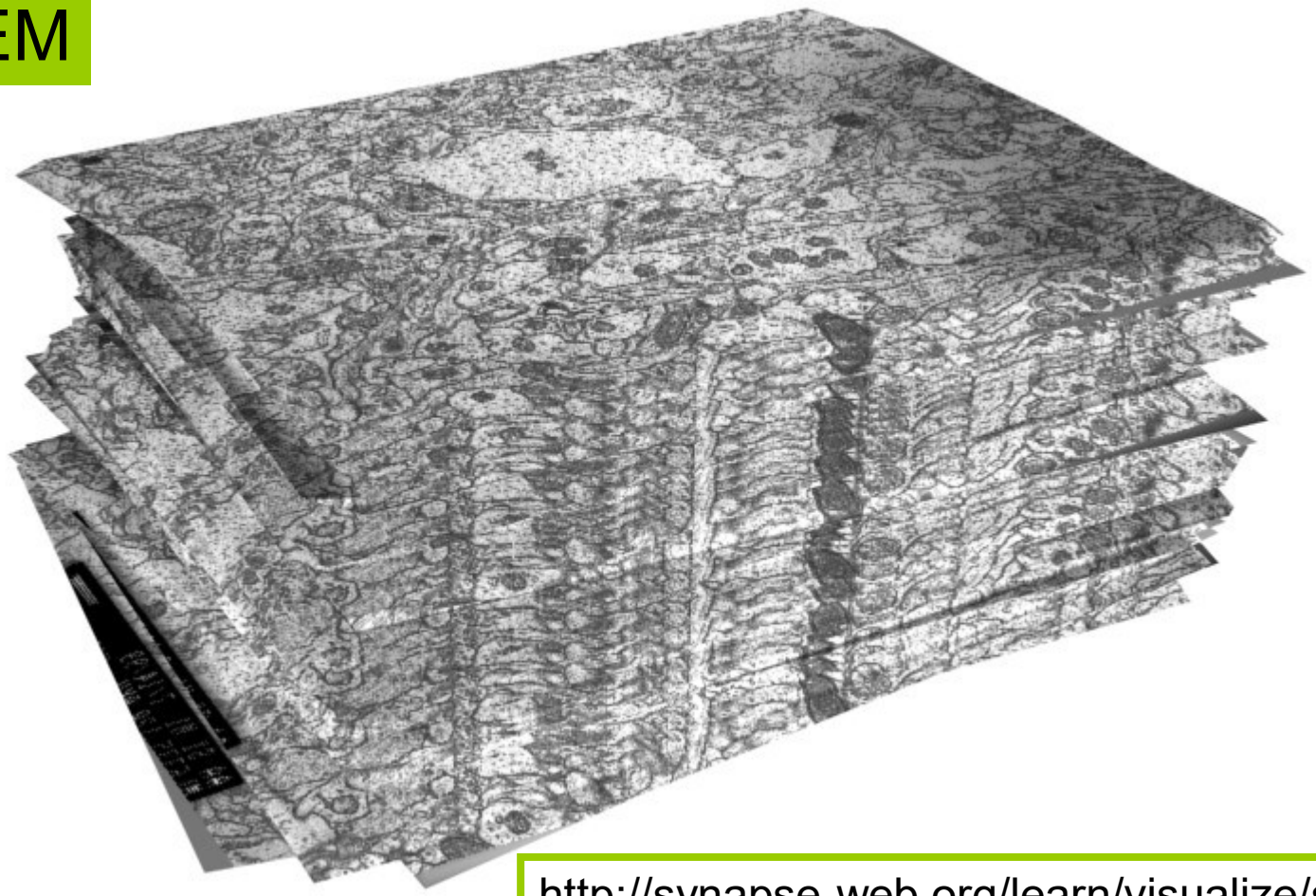

http://synapse-web.org/learn/visualize/serial.stm

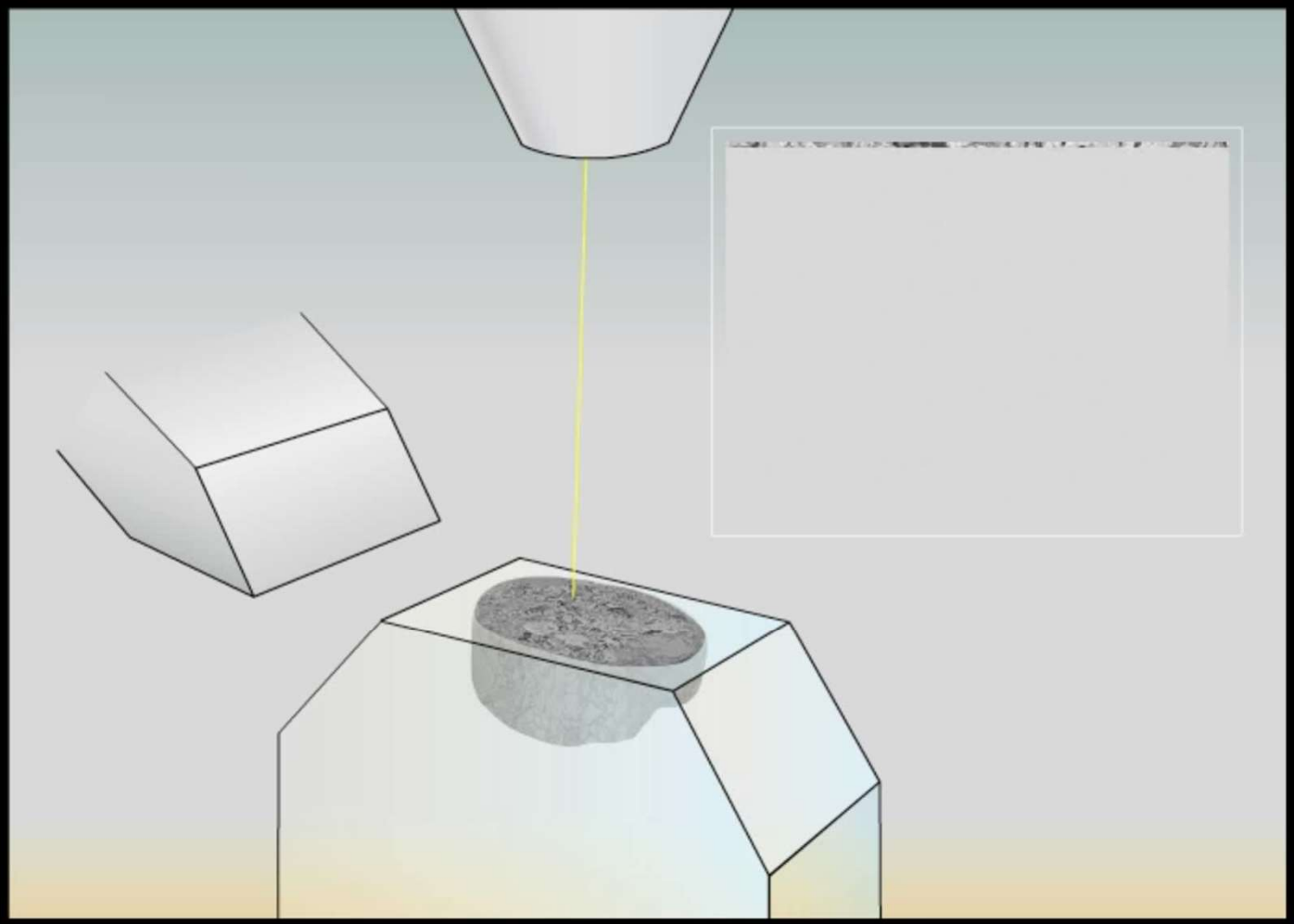

Animation: Julia Kuhl

Denk and Horstmann 2004, Leighton 1981

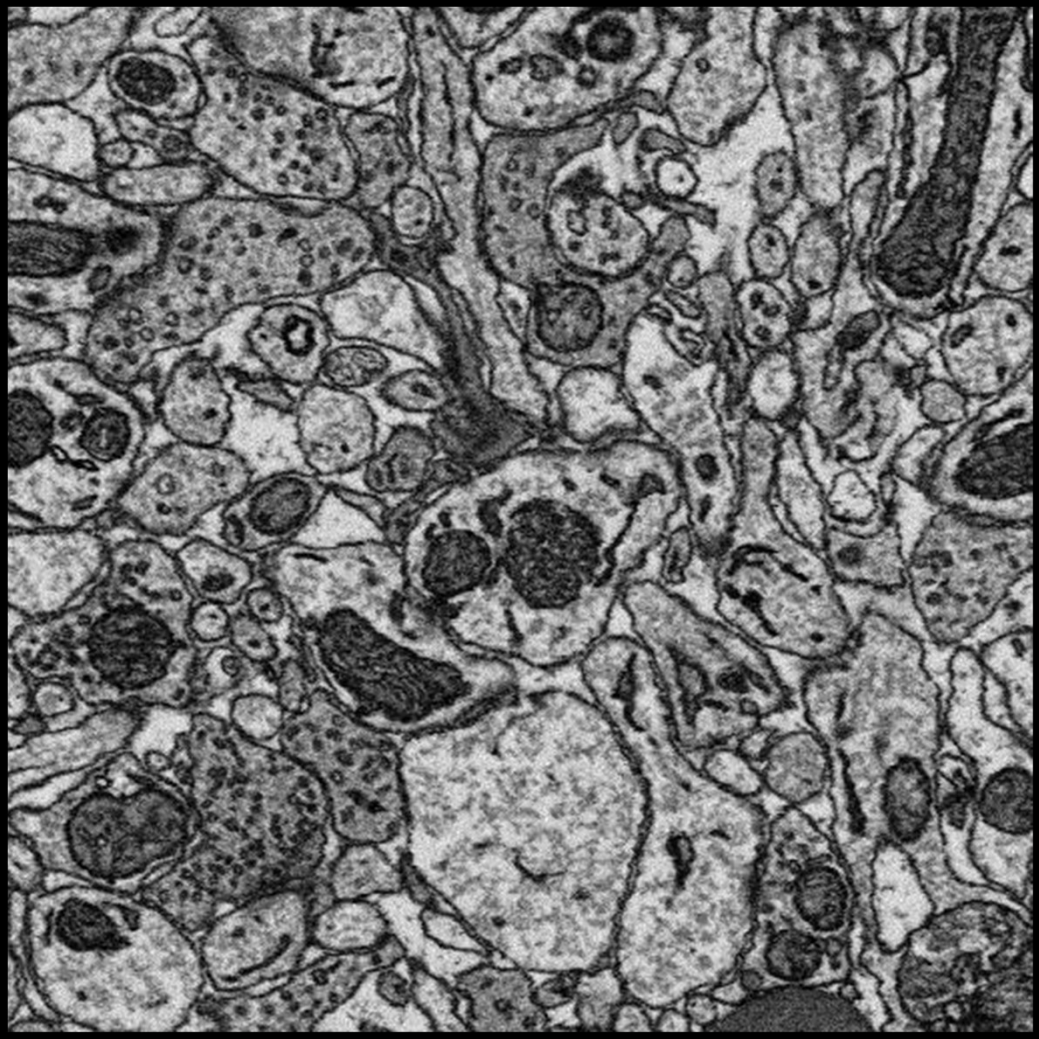

Joergen Kornfeld

EM contrast is provided by highly charged (heavy) nuclei

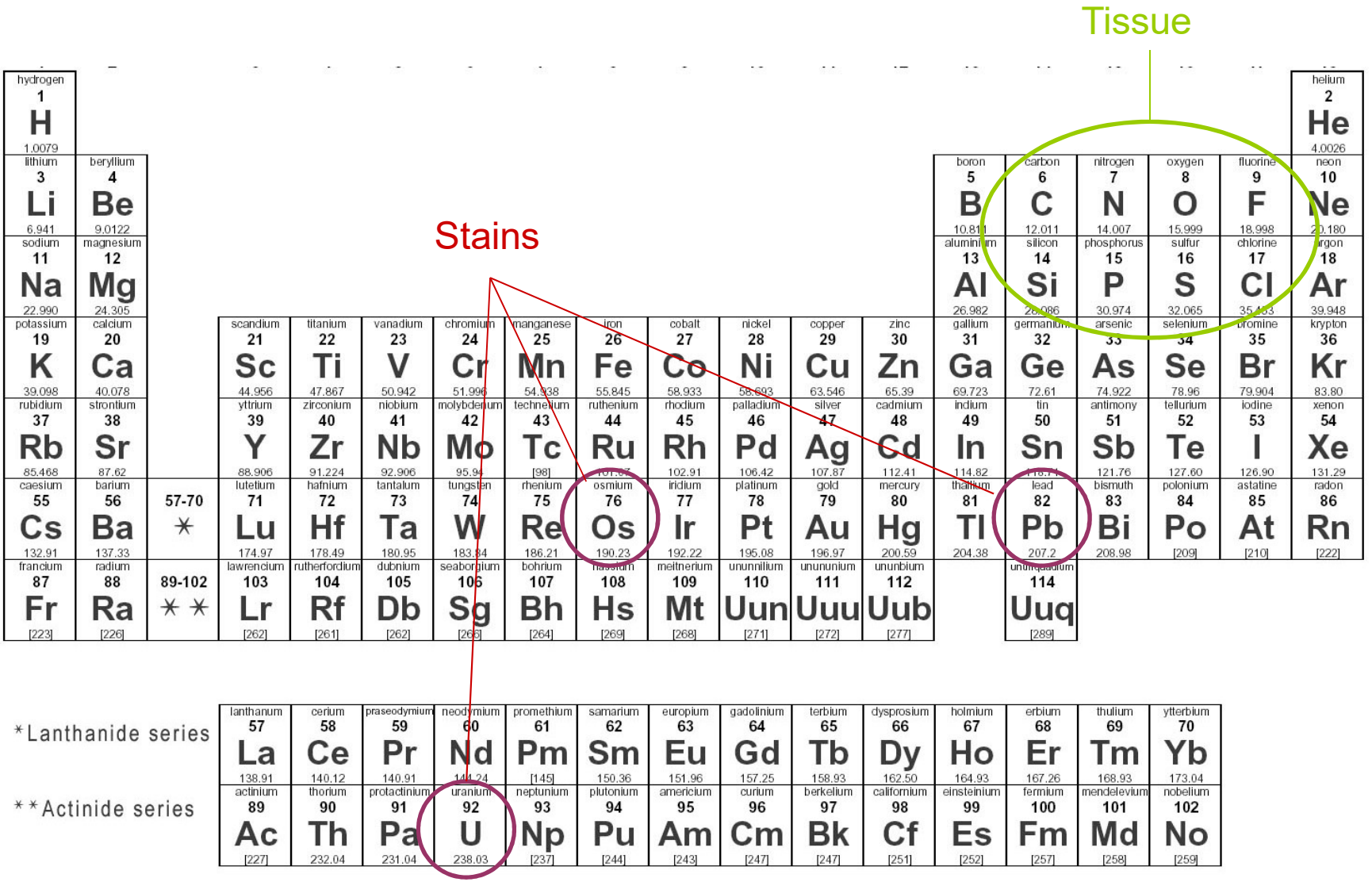

Slide by Kevin Briggman

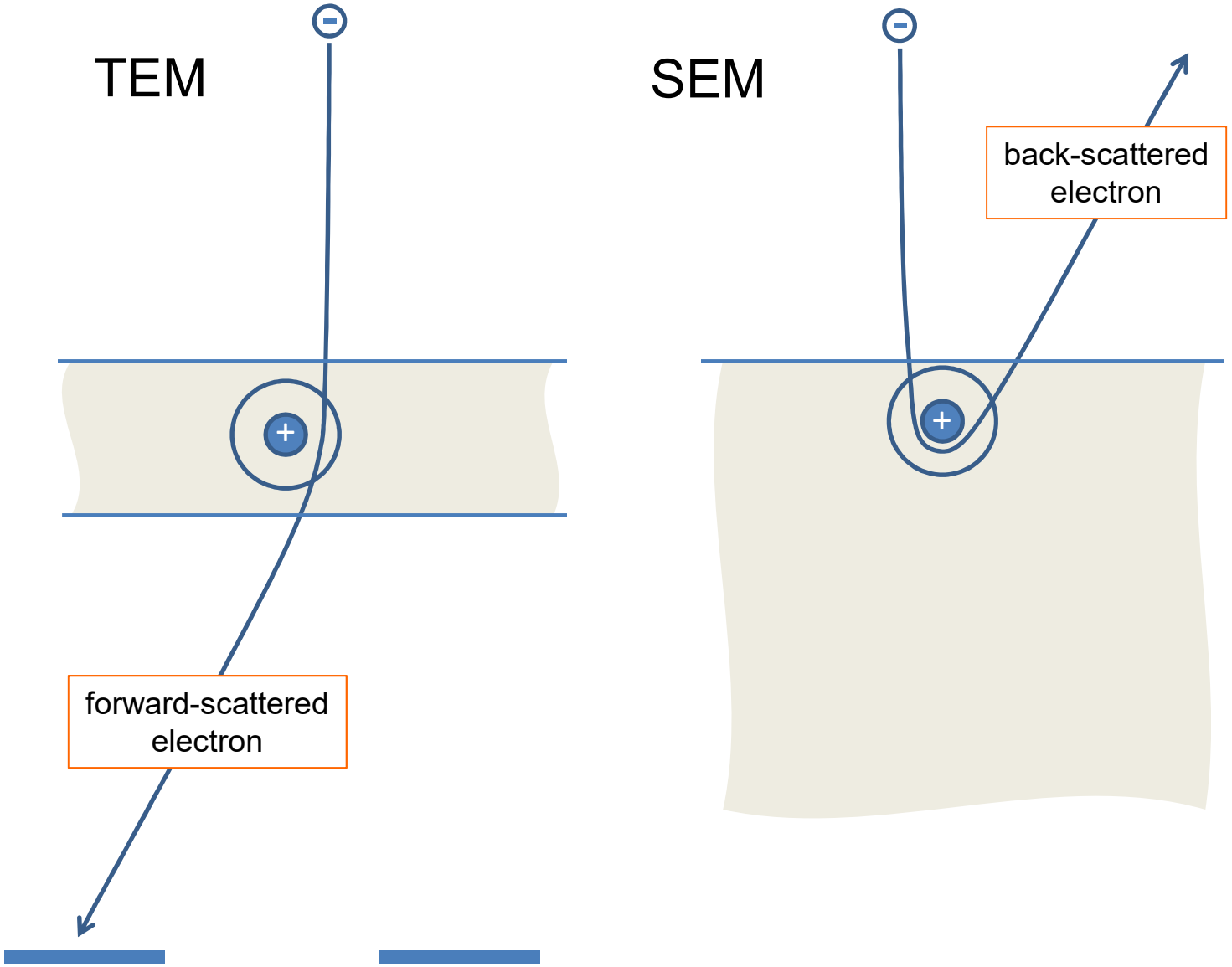
TEM
forward-scattered electron
SEM
back-scattered electron

3D-EM Techniques

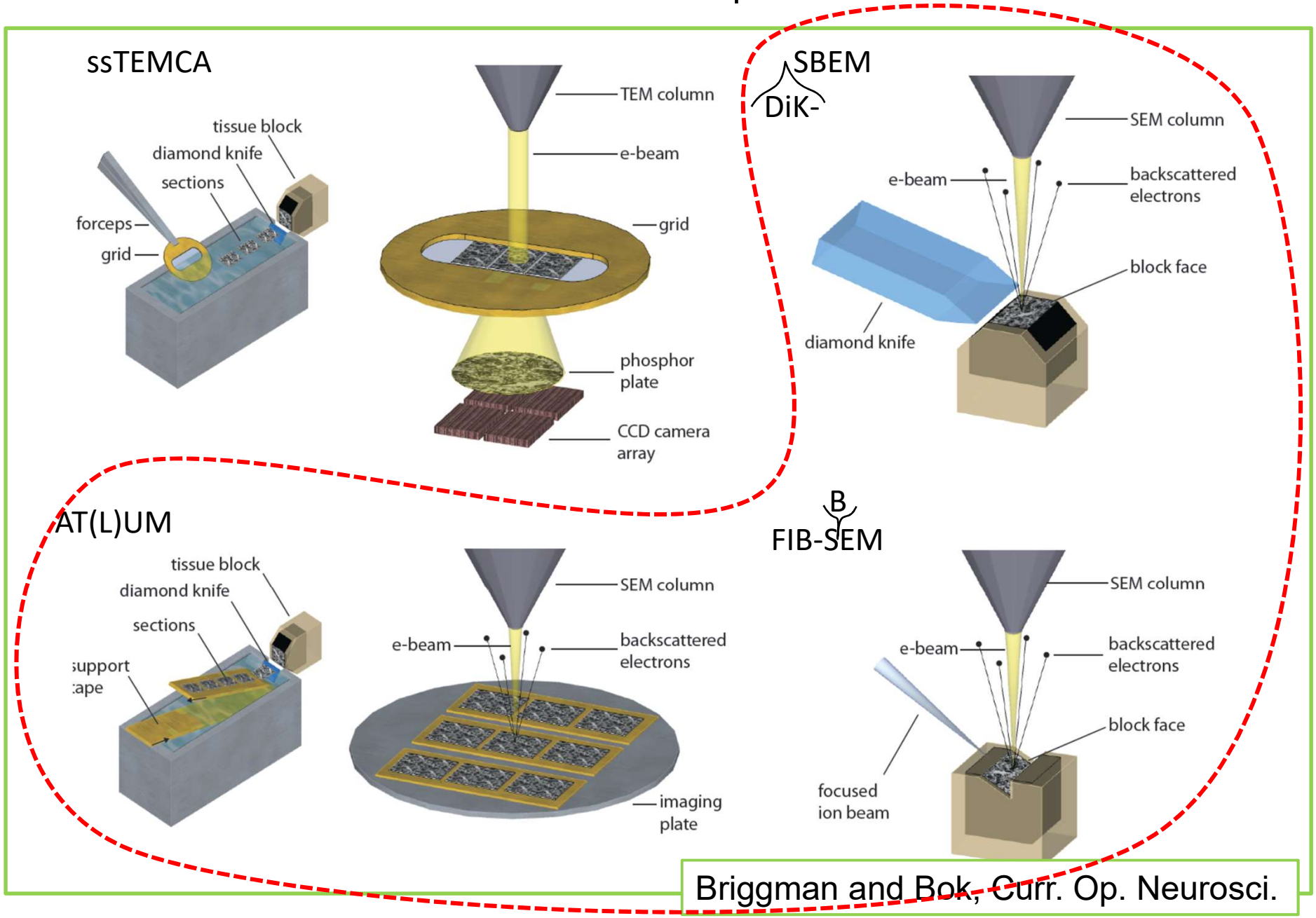

Briggman and Bok, Curr. Op. Neurosci.

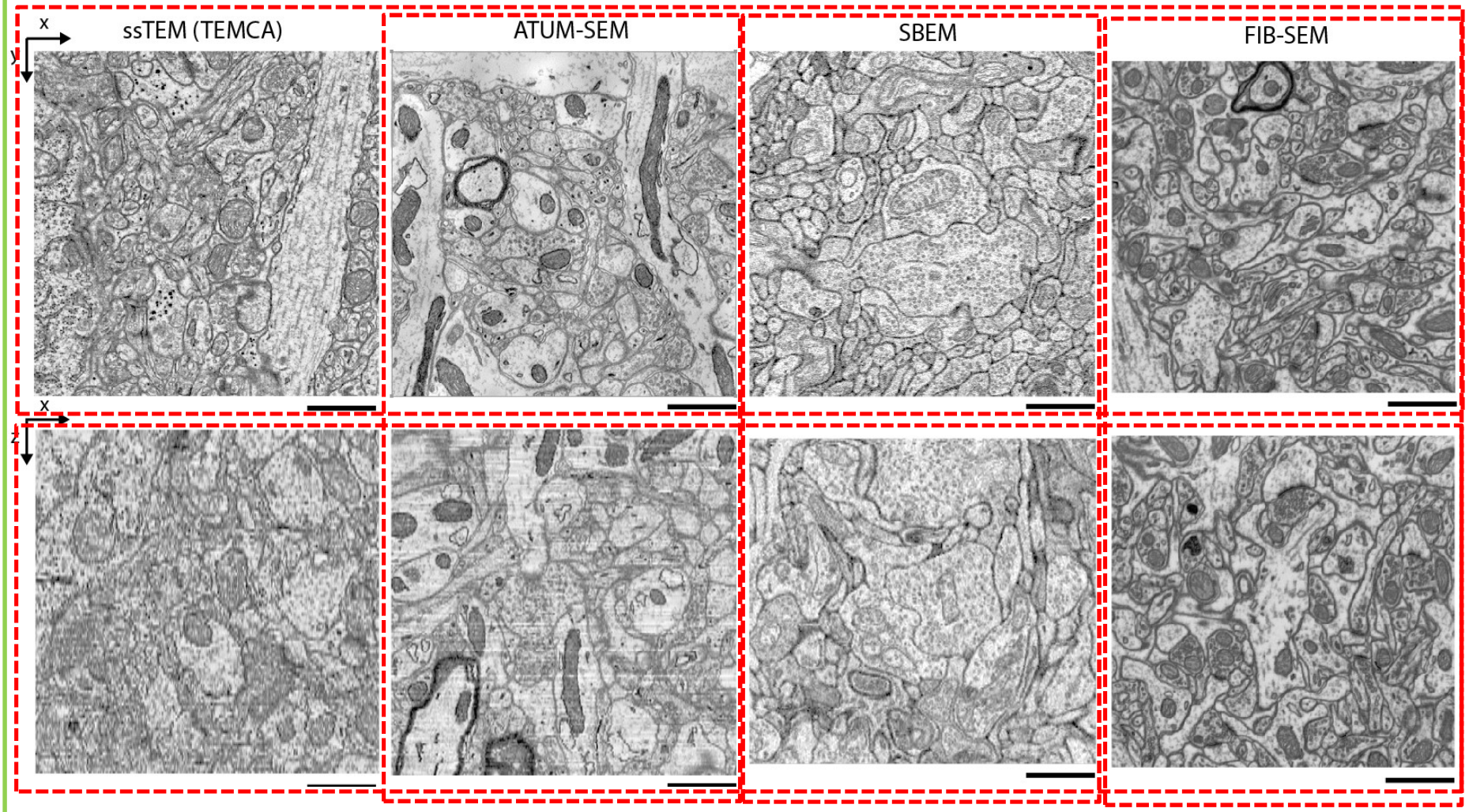

A) ssTEMCA: mouse visual cortex at 4 x 4 x 45 nm^3. B) ATUM-SEM: Mouse cortex at 3 x 3 x 29 nm^3 C) SBEM: mouse retina at 12 x 12 x 25 nm^3. D) FIB-SEM: cortex at 5 x 5 x 5 nm^3. Images by: D. Bock (A), K. Hayworth, J. Lichtman (B), K. Briggman (C), and G. Knott (D).

Briggman and Bok, Curr. Op. Neurosci.

Monte-Carlo simulations yield point-spread functions for block-face imaging

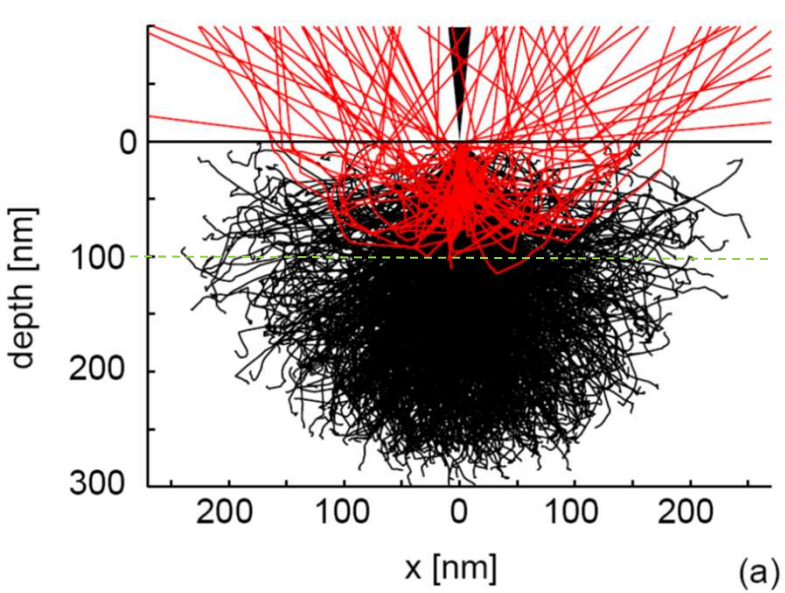

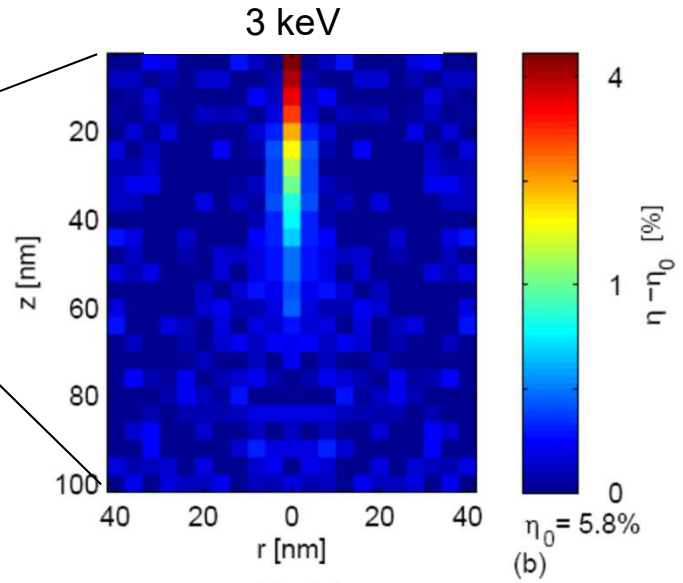

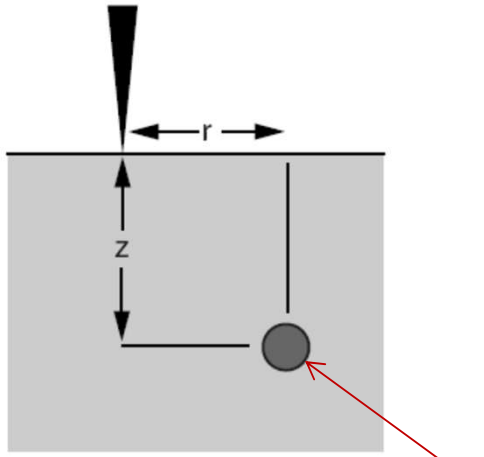

Os

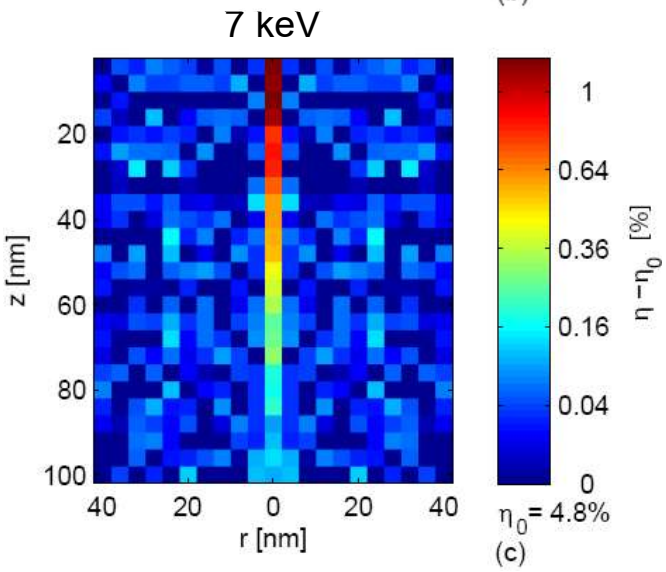

Hennig and Denk, 2007

Scanning Microscopy Vol. 12, No. 1, 1998 (Pages 185-192)
Scanning Microscopy International, Chicago (AMF O'Hare), IL 60666 USA
0891-7035/98$5.00+.25

BACKSCATTERING COEFFICIENTS FOR LOW ENERGY ELECTRONS

A.M.D. Assa'd and M.M. El Gomati*

The Department of Electronics, University of York, York YO1 5DD, U.K.

(Received for publication August 6, 1996 and in revised form December 9, 1996)

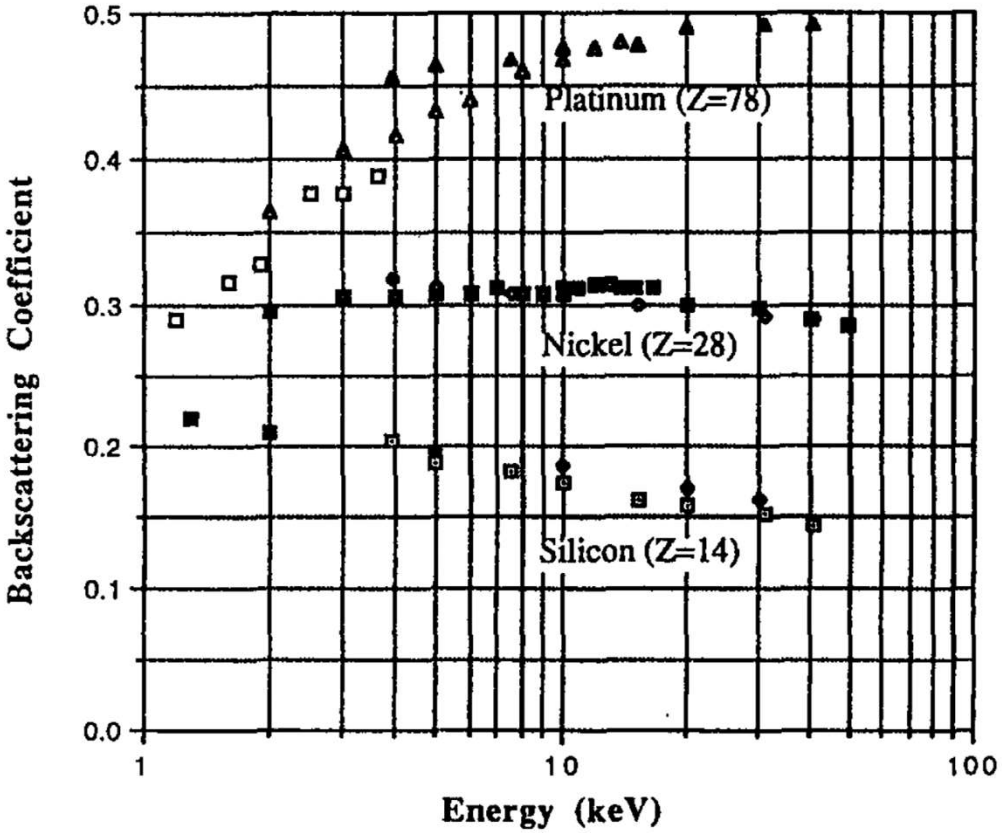

Joy&Joy, 1996

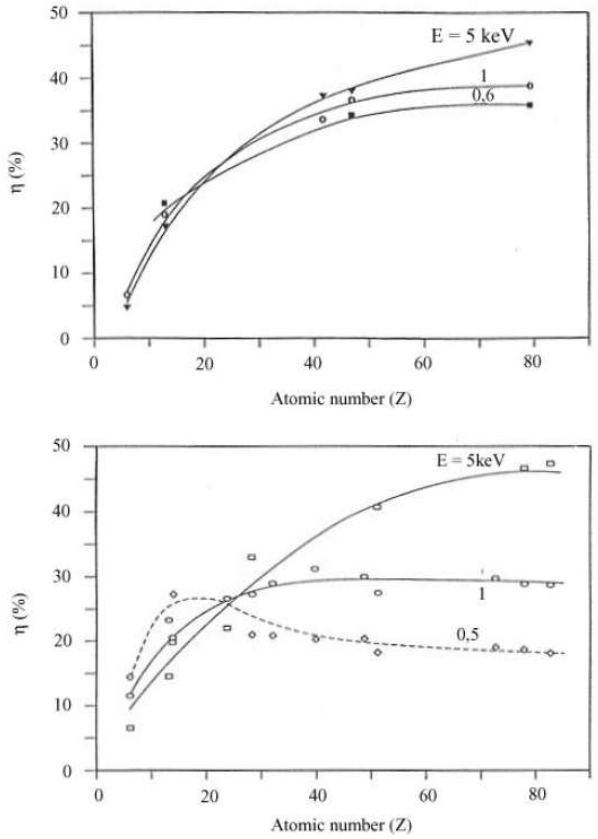

Figure 4. The backscattered electron coefficient as a function of the atomic number for different electron beam energies (**a**) for Ar ion cleaned surfaces, (**b**) as inserted from Bongeler *et al.* (1993).

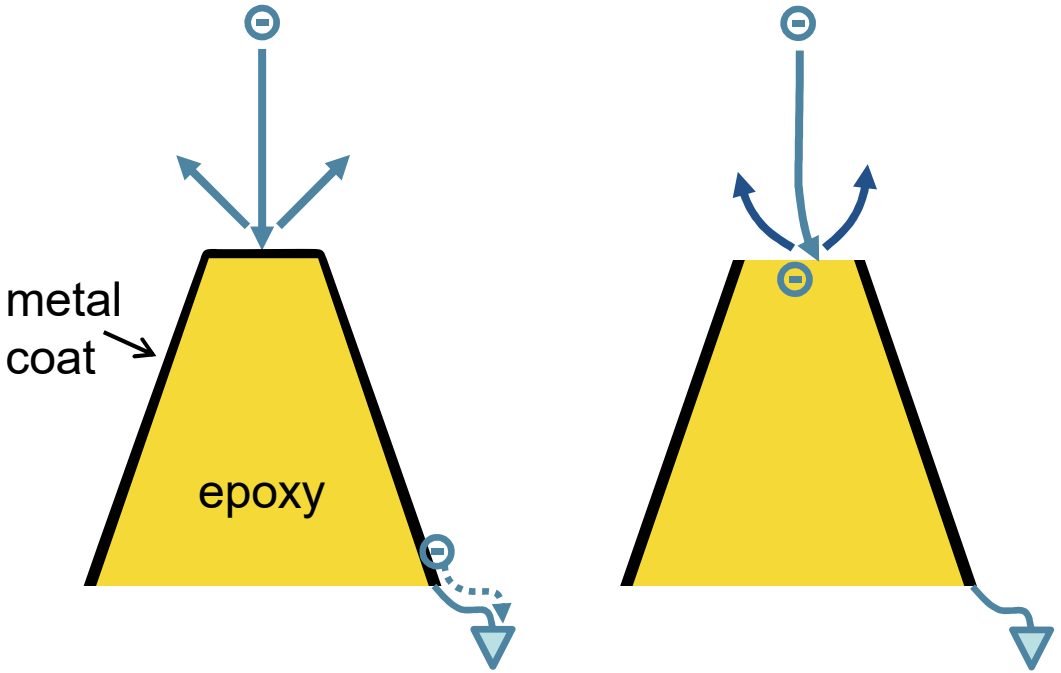
metal
coat
epoxy

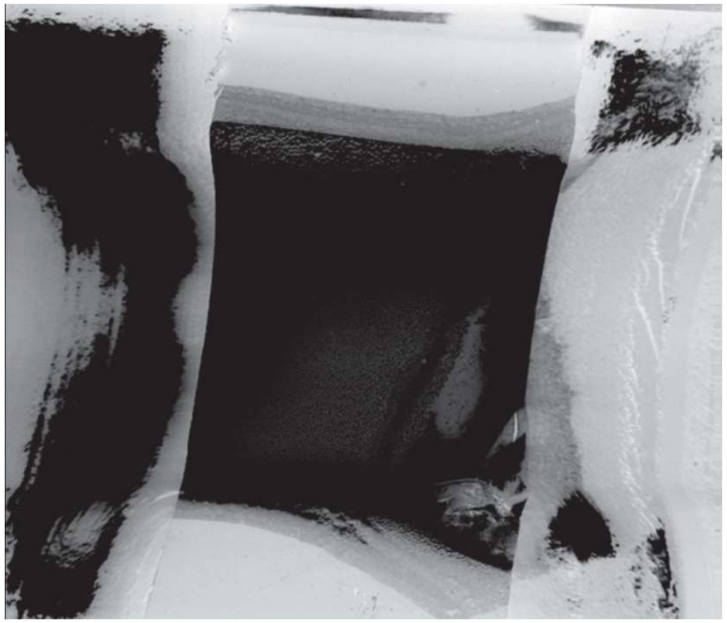
~100μm

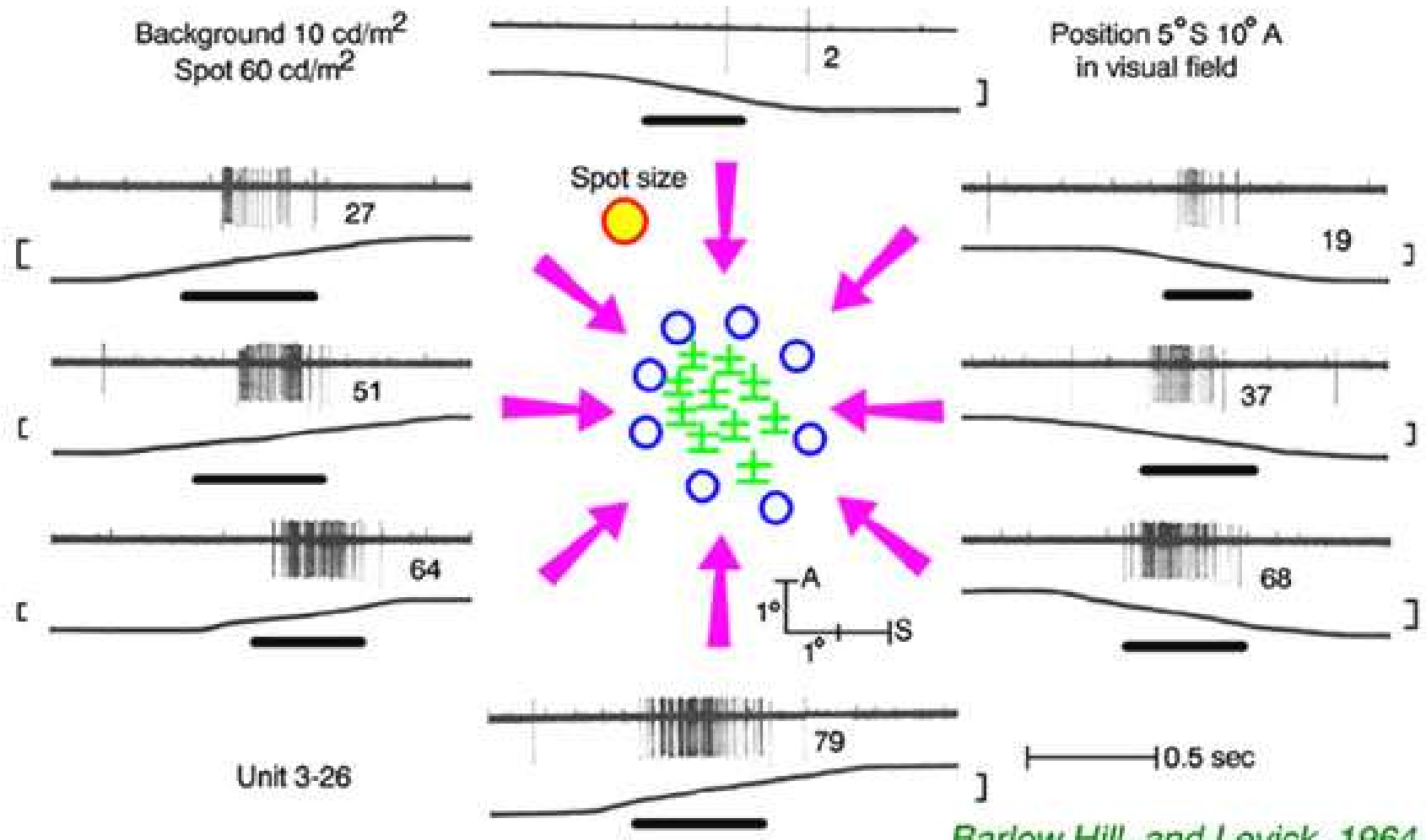
Background 10 cd/m2
Spot 60 cd/m2
Position 5° S 10° A
in visual field
Spot size
2
27
19
51
37
64
68
79
A
1°
S
1°
Unit 3-26
0.5 sec
Barlow,Hill, and Levick, 1964

Kevin
Briggman

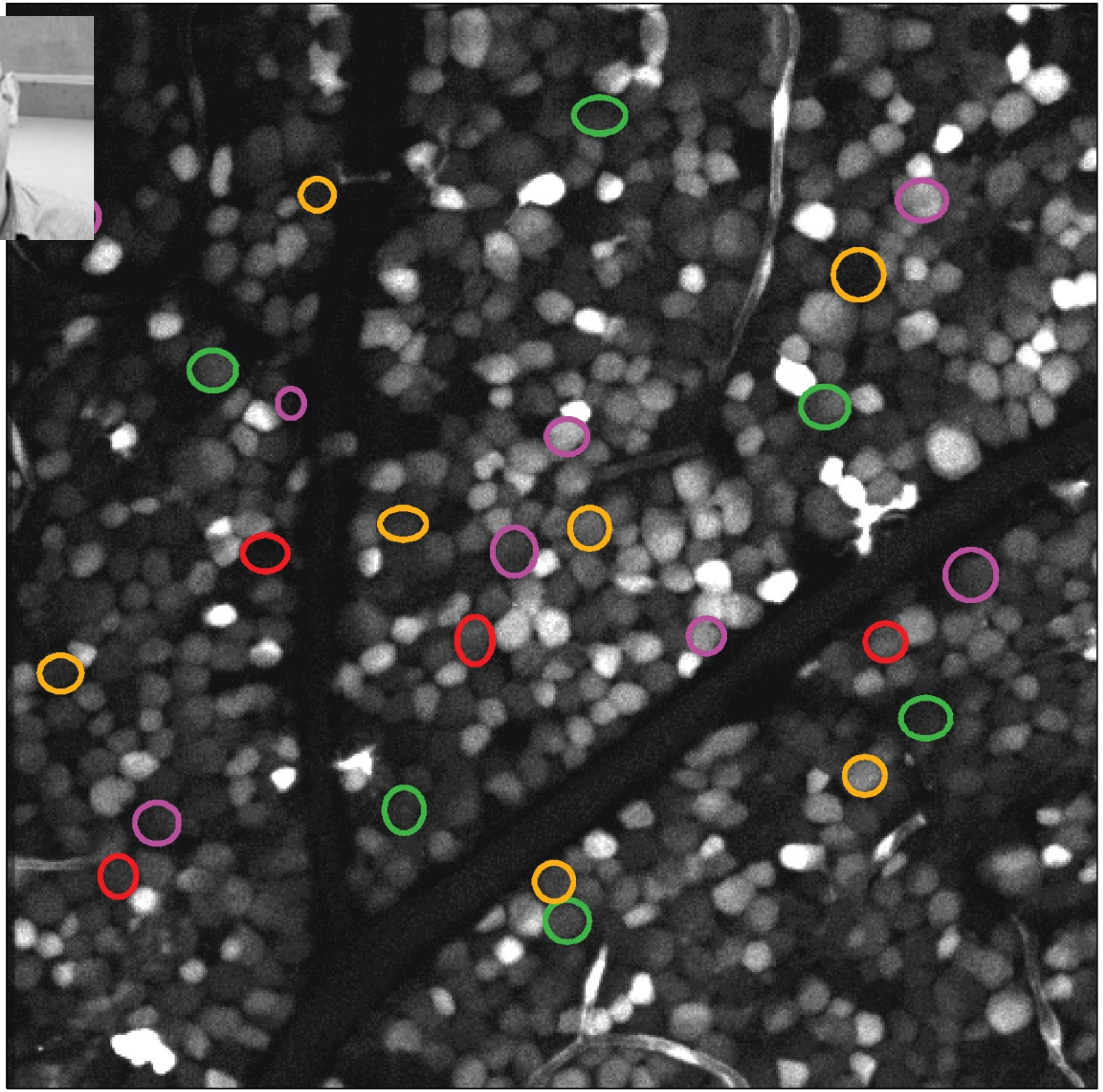

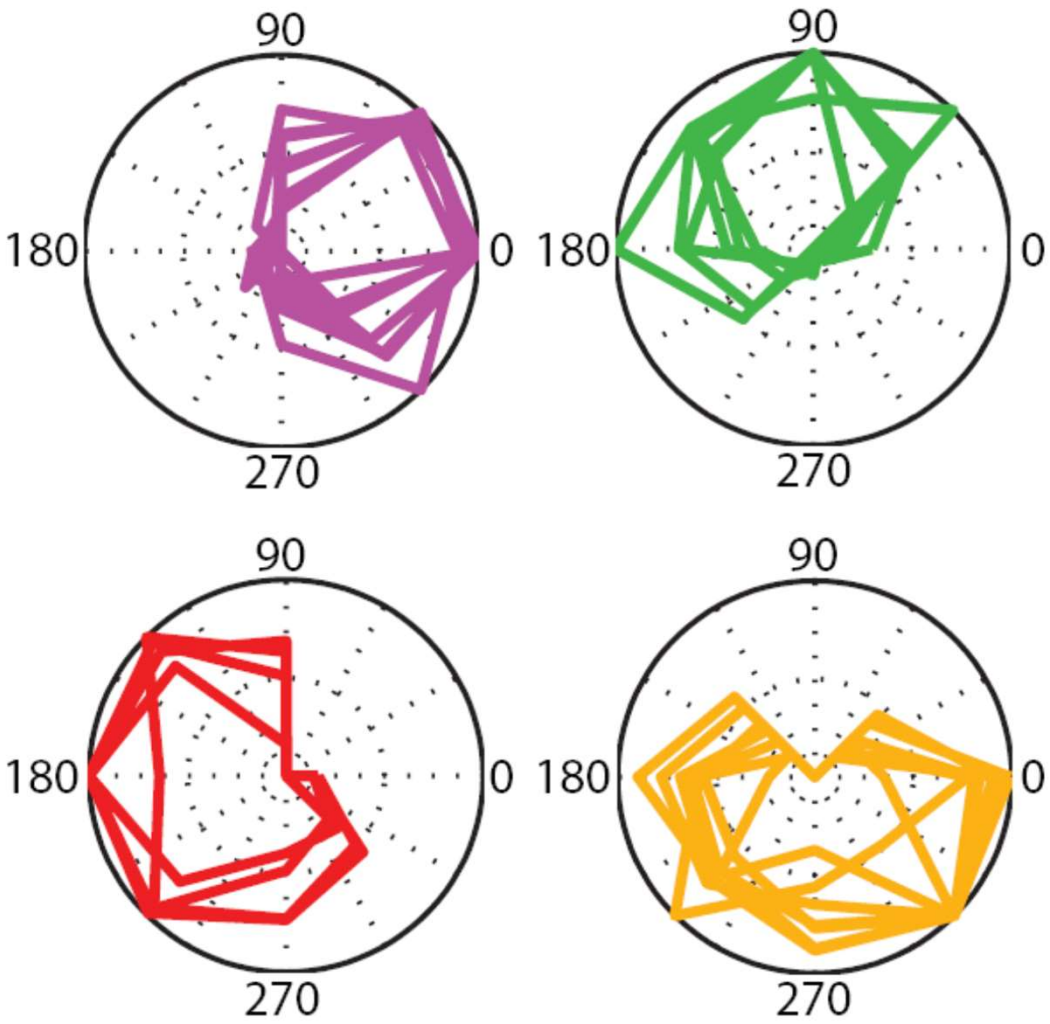

Kevin Briggman

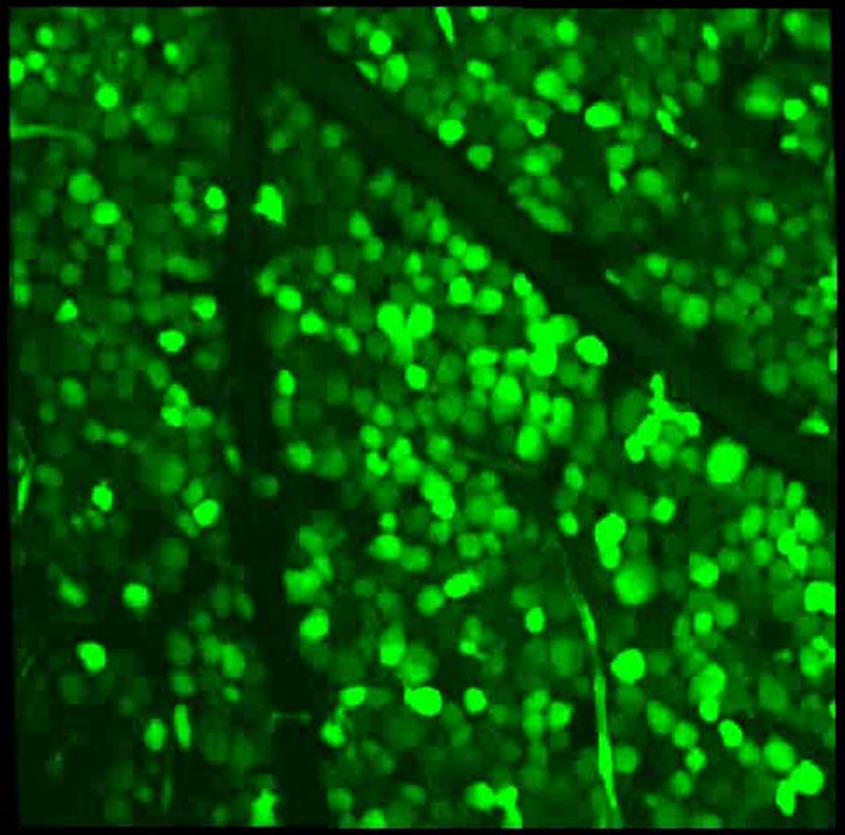

Kevin Briggman

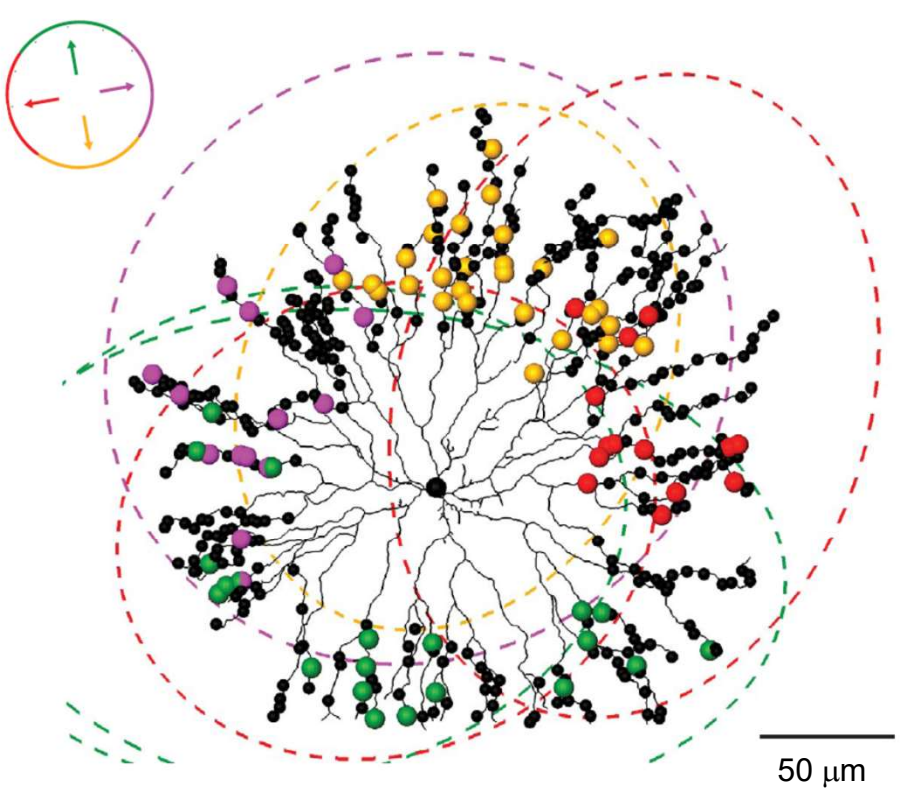

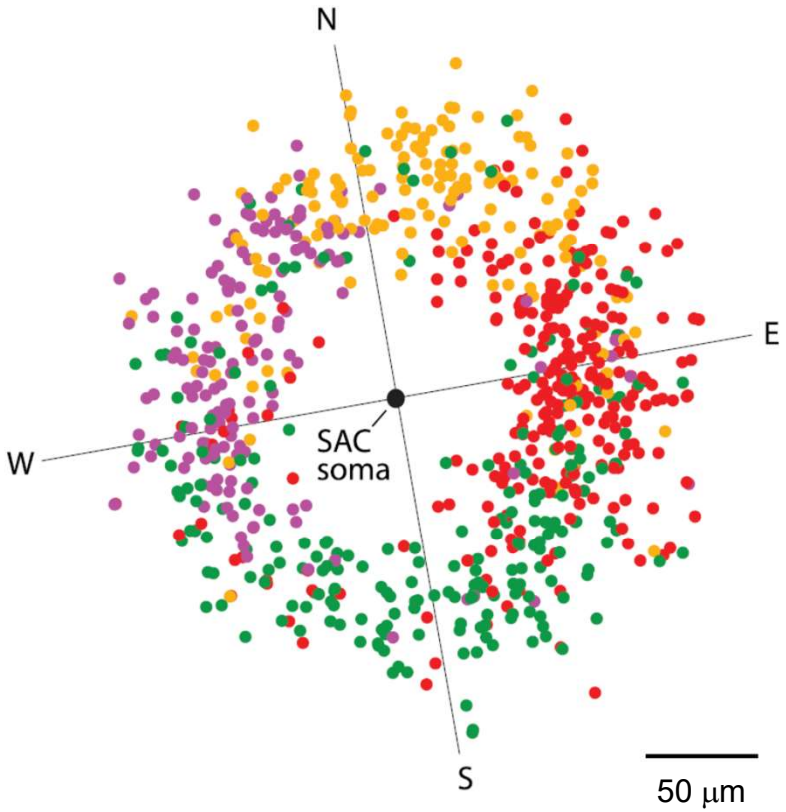

Briggman et al. 2011

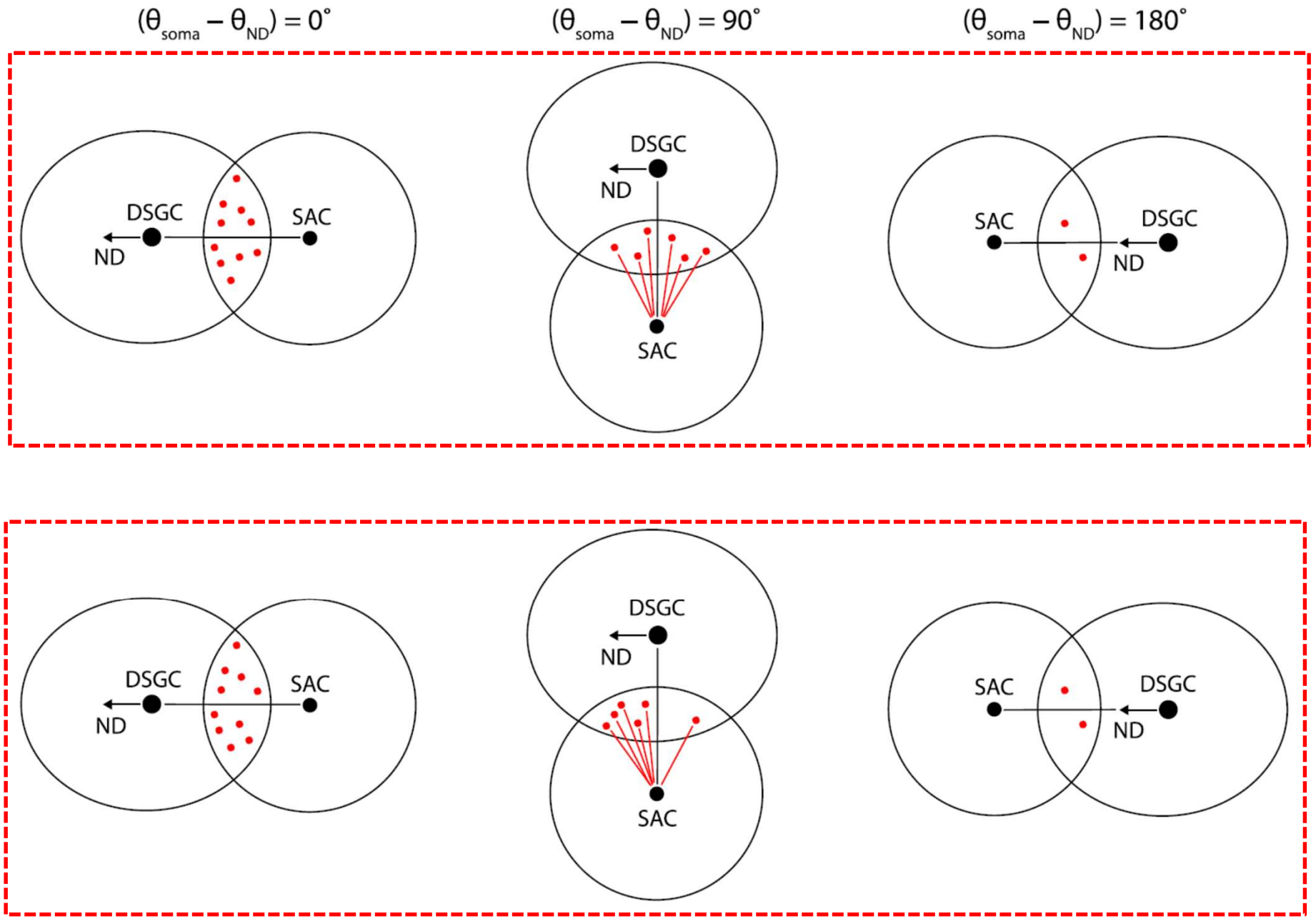

Briggman et al. 2011

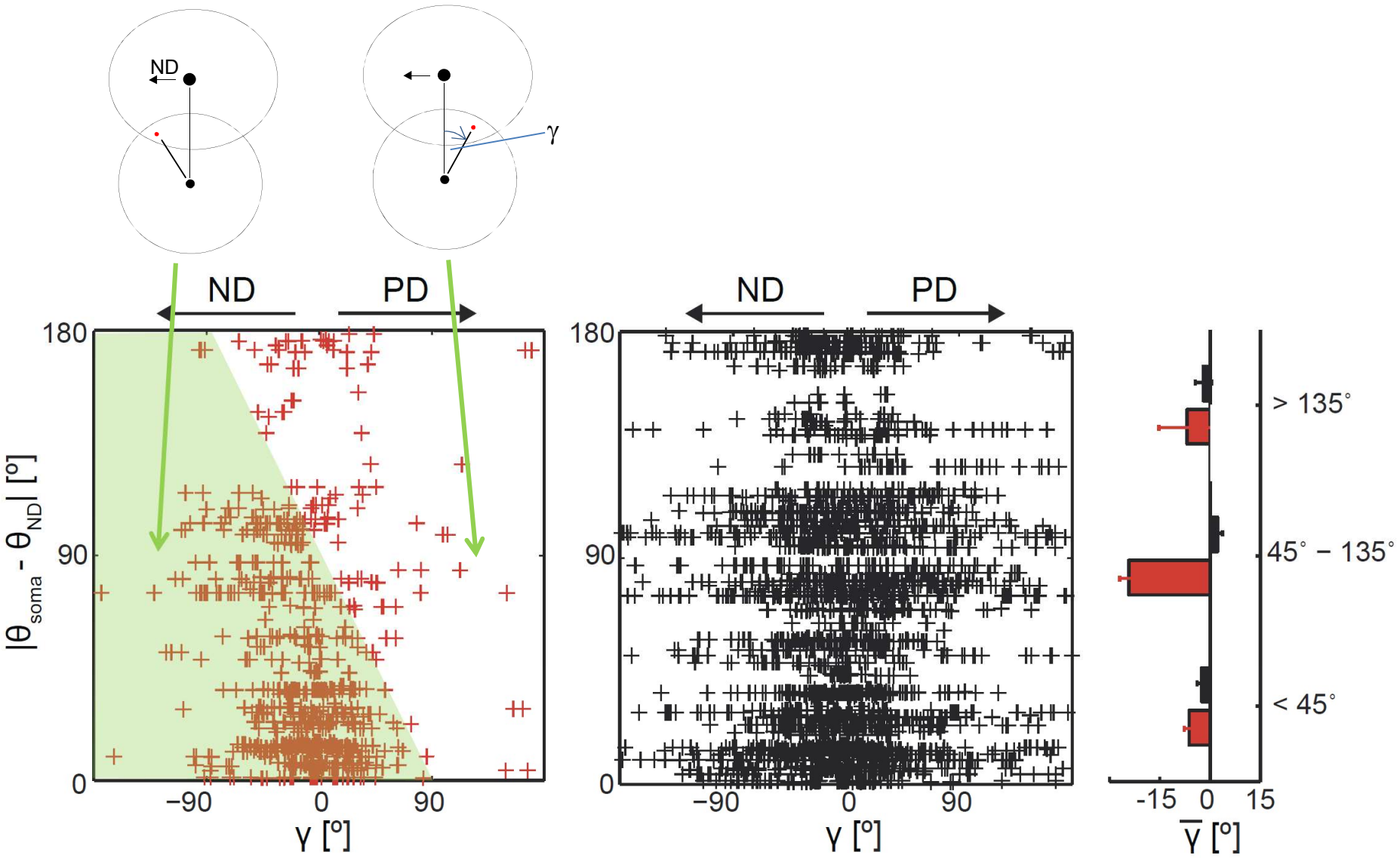

‘synapses’

all contacts

Briggman et al. 2011

“Connectomics”…

Moritz
Helmstaedter

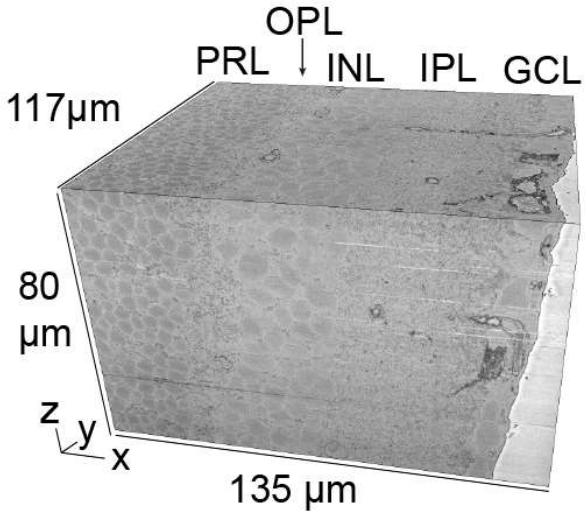

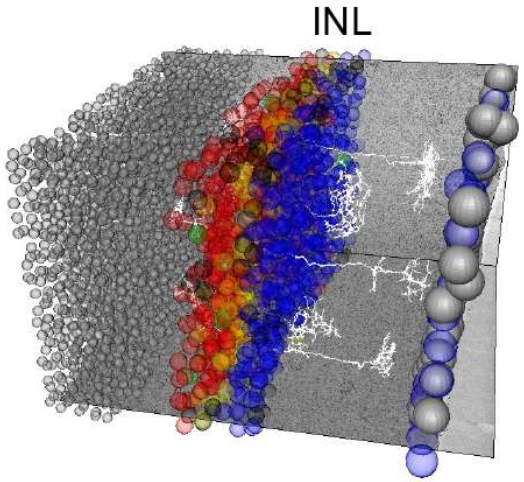

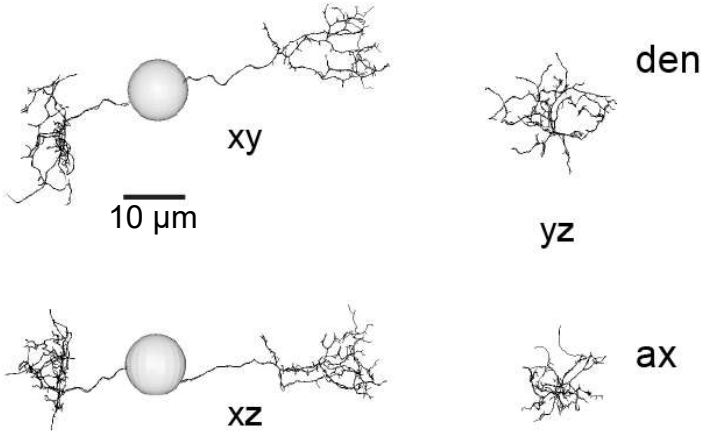

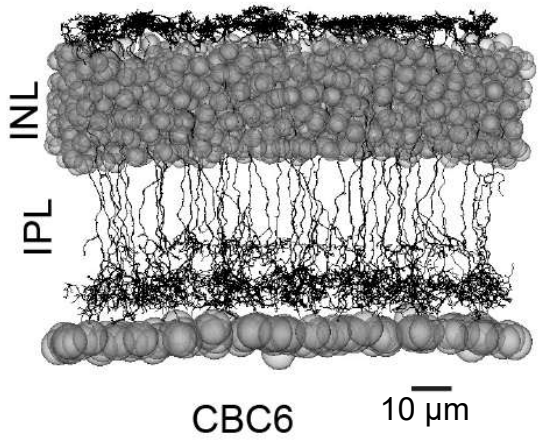

Helmstaedter, M., K. B. Briggman, et al. (2013). "Connectomic reconstruction of the inner plexiform layer in the mouse retina." Nature: (in press).

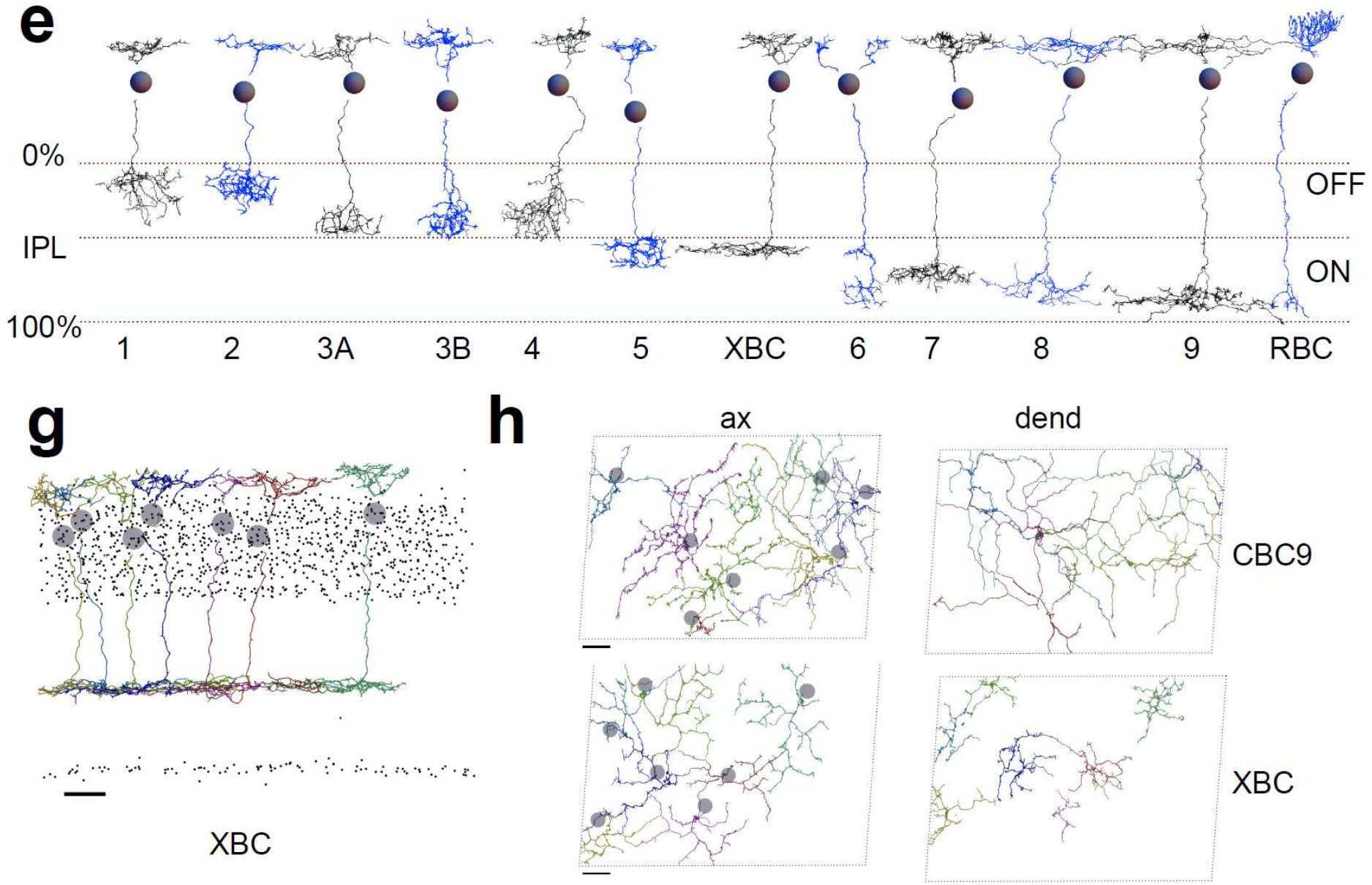

Helmstaedter, Briggman, Turaga, Jain, Seung, Denk, 2013

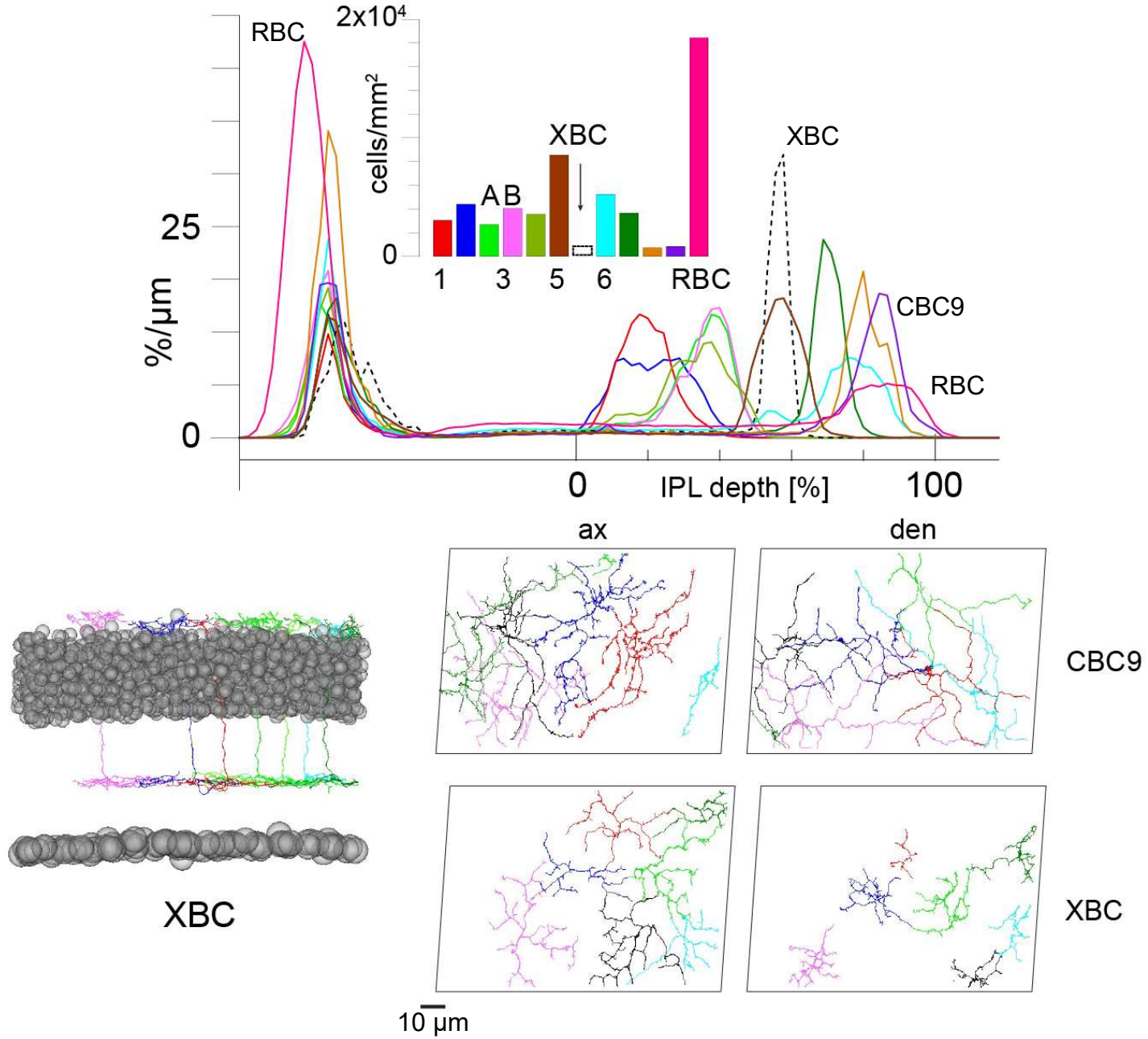

Helmstaedter, M., K. B. Briggman, et al. (2013). "Connectomic reconstruction of the inner plexiform layer in the mouse retina." Nature: (in press).

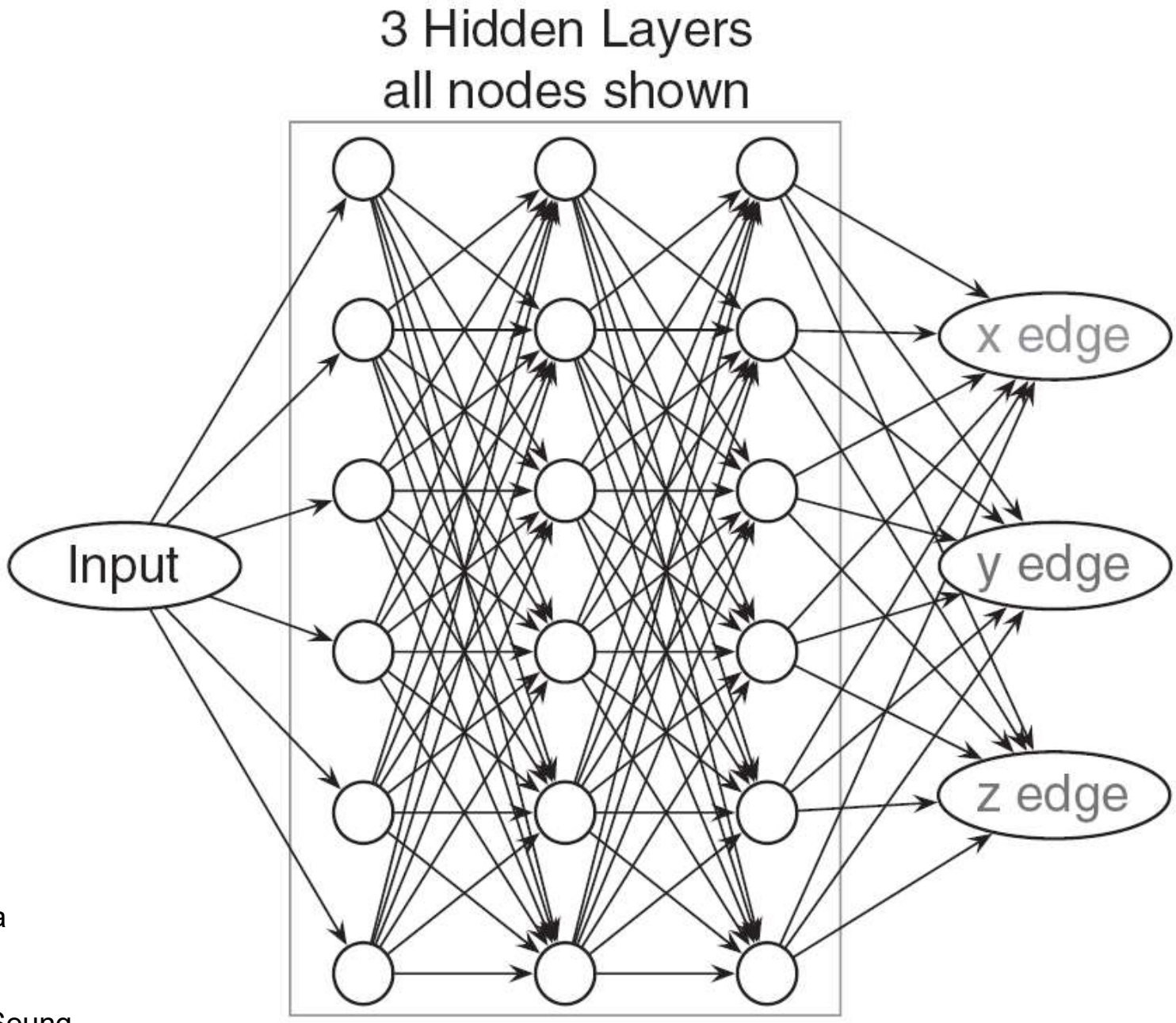

Srini Turaga
Viren Jain
…
Sebastian Seung
MIT

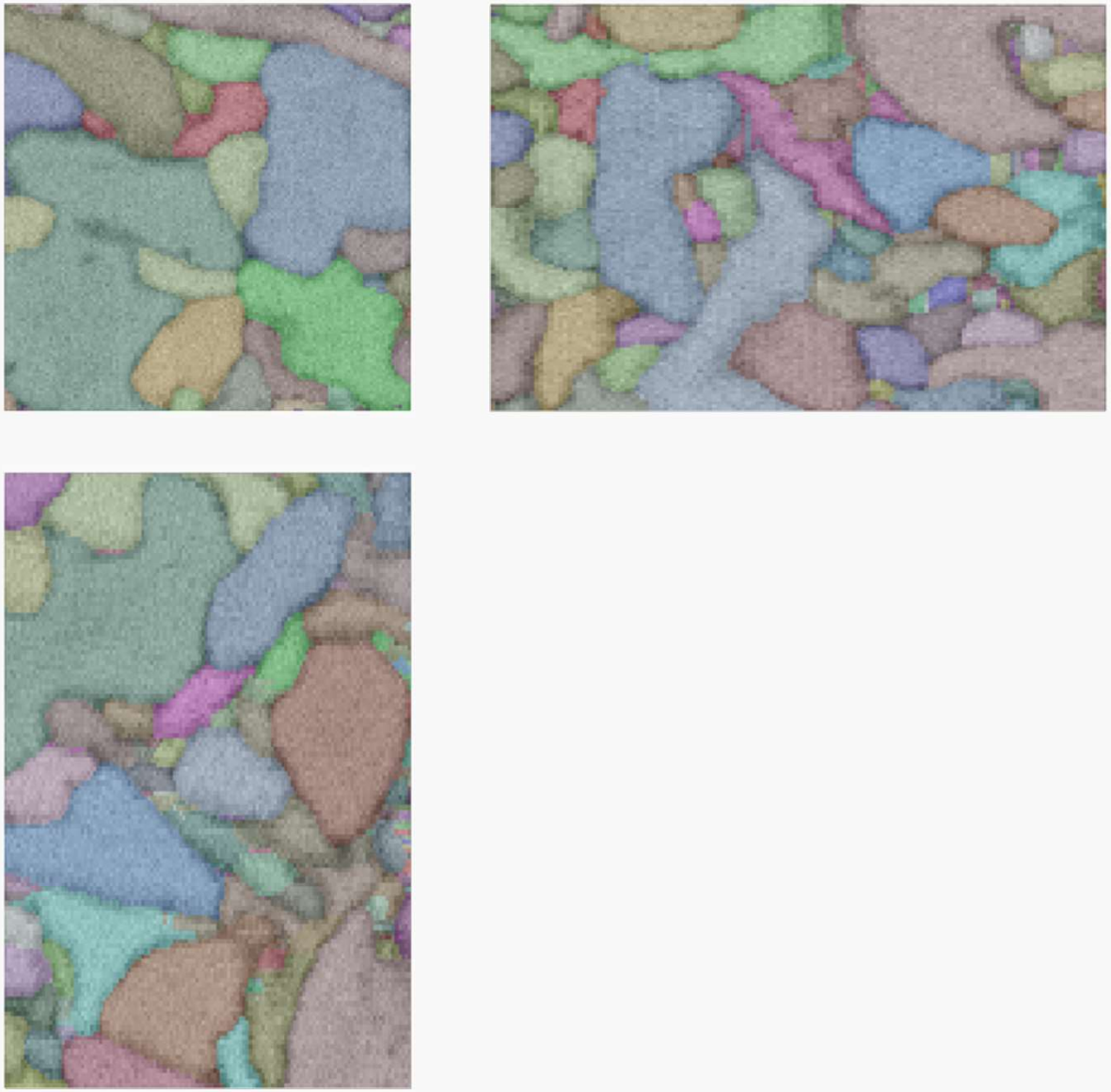

Helmstaedter, M., K. B. Briggman, et al. (2013). "Connectomic reconstruction of the inner plexiform layer in the mouse retina." Nature: (in press).

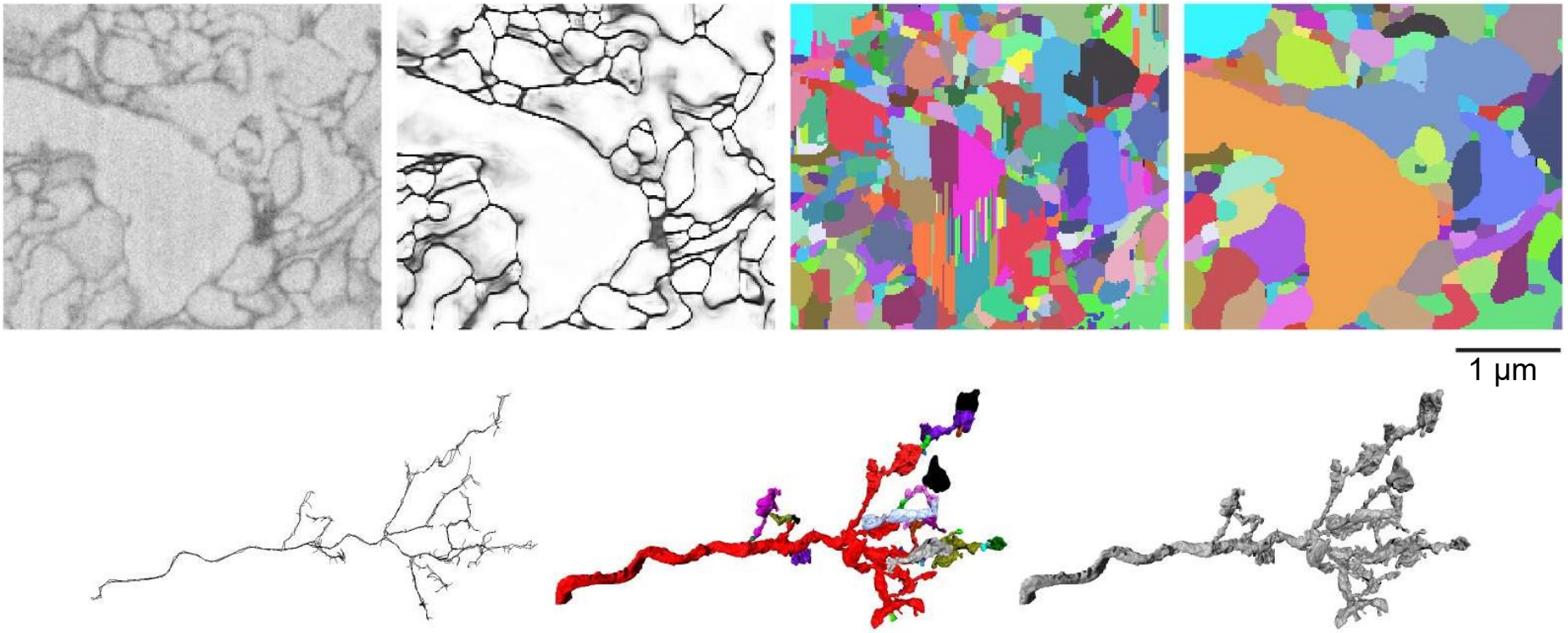

Helmstaedter, M., K. B. Briggman, et al. (2013). "Connectomic reconstruction of the inner plexiform layer in the mouse retina." Nature: (in press).

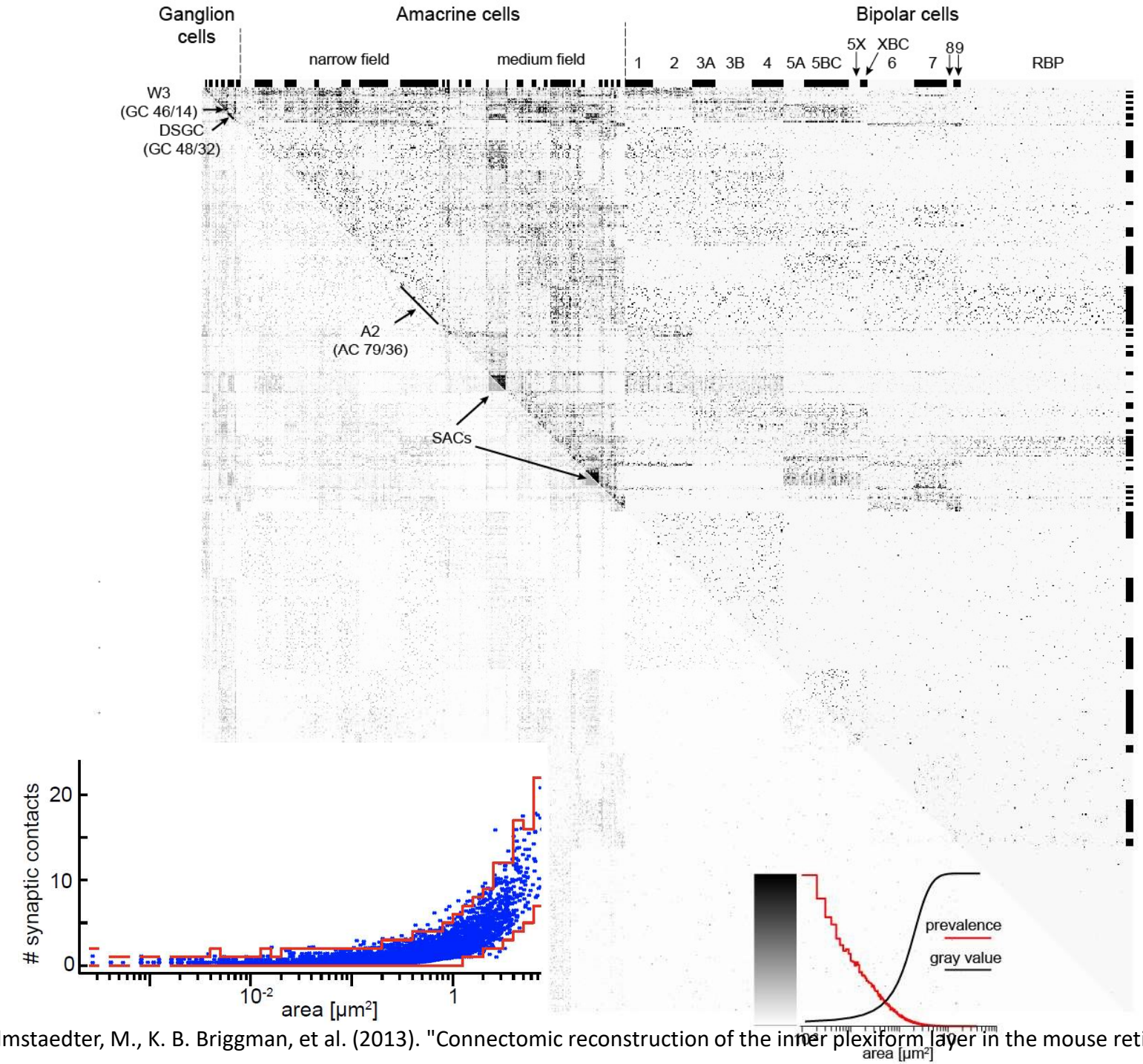

Helmstaedter, M., K. B. Briggman, et al. (2013). "Connectomic reconstruction of the inner plexiform layer in the mouse retina." Nature: (in press).

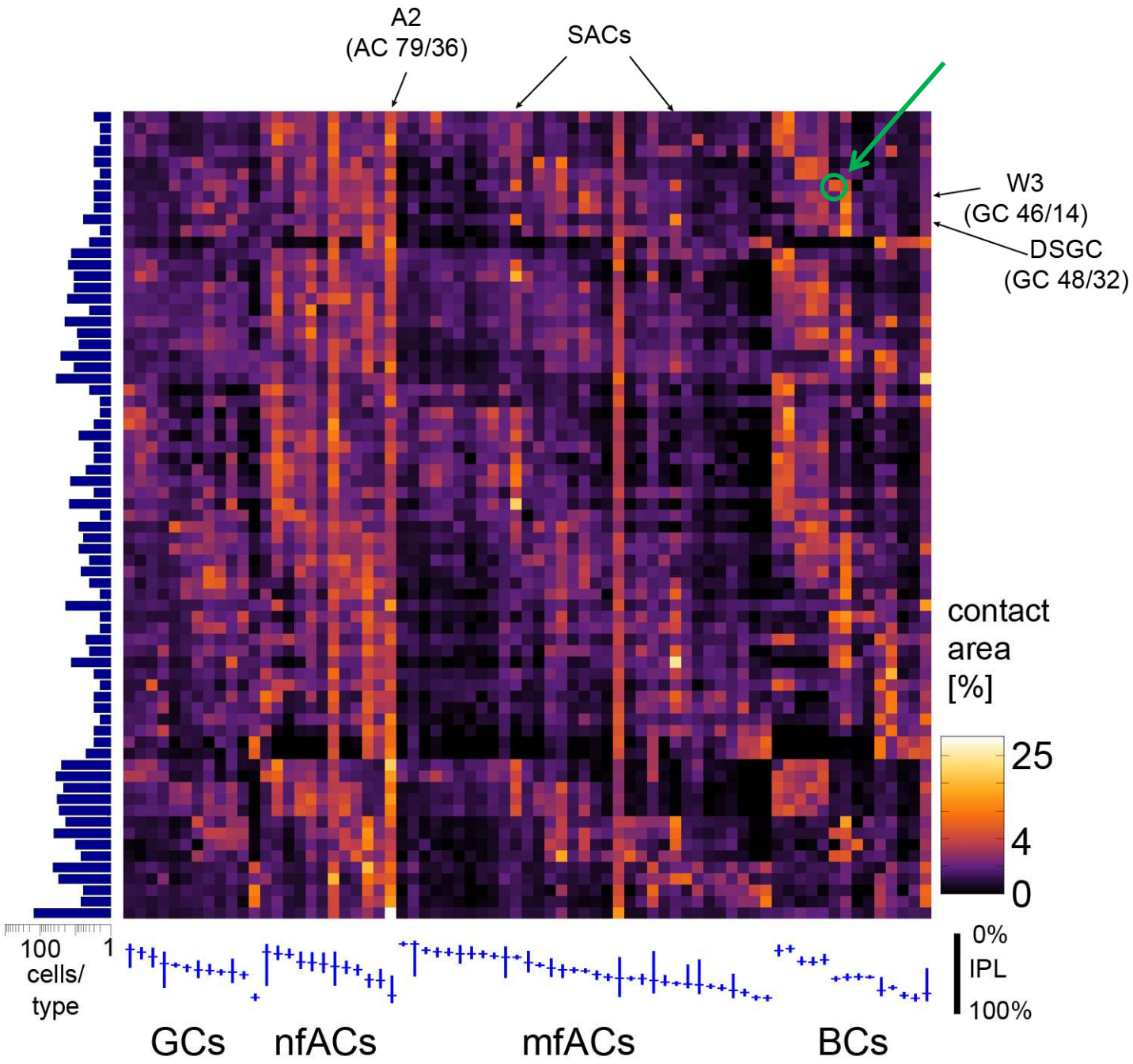

Helmstaedter, M., K. B. Briggman, et al. (2013). "Connectomic reconstruction of the inner plexiform layer in the mouse retina." Nature: (in press).

Joergen Kornfeld

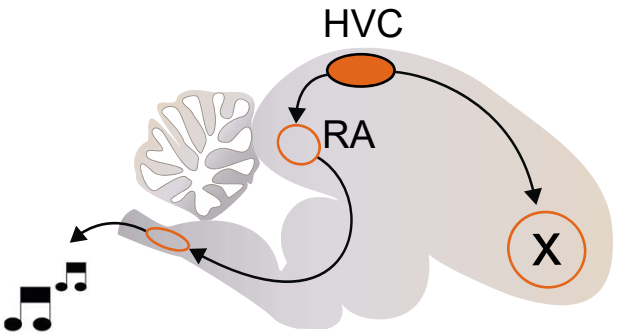

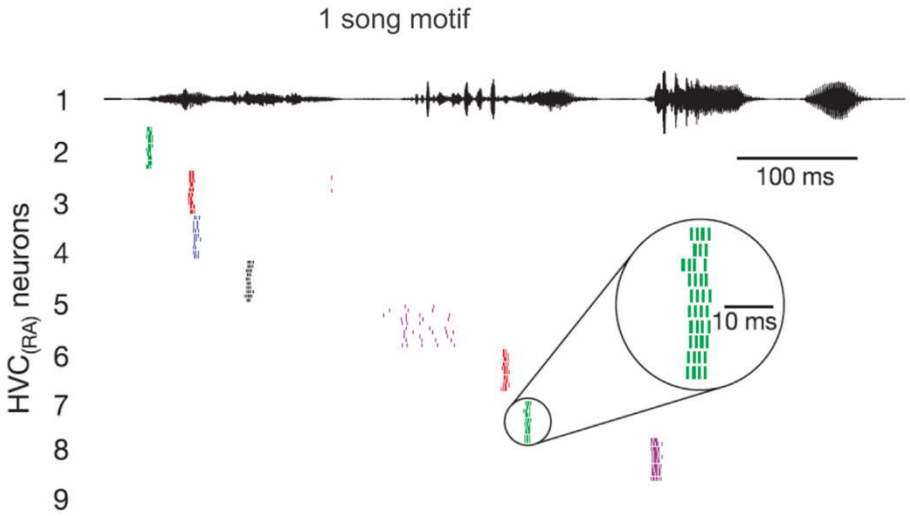

Hahnloser et al., 2002: Sparse time code

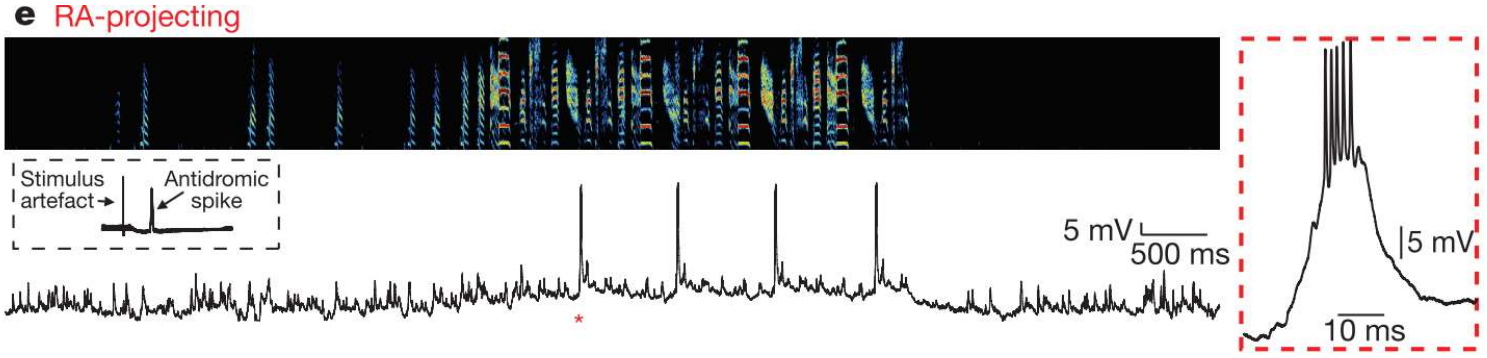

Long et al., 2010: Rapid depolarization underlies the burst

+biotinylated dextran amine (BDA)

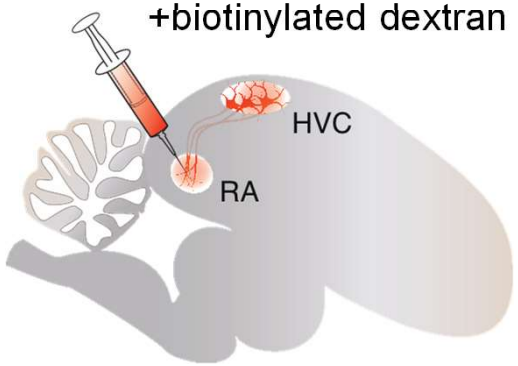

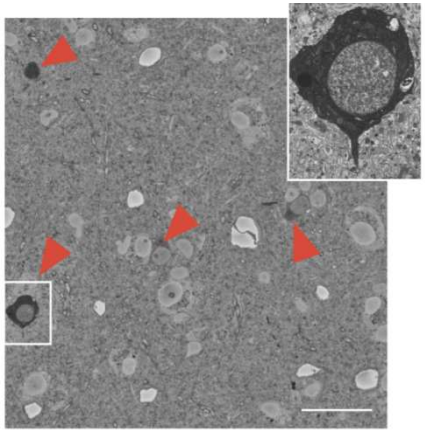

BDA labeled
HVC(RA) neurons

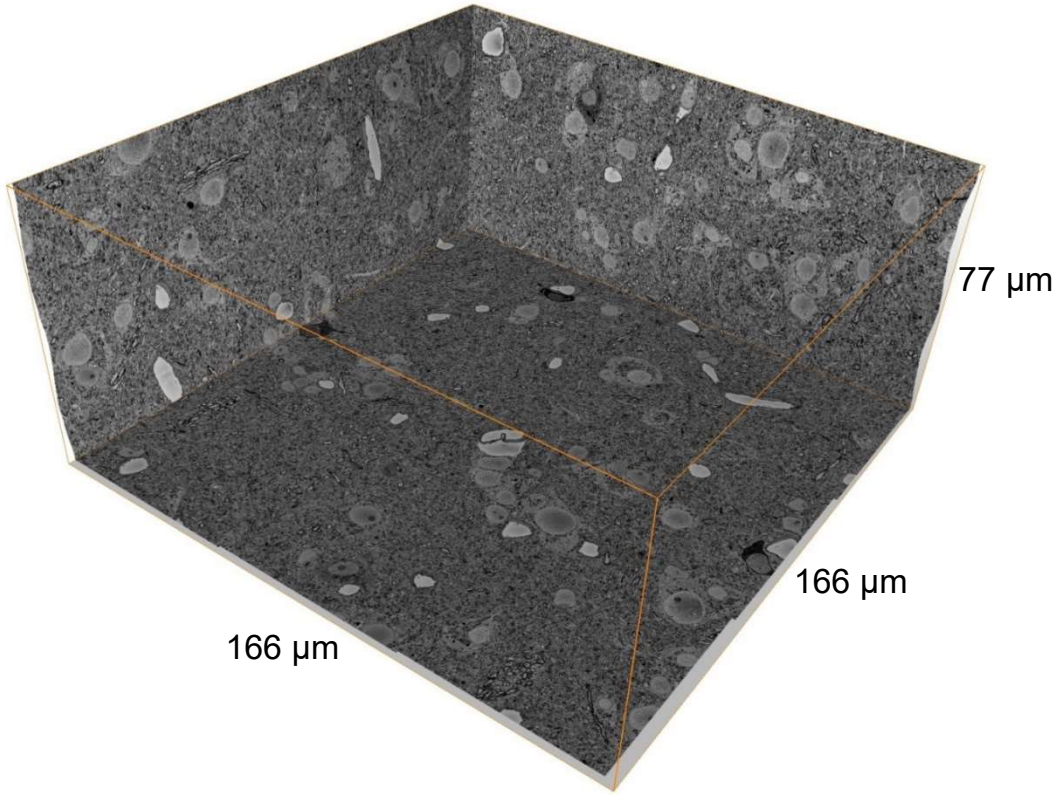

11x11x29 nm, ROTO stain combined with HRP-DAB protocol for labeling, ECS preservation

Kornfeld et al. (under review)

$HVC_{(RA)}$ axons with synapses colored by postsynaptic type

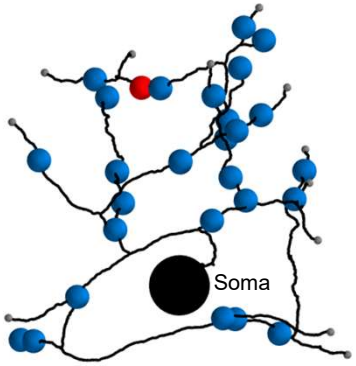

20μm

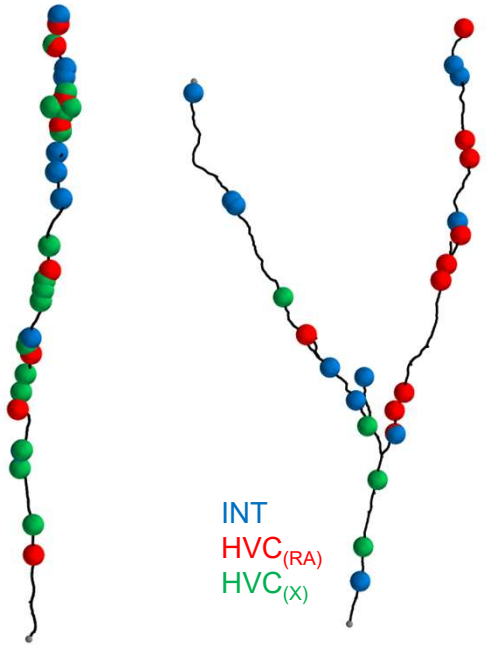

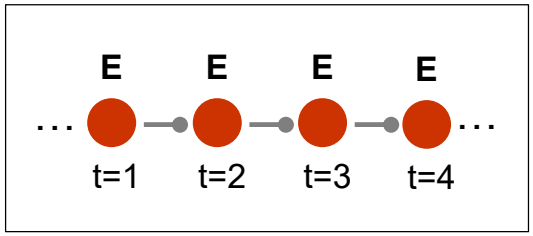

Quantified for 9 axons,
504 postsynaptic dendrites

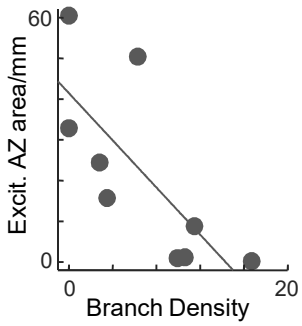

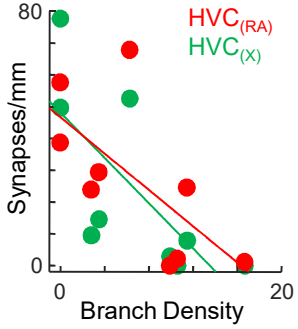

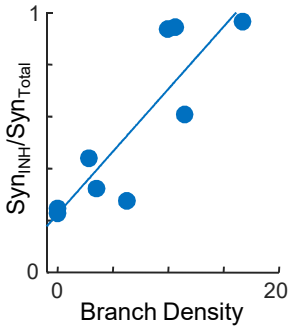

Kornfeld et al. 2017

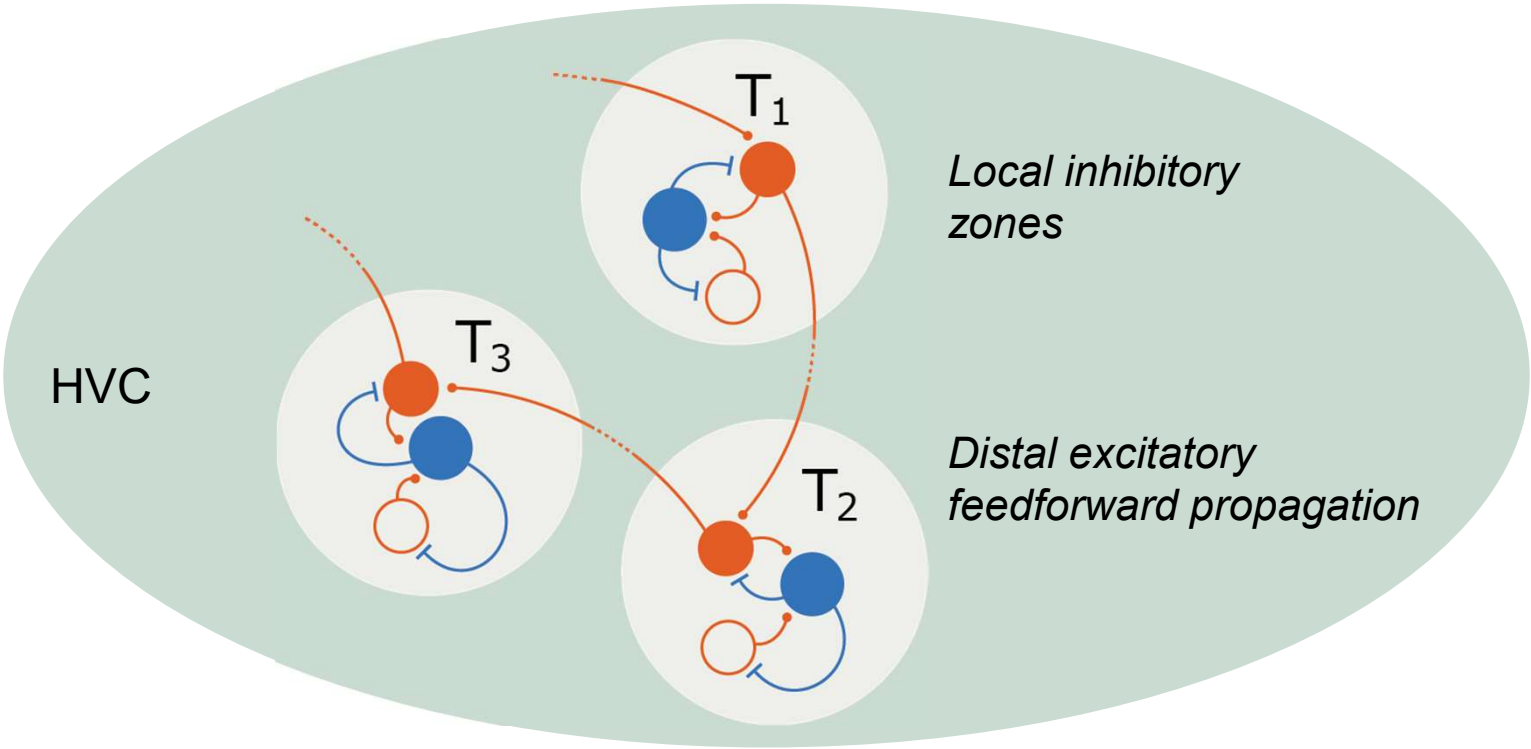

Similar network architecture proposed by Binas et al., 2014
for cortical sequence generation (coupled winner-take-all)

Kornfeld et al. 2017

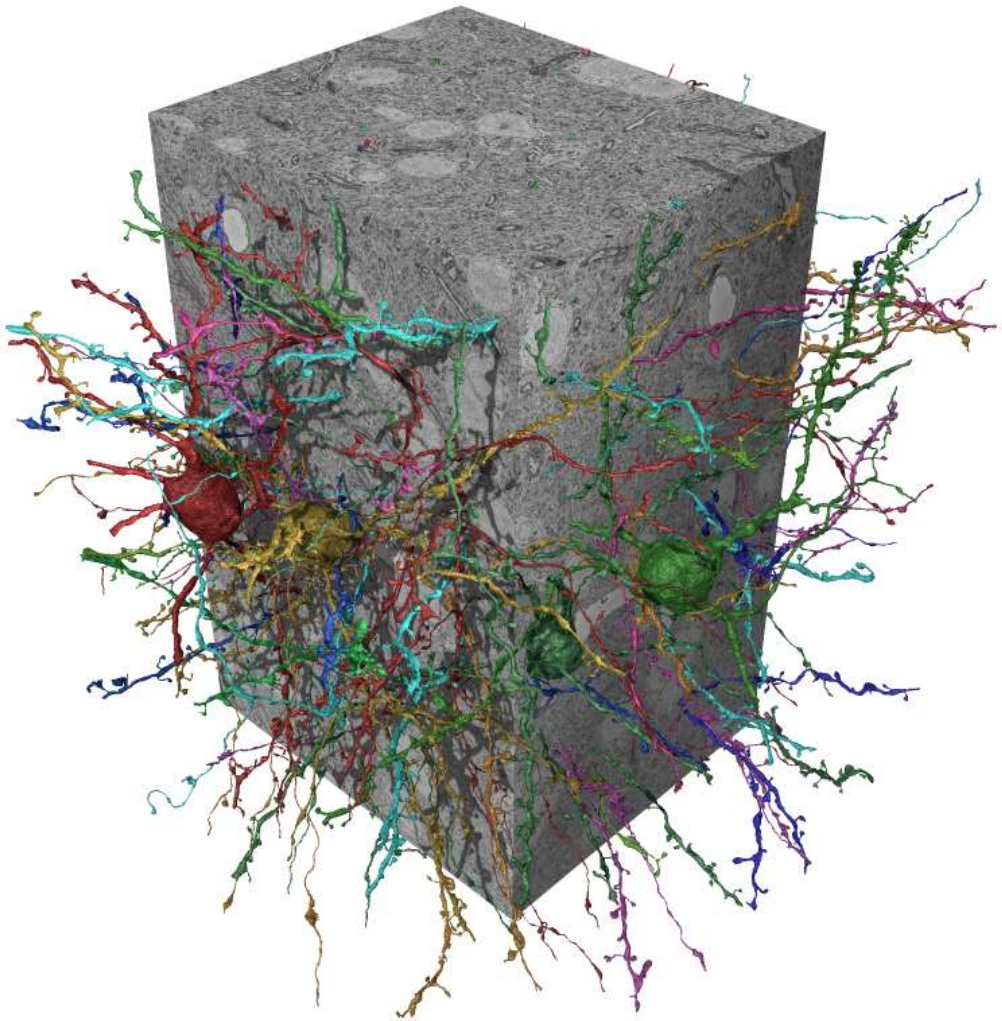

Jörgen Kornfeld

2015

2017

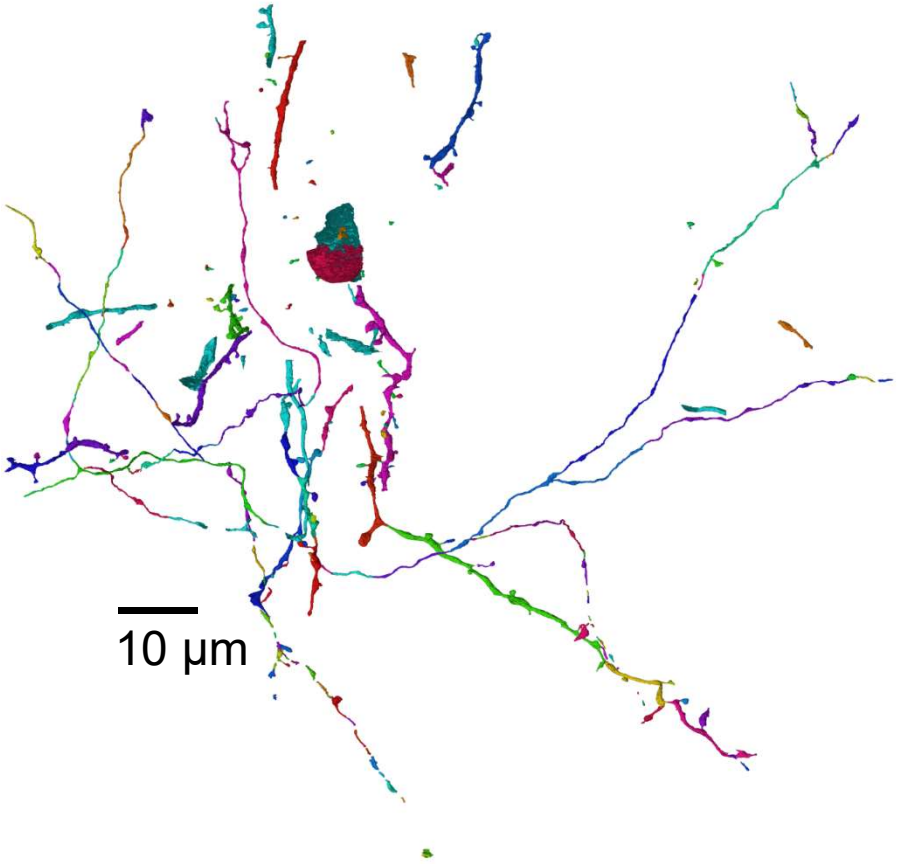

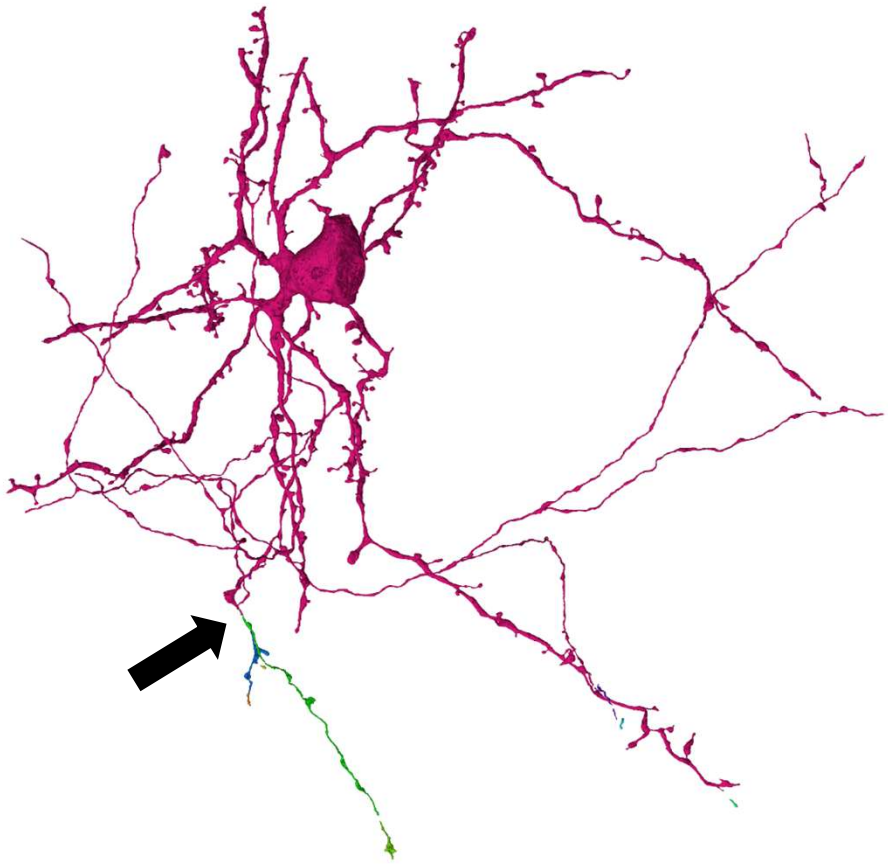

~0.01 mm error free path length

> 1 mm error free path length

Januszewski, Kornfeld, Li, Pope, Blakely, Maitin-Shepard, Tyka, Denk, Jain. **arXiv 2017**

Michal Januszewski (Google), Jeremy Maitin-Shepard (Google), Peter Li (Google), Joergen Kornfeld (MPINB), Viren Jain (Google)

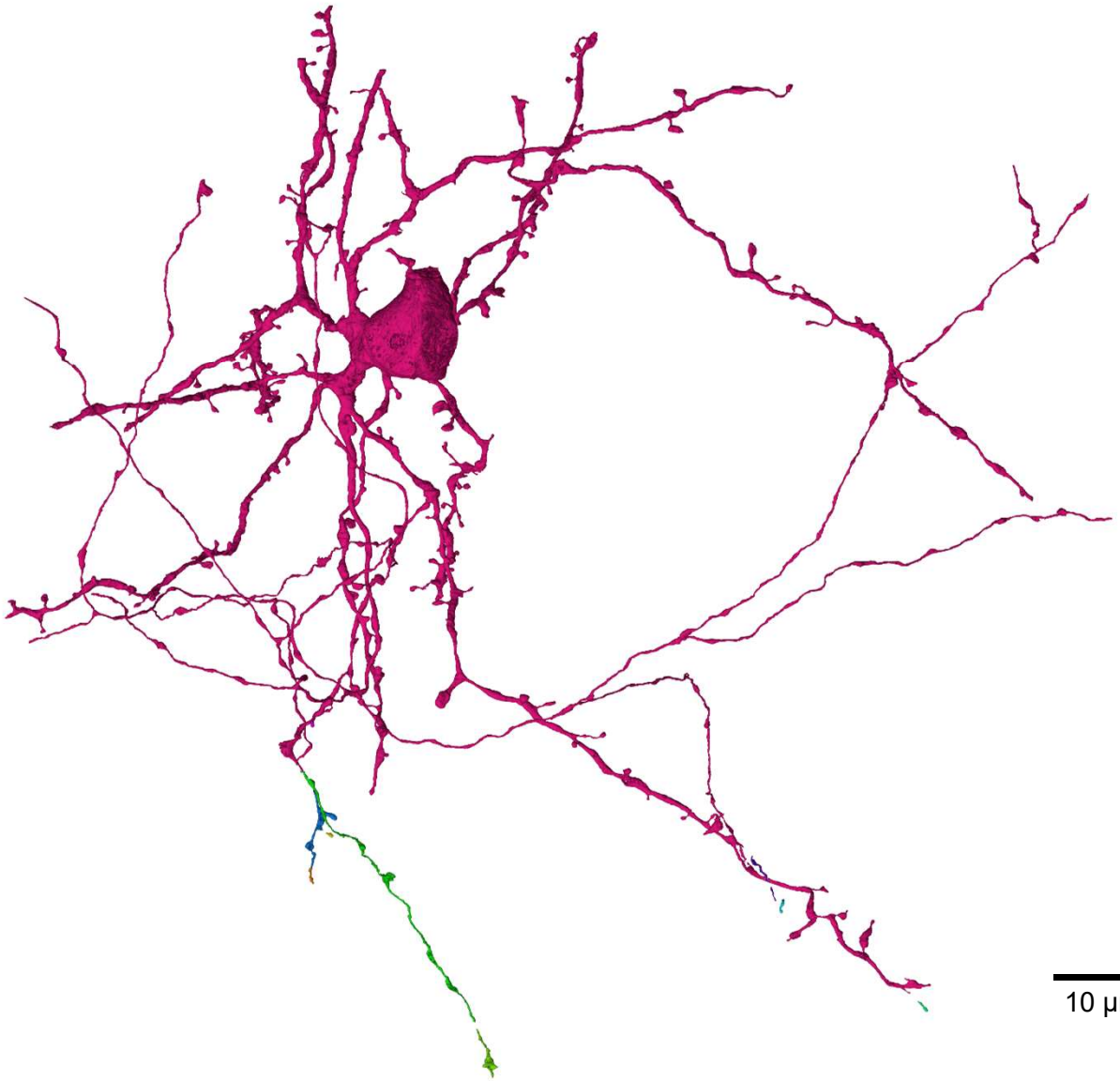

M. Januszewski

V. Jain

Completed reconstruction through targeted tracing with KNOSSOS
Total workload for small data set: ~900 hours

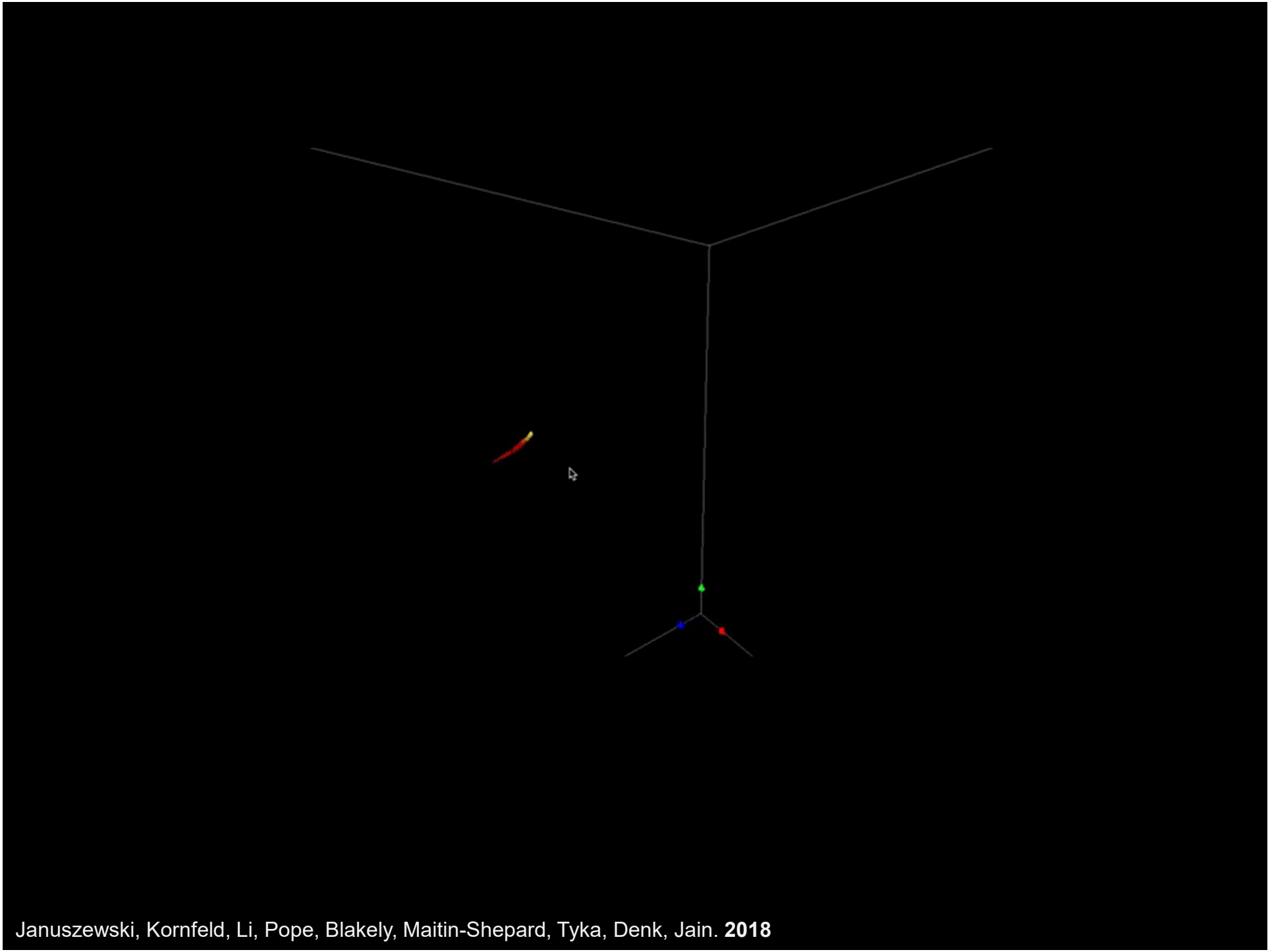

Januszewski, Kornfeld, Li, Pope, Blakely, Maitin-Shepard, Tyka, Denk, Jain. **2018**

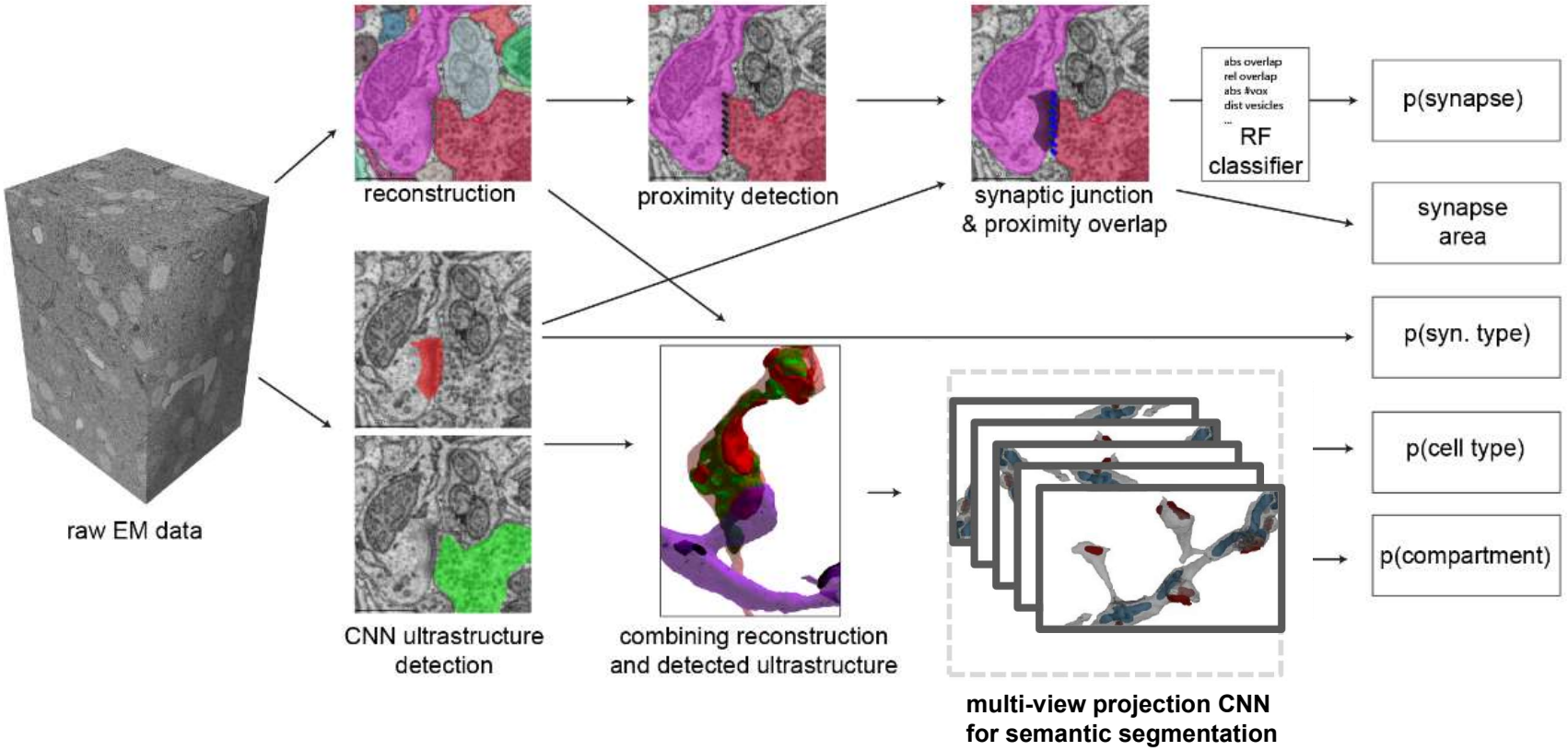

Automated synaptic connectivity inference for volume electron microscopy

Sven Dorkenwald, Philipp J Schubert, Marius F Killinger, Gregor Urban, Shawn Mikula, Fabian Svara & Joergen Kornfeld ✉

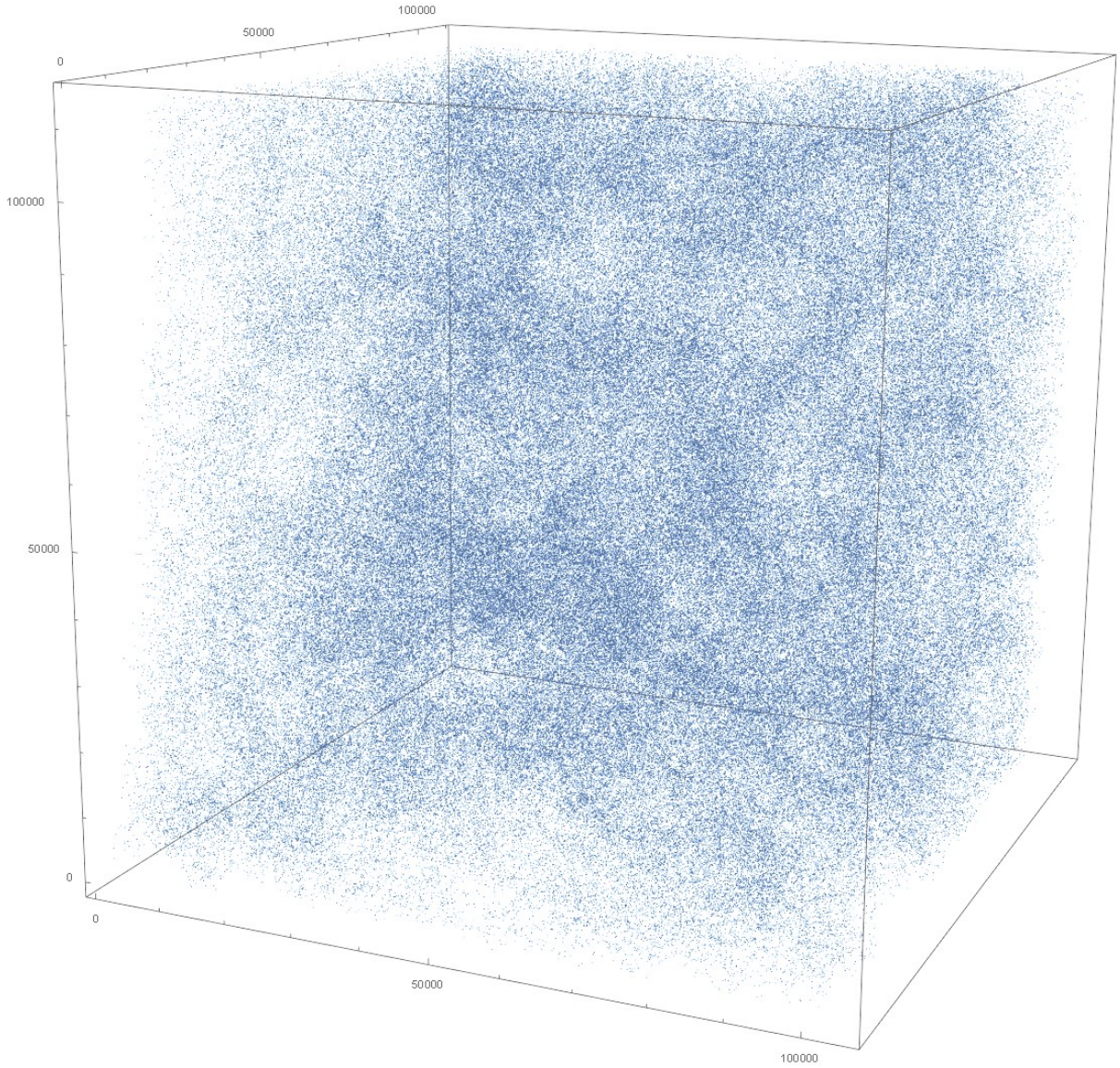
100000
50000
0
100000
50000
0
0
50000
100000

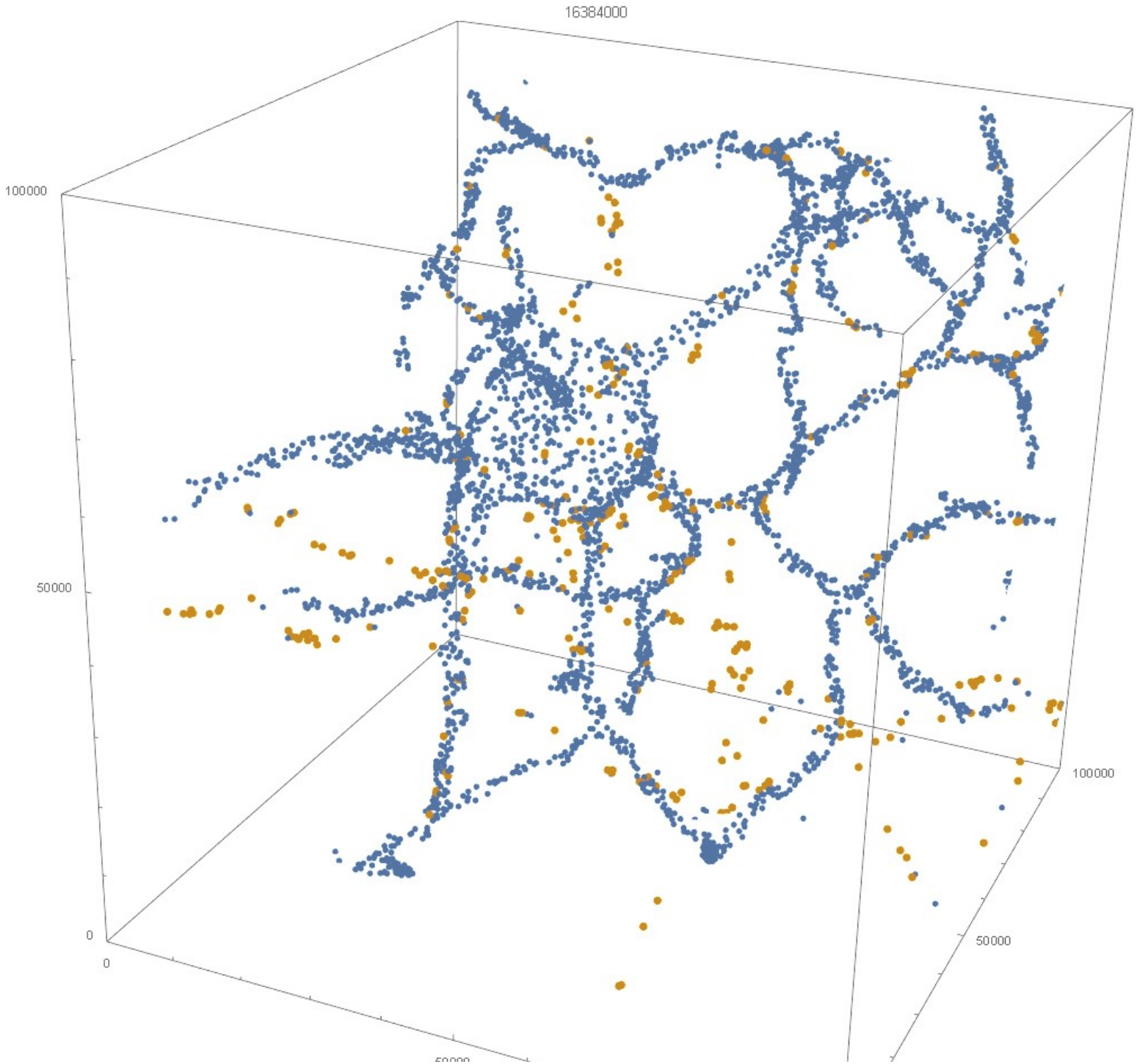
16384000
100000
50000
0
0
50000
100000

Songbird basal ganglia datasets

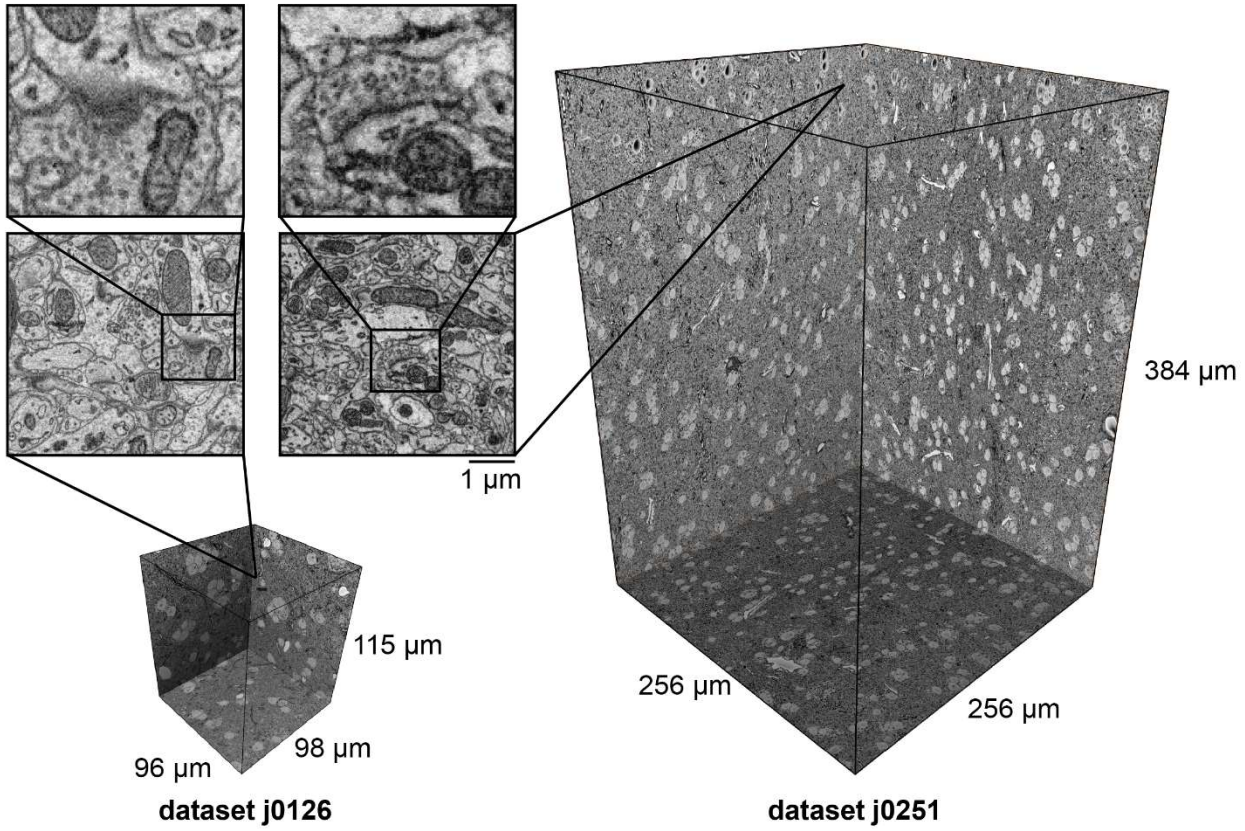

450 somata

11,000 somata

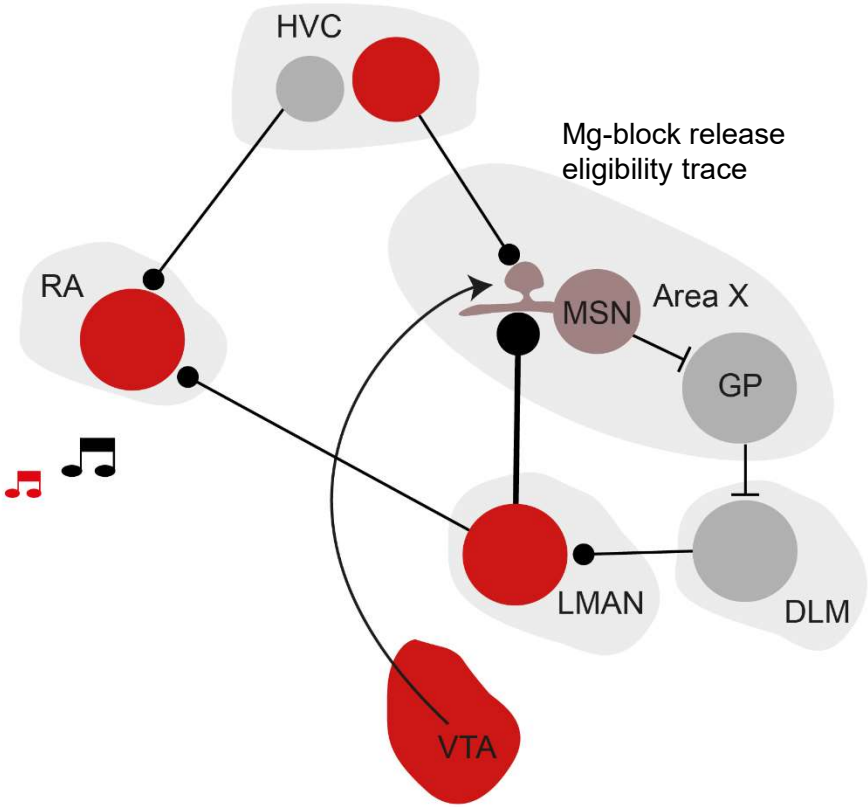
HVC
Mg-block release
eligibility trace
RA
MSN
Area X
GP
LMAN
DLM
VTA

The three ingredients for reinforcement learning

1 Behavorial context (relative song time)

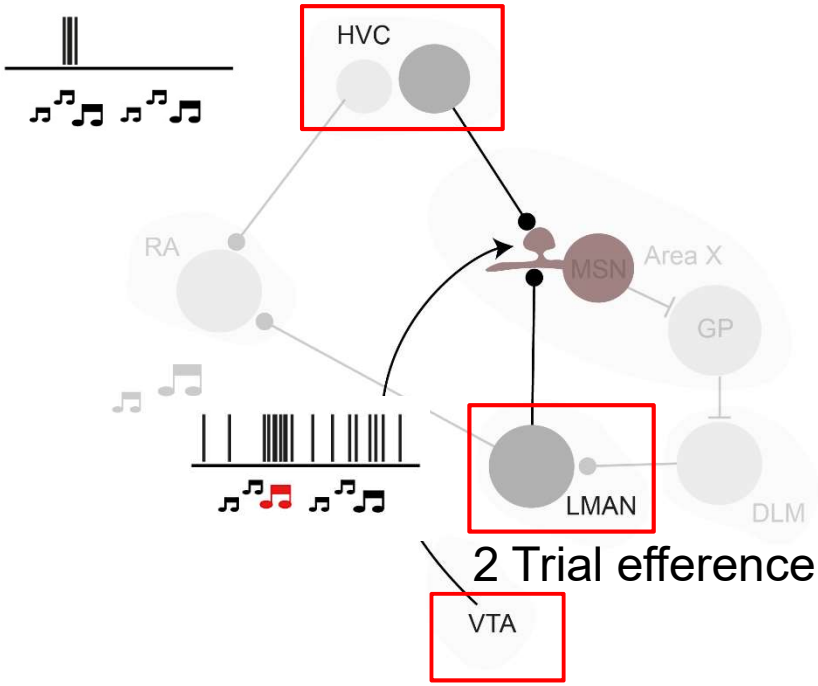

2 Trial efference copy (random song change)

3 Reward signal (dopaminergic reward prediction error)

M. Fee

Goldberg and Fee. J Neuroscience 2011
Fee. Current Opinion in Neurobiology 2014

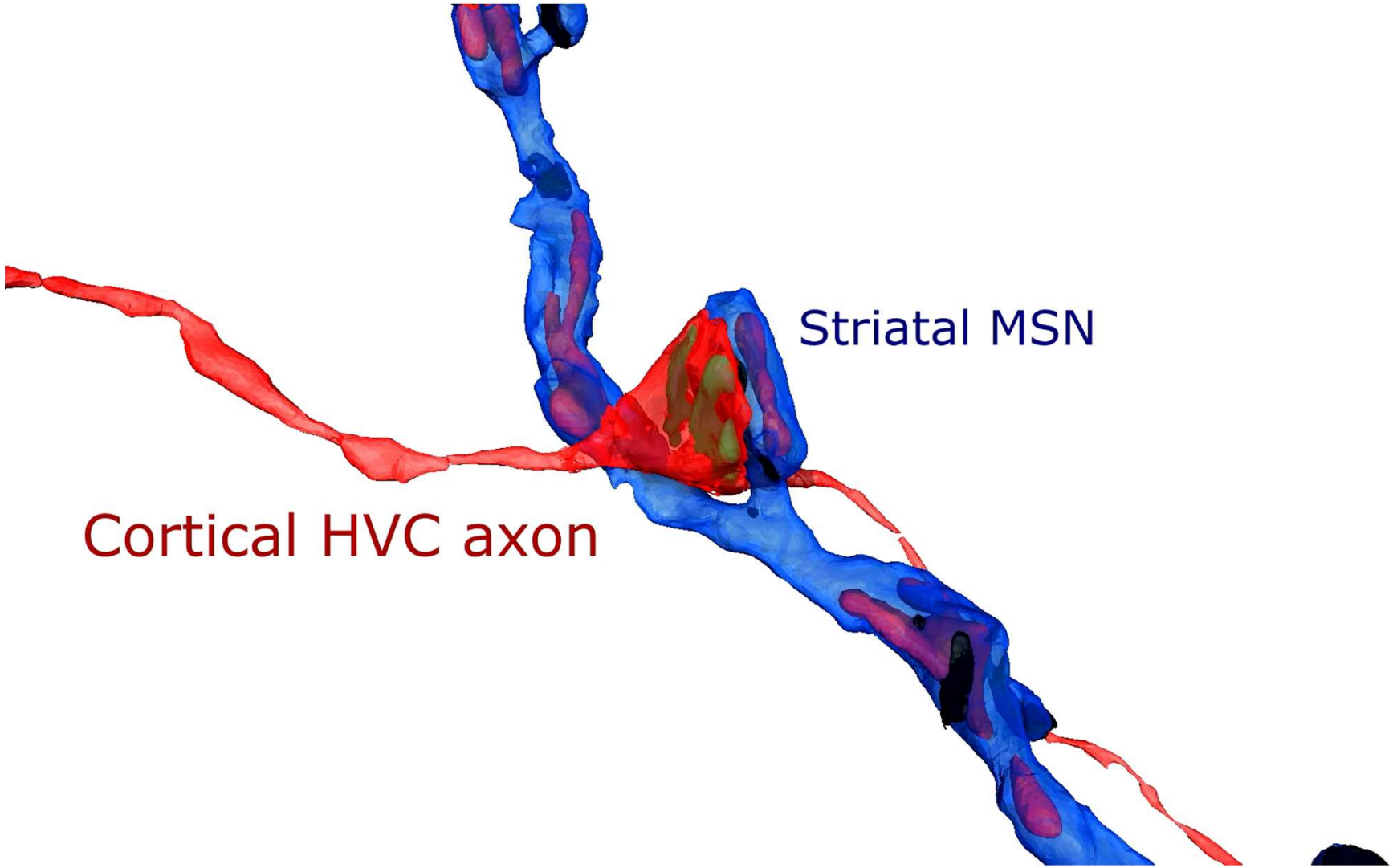
Striatal MSN
Cortical HVC axon

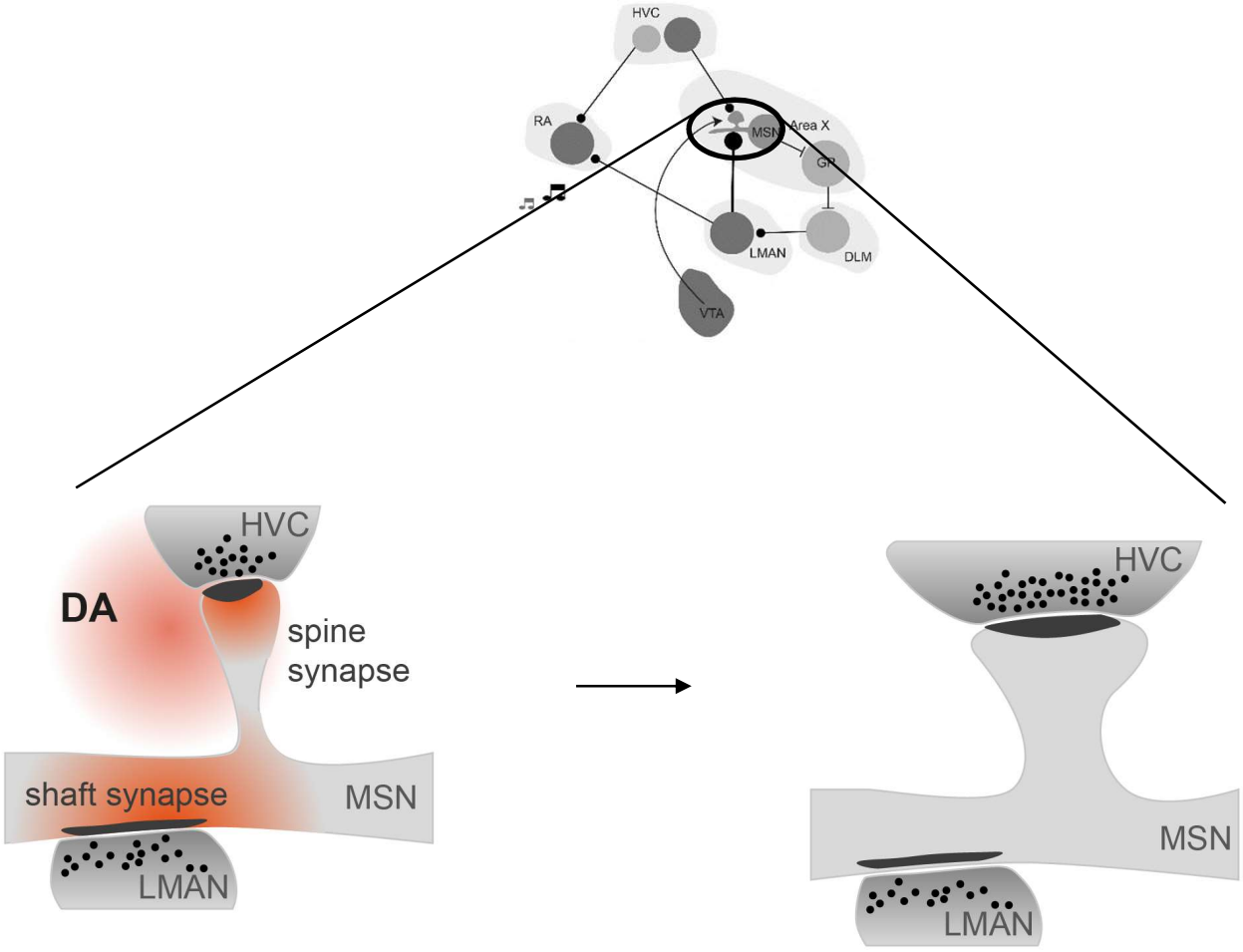

Links between plasticity and spines e.g. Yuste and Bonnhoefer. Ann. Rev. Neuroscience 2001

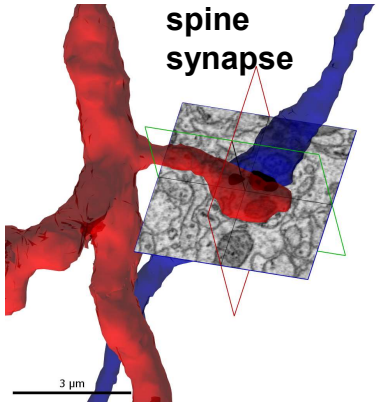

HVC synapse

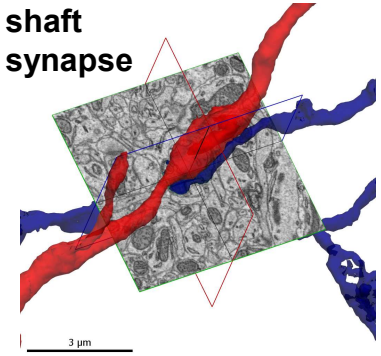

LMAN synapse

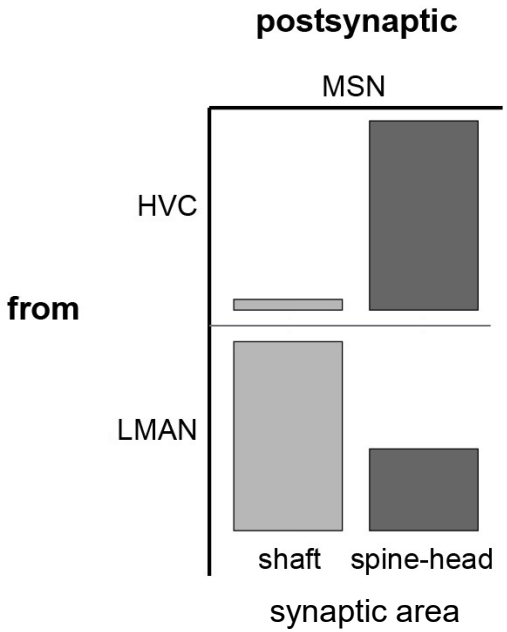

Preliminary analysis with manually identified cells
11-fold higher synaptic area of LMAN shaft synapses in comparison to HVC synapses

Fumi
Kubo

Fabian
Svara

Rotation
(clockwise)

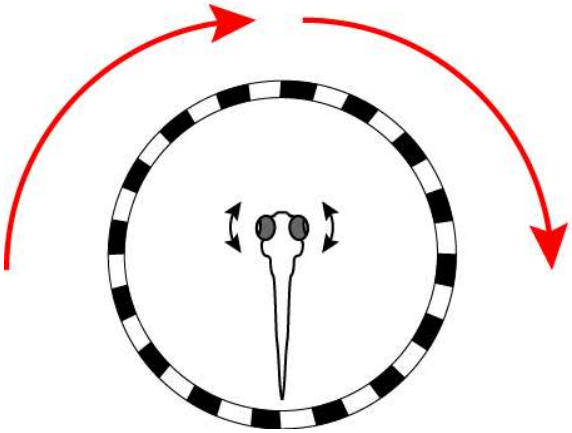

Optokinetic response (OKR)
(Eye movements)

Translation
(forward)

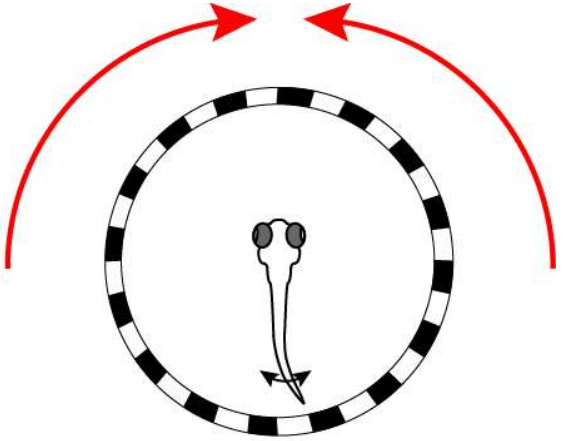

Optomotor response (OMR)
(Swimming)

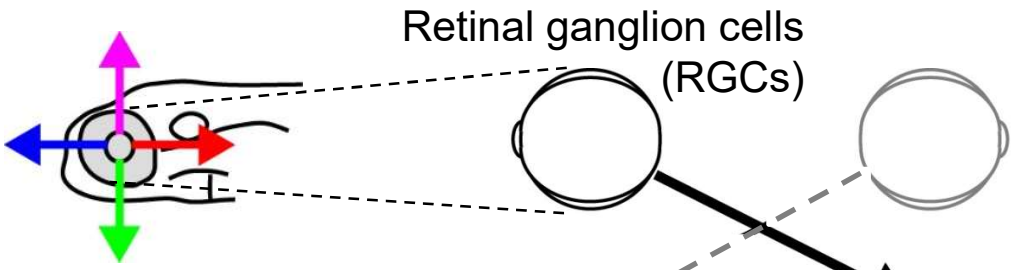

Retinal ganglion cells
(RGCs)

Pretectum

Premotor/motor pathways

* Pretectum

Premotor/motor pathways

Direction-selective cells

*Accessory optic system (AOS) / Nucleus of the optic tract (NOT) in mammals

All RGC axons cross the midline in fish; binocular integration therefore requires additional crossings.

Modified from Masseck and Hoffmann (2009)

From functional imaging to electron microscopy (EM) reconstruction

Pretectal Ca^{2+} imaging

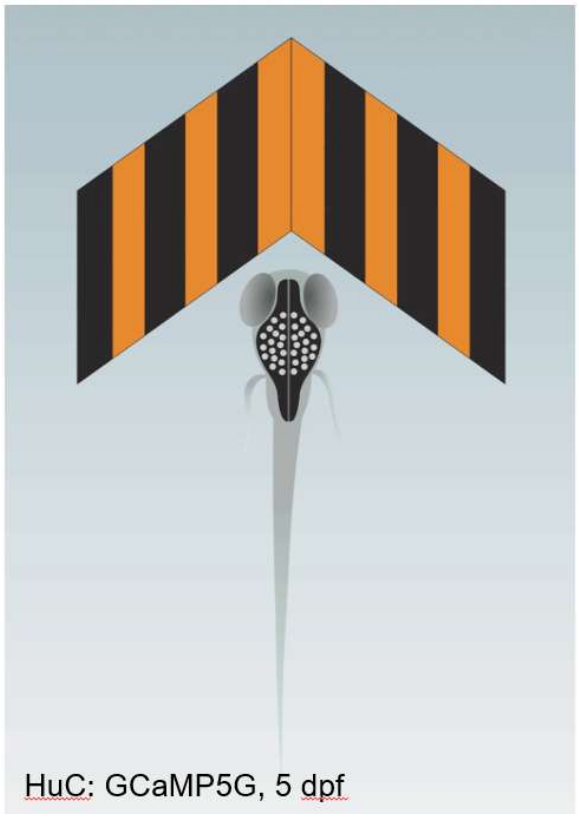

approx. 4-30 neurons per each type
(approx. 200 neurons in total)

Fixation
and staining

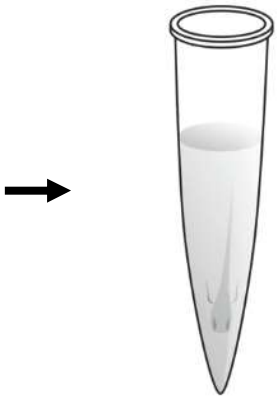

Serial block-face EM
of whole larval brain

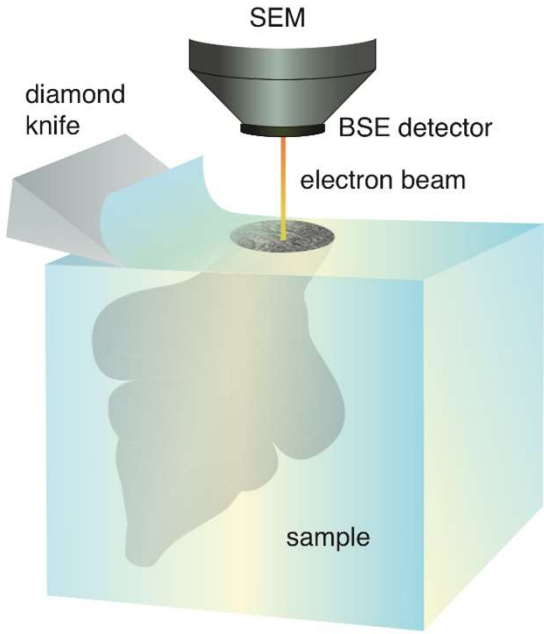

14 x 14 x 25 nm in x,y,z axis
Data size: ~12 TB

Larval Zebrafish Whole-Brain EM

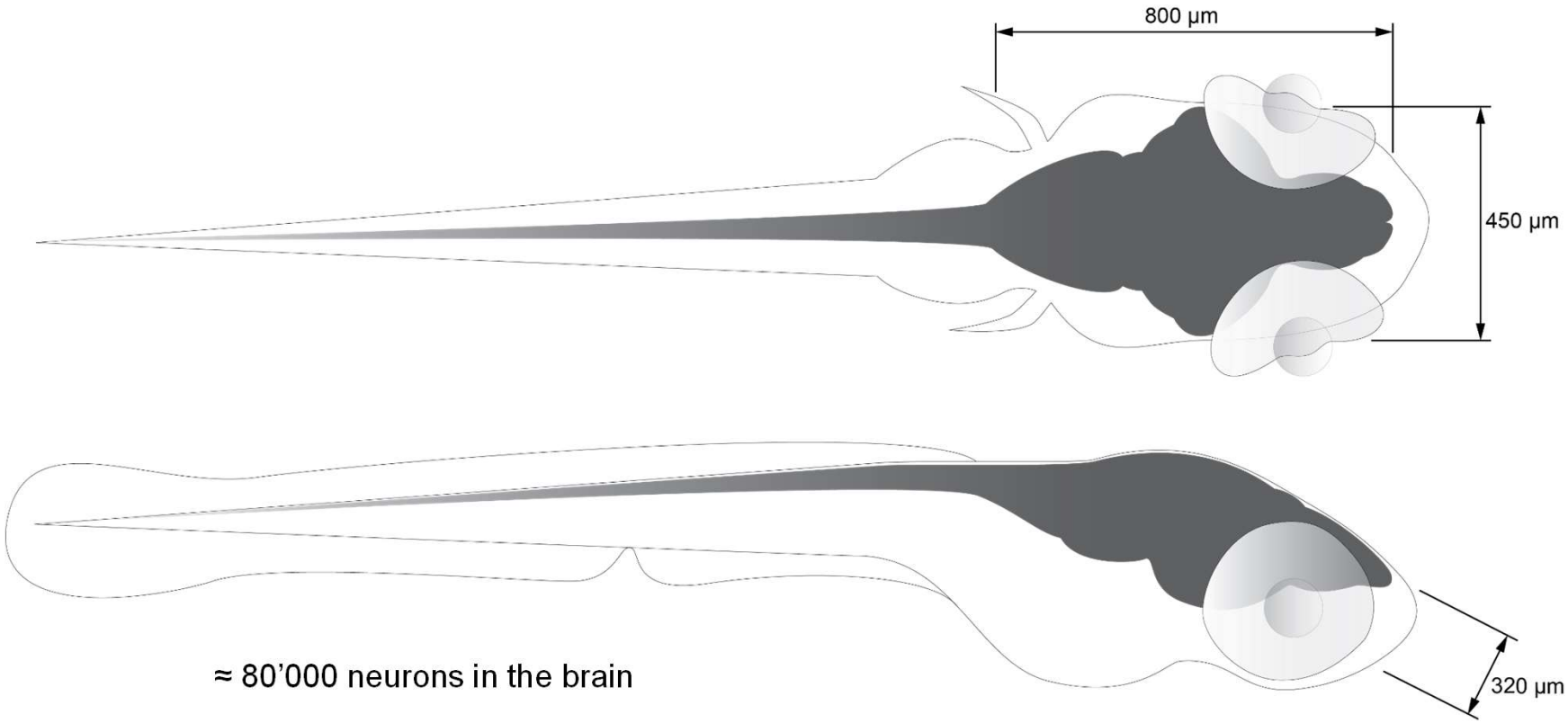

≈ 80’000 neurons in the brain

≈ **7 months, 28000 sections** at 25 nm
(at 14 x 14 nm resolution, with standard SBEM setup)

Fish drawing: Julia Kuhl

X-ray microCT

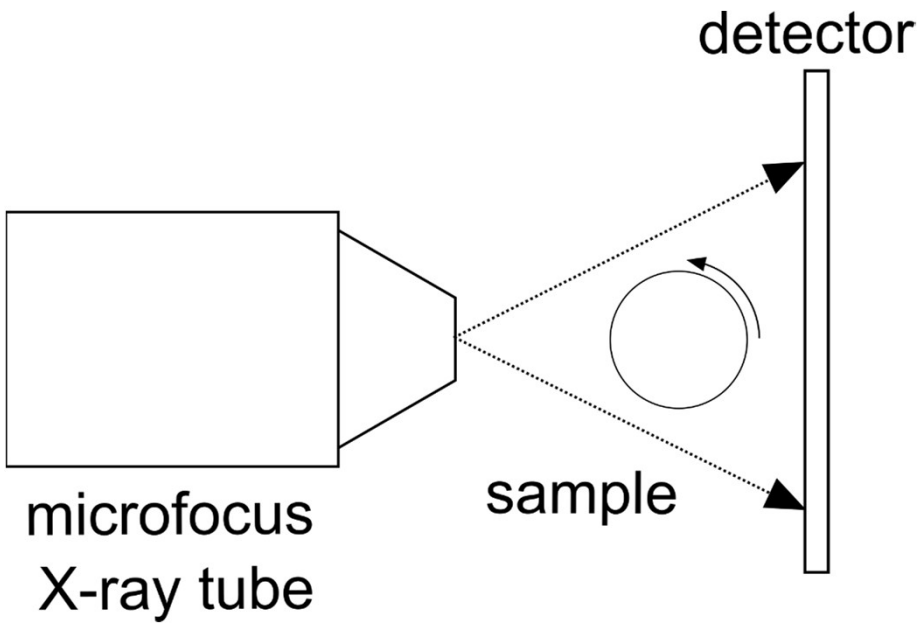

Allows exact measurement of sample geometry after embedding,
even in opaque epoxy

microCT illustration adapted from
documentation by SCANCO medical AG

microCT

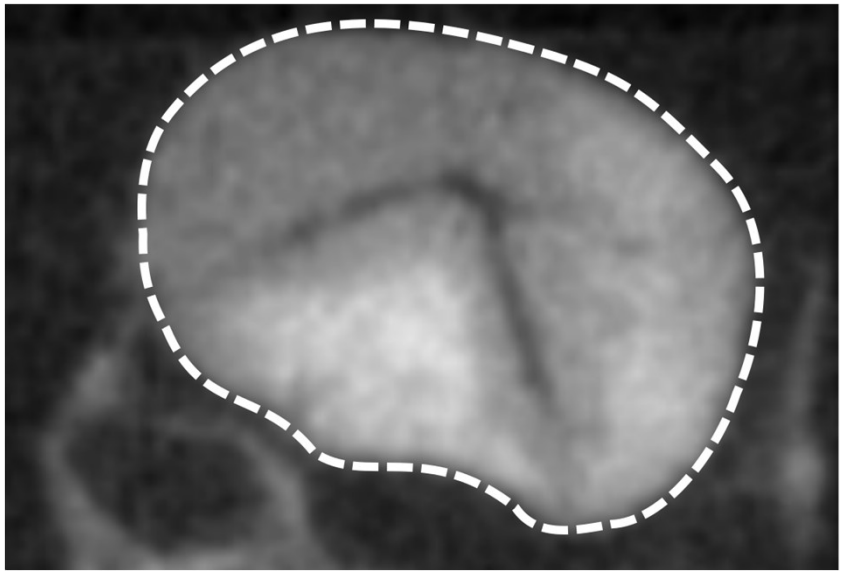

Linescanning + dynamic mosaic

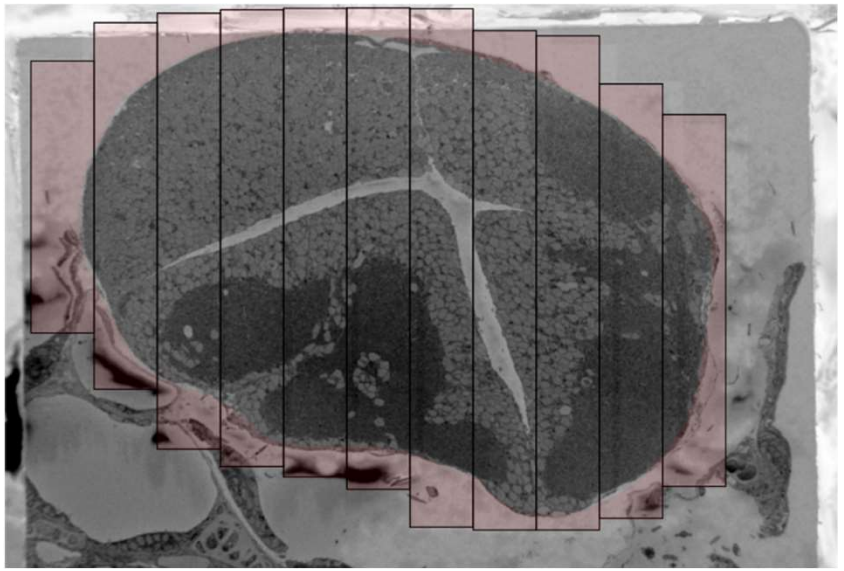

50 µm

Reconstruction of functionally characterized pretectal cells: Current status

Simple	Complex
MoNL	FEL
MoNR	FER
MoNL	BEL
MoTR	BER
	FELR
	BSP
	FSP

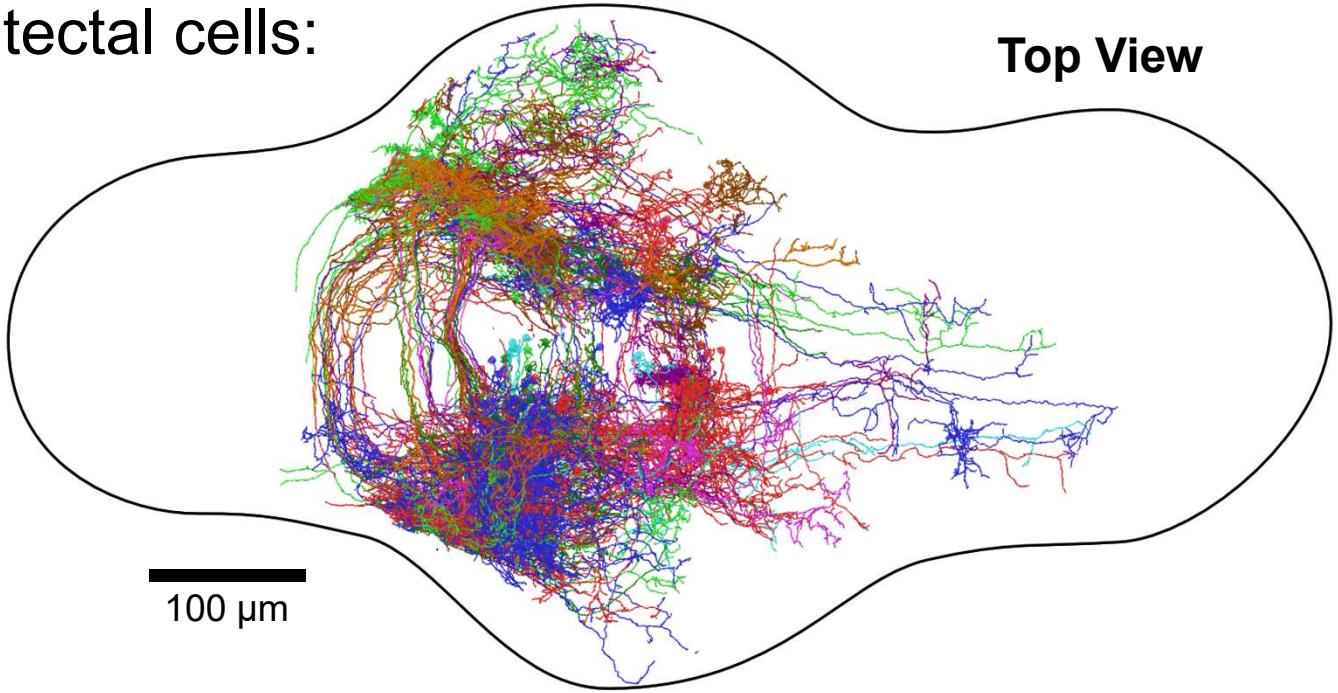

195 cells traced
(partially consolidated)

Consensus path
length: 49 cm

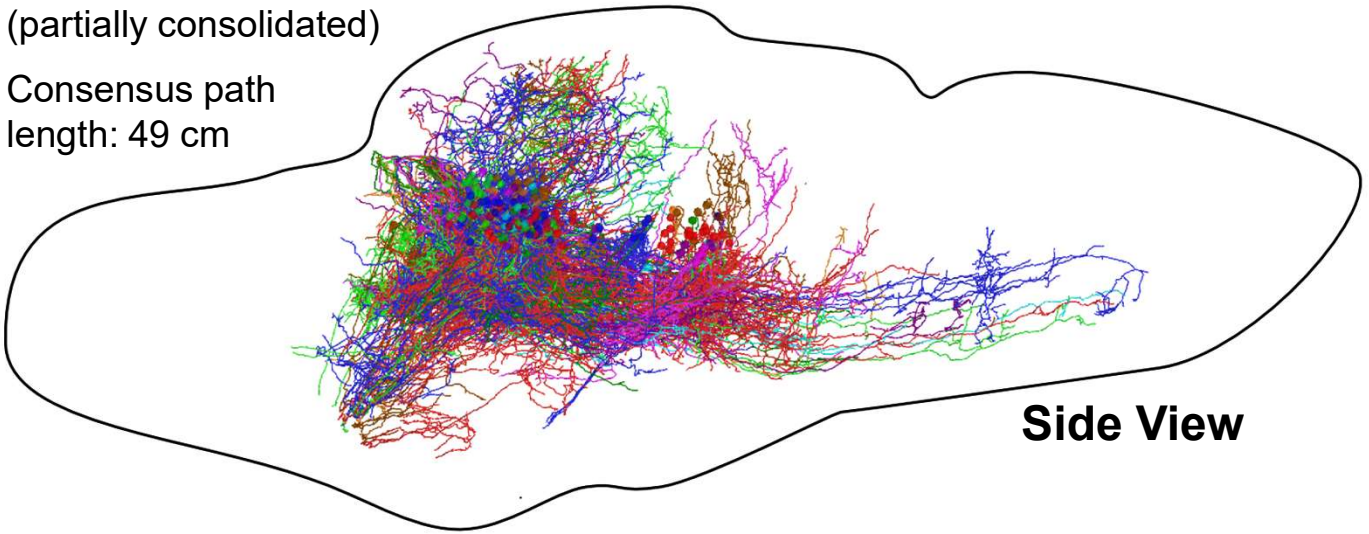

Tracing:
ariadne-service GmbH

C. elegans

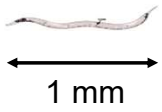

10^{-3} mm^3
10^2 neurons

Fly brain

10^{-1} mm^3
10^5 neurons

Mouse cortical column

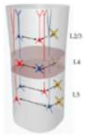

10^{-2} mm^3
10^4 neurons

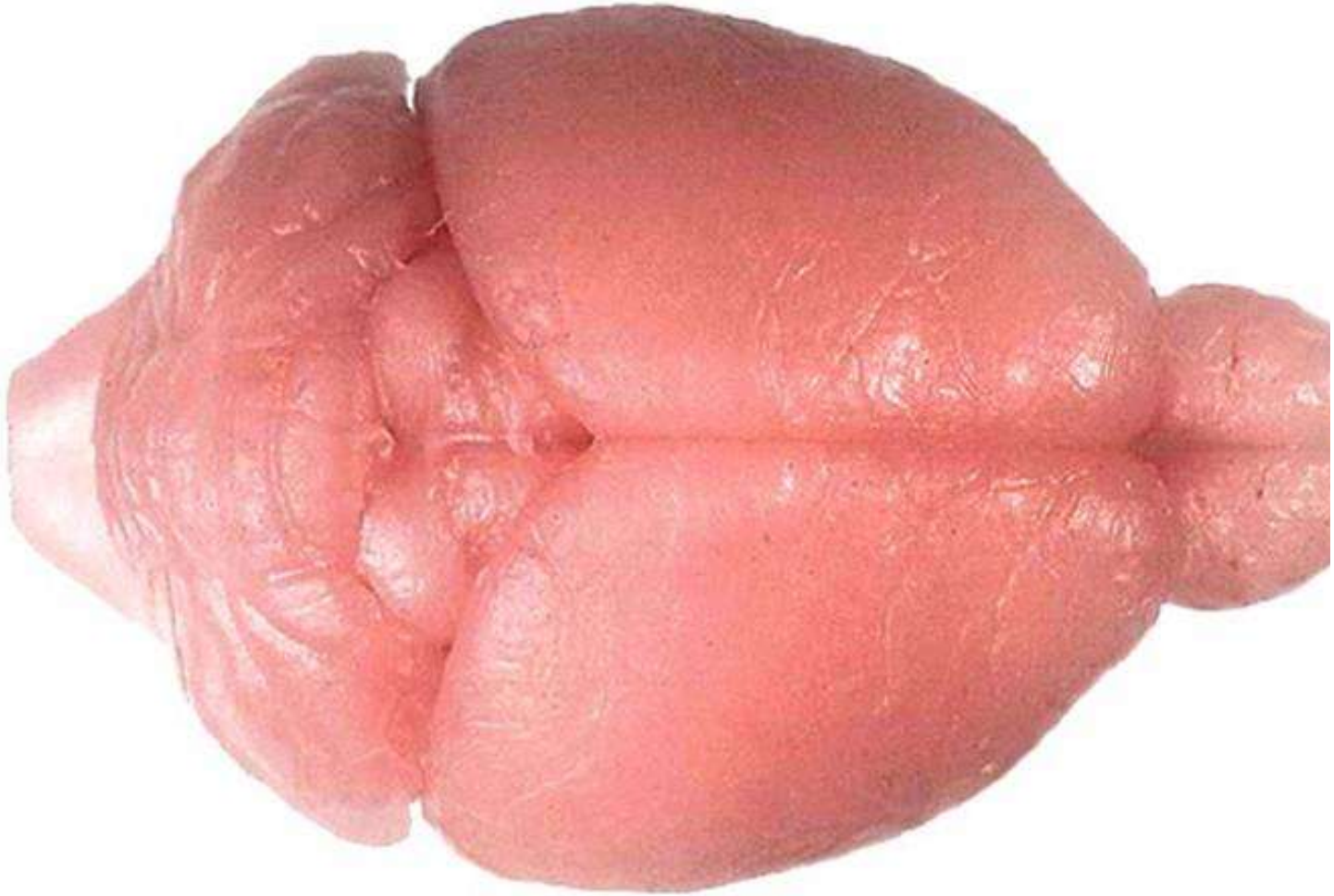

Mouse brain

10^3 mm^3
10^8 neurons

slide by Kevin Briggman

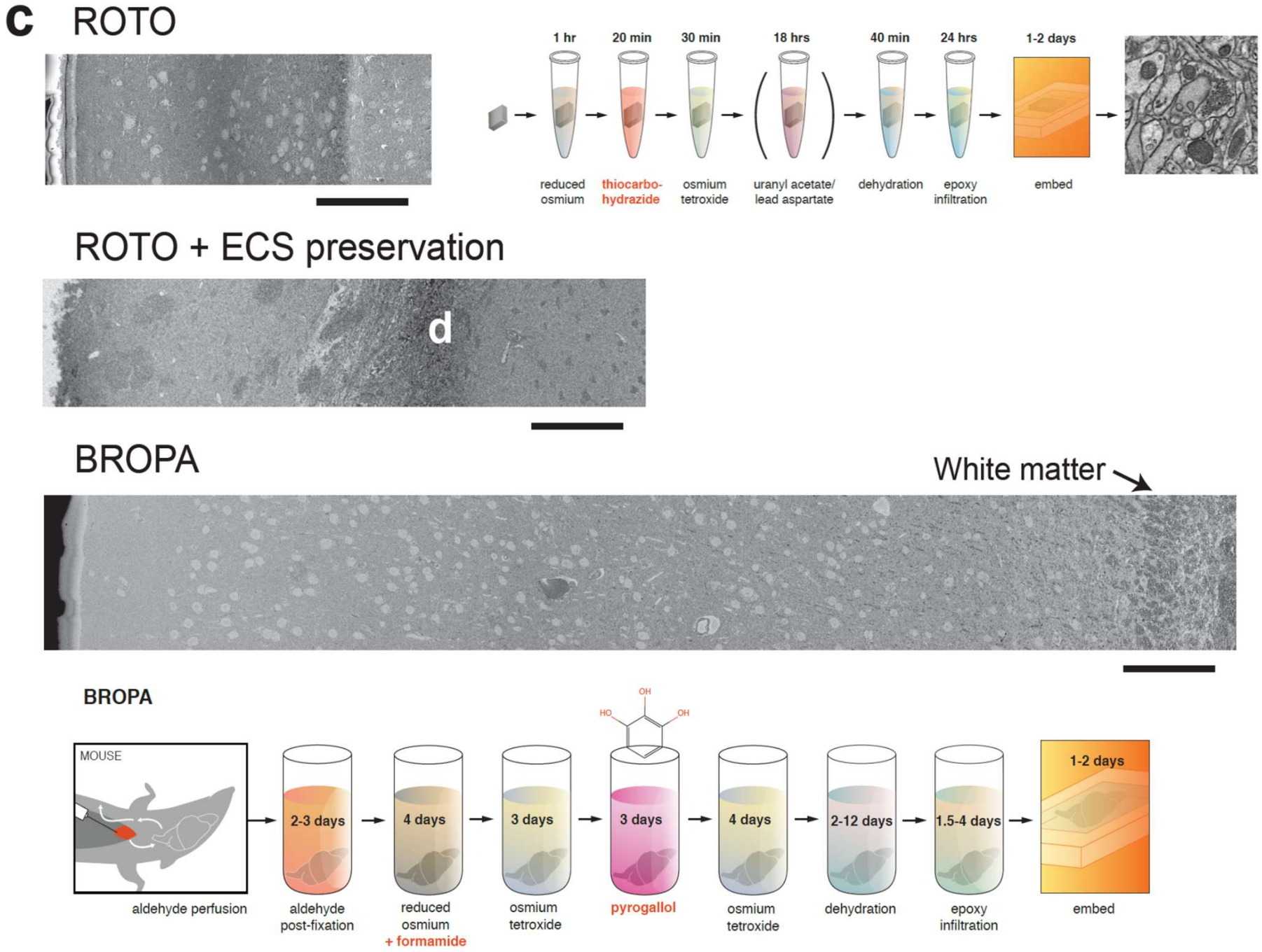

Mikula & Denk 2015

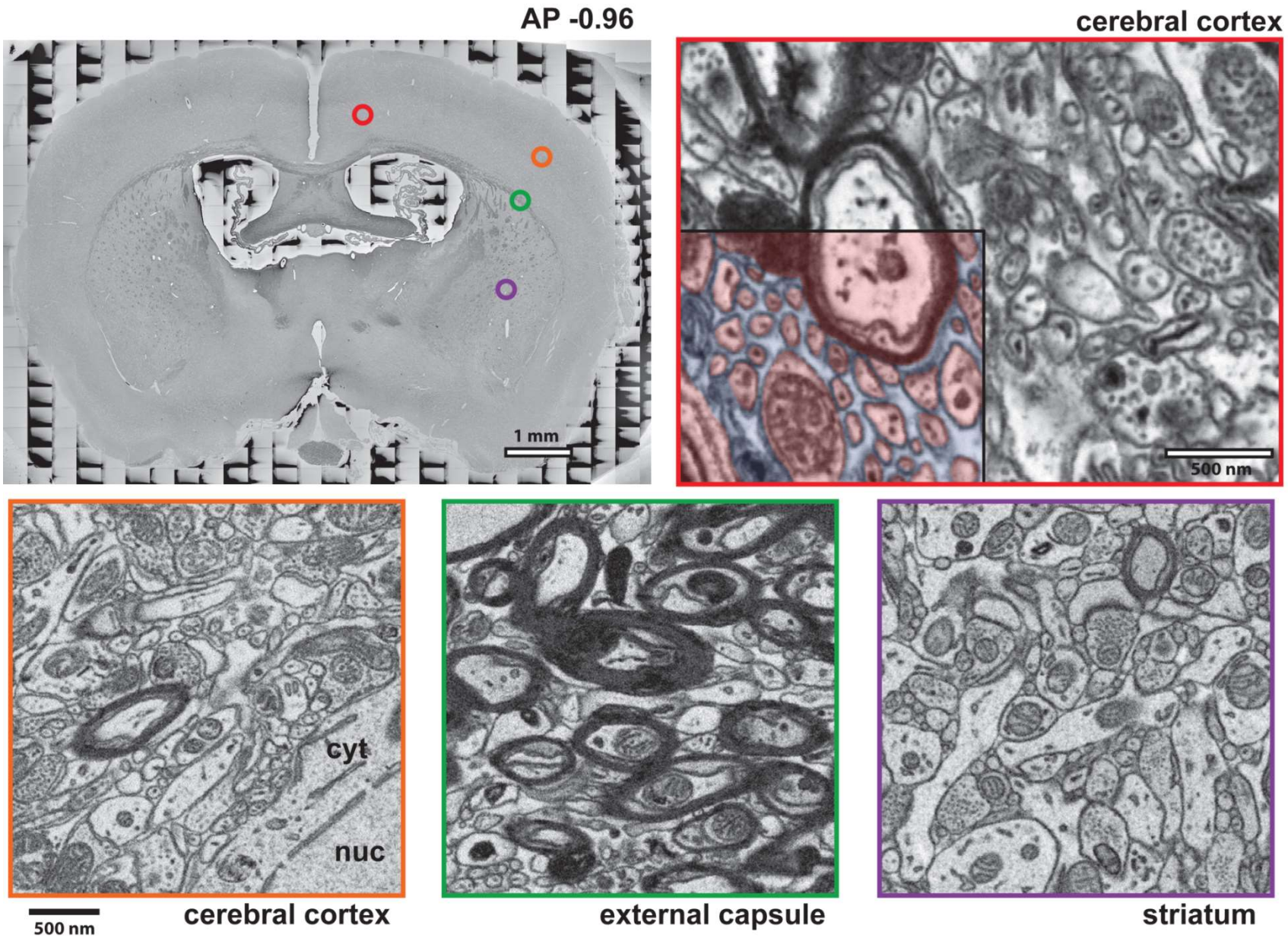

Mikula & Denk 2015

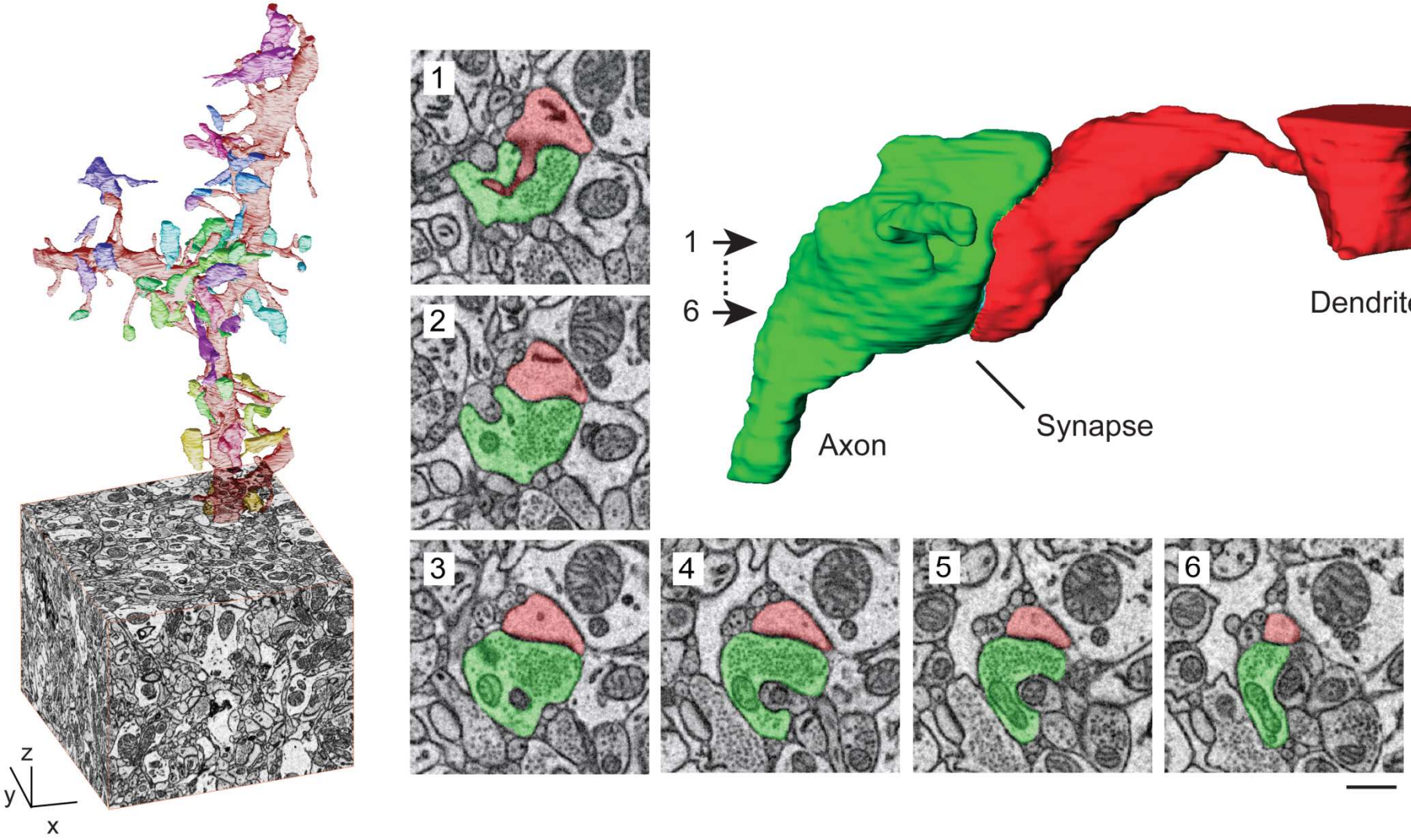

Mikula & Denk 2015

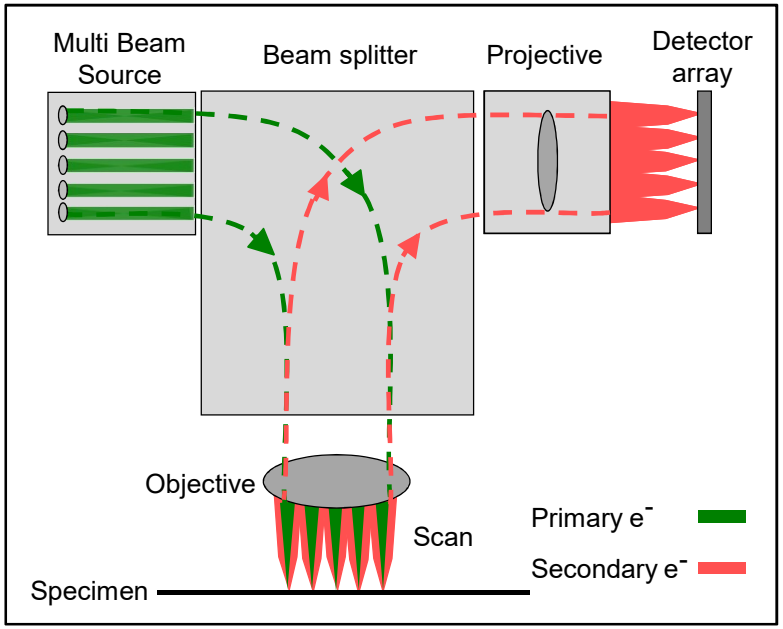

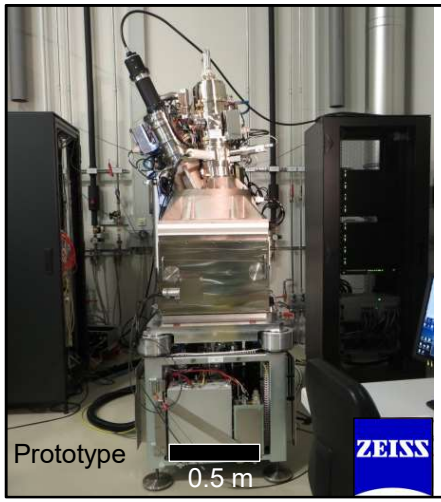

Specifications:

- 61 parallel beams
- Acq. rate: 1.22 Gpixel/s
- Resolution: 4-10 nm

Zeiss Team:

- Pascal Anger
- Thomas Kemen
- Mario Mützel
- Stefan Schubert
- Dirk Zeidler

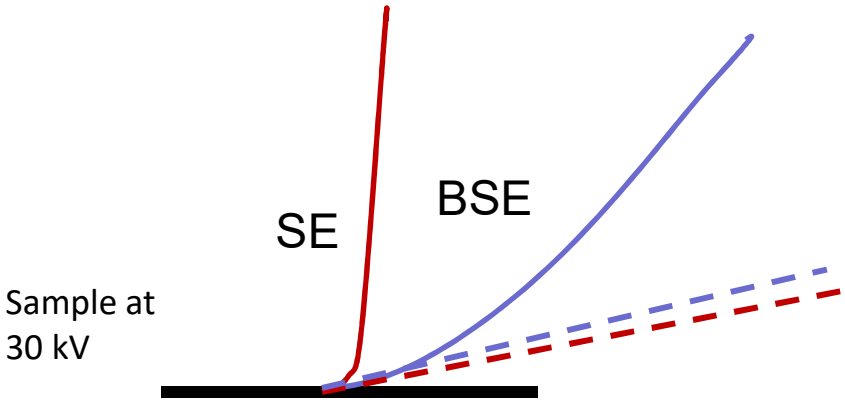

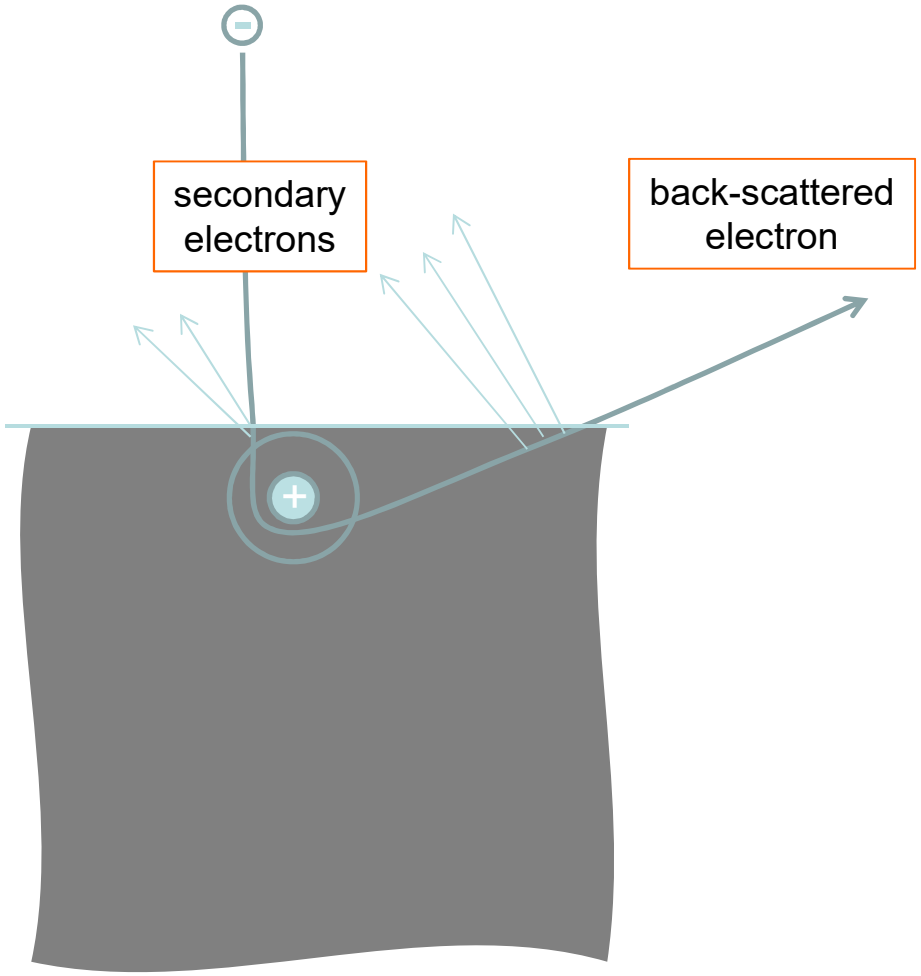
secondary electrons
back-scattered electron

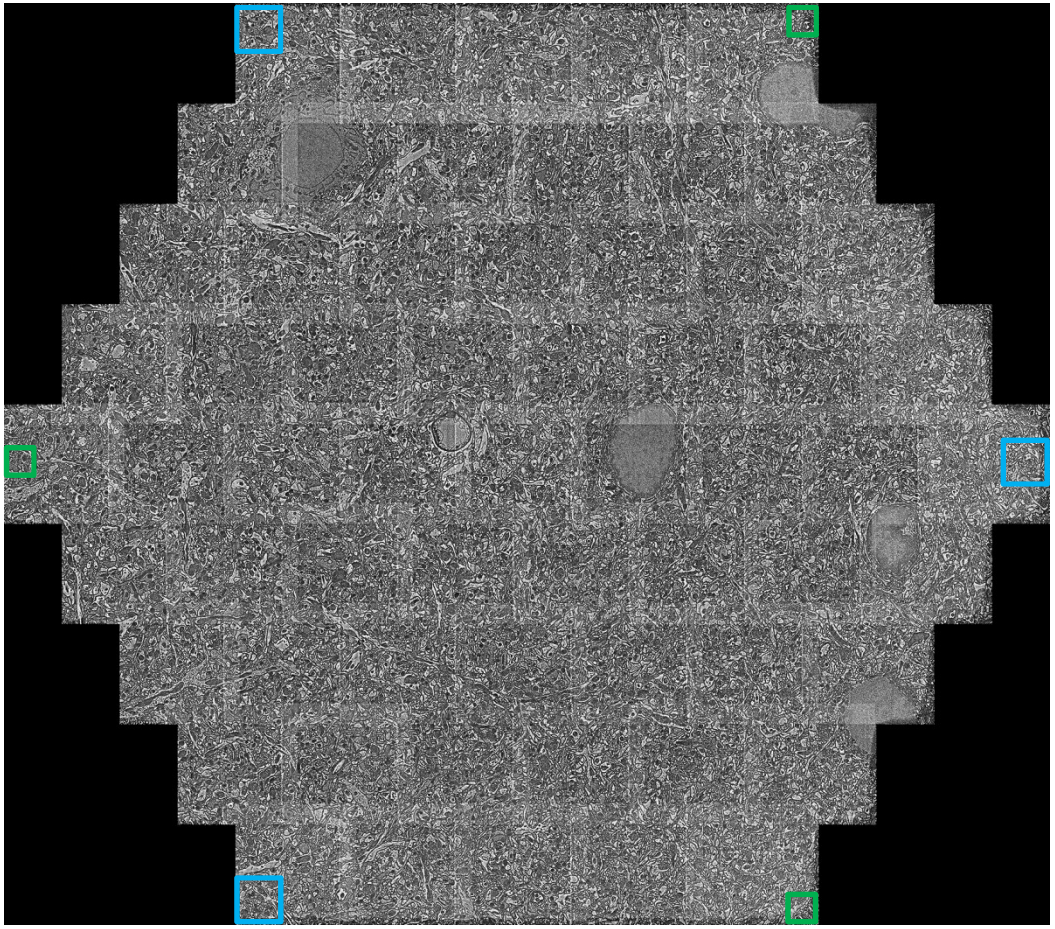

10 µm

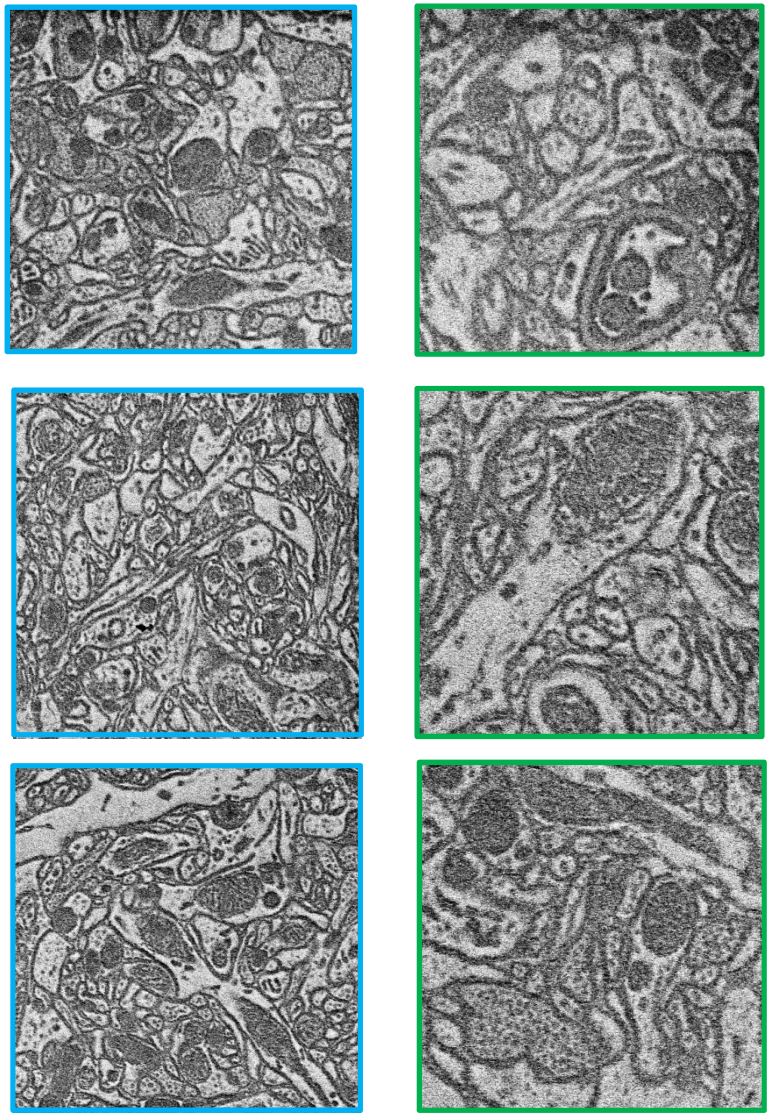

1 µm

500 nm

Landing energy:	**1.5 kV**
Beam deceleration:	**30 kV**
Pixel size:	**6 nm**
Dwell time:	**50 nS**
Acquisition rate:	**1.22 GHz**

Sample: Shawn Mikula
Coating: Benjamin Titze
Imaging: Tomasz Garbowski & Dirk Zeidler
(Carl Zeiss Microscopy GmbH)
mSEM prototype system in development

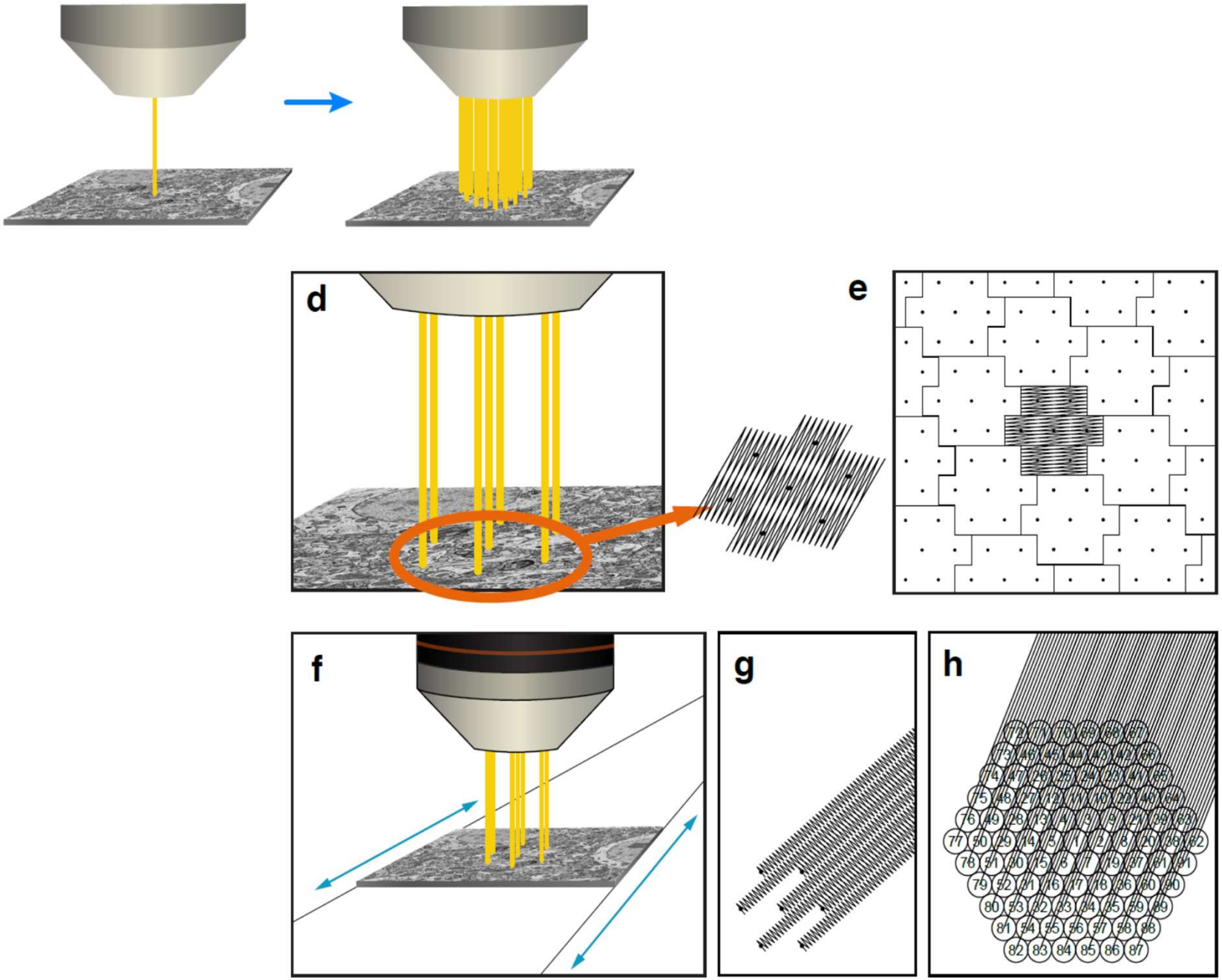
d
e
f
g
h

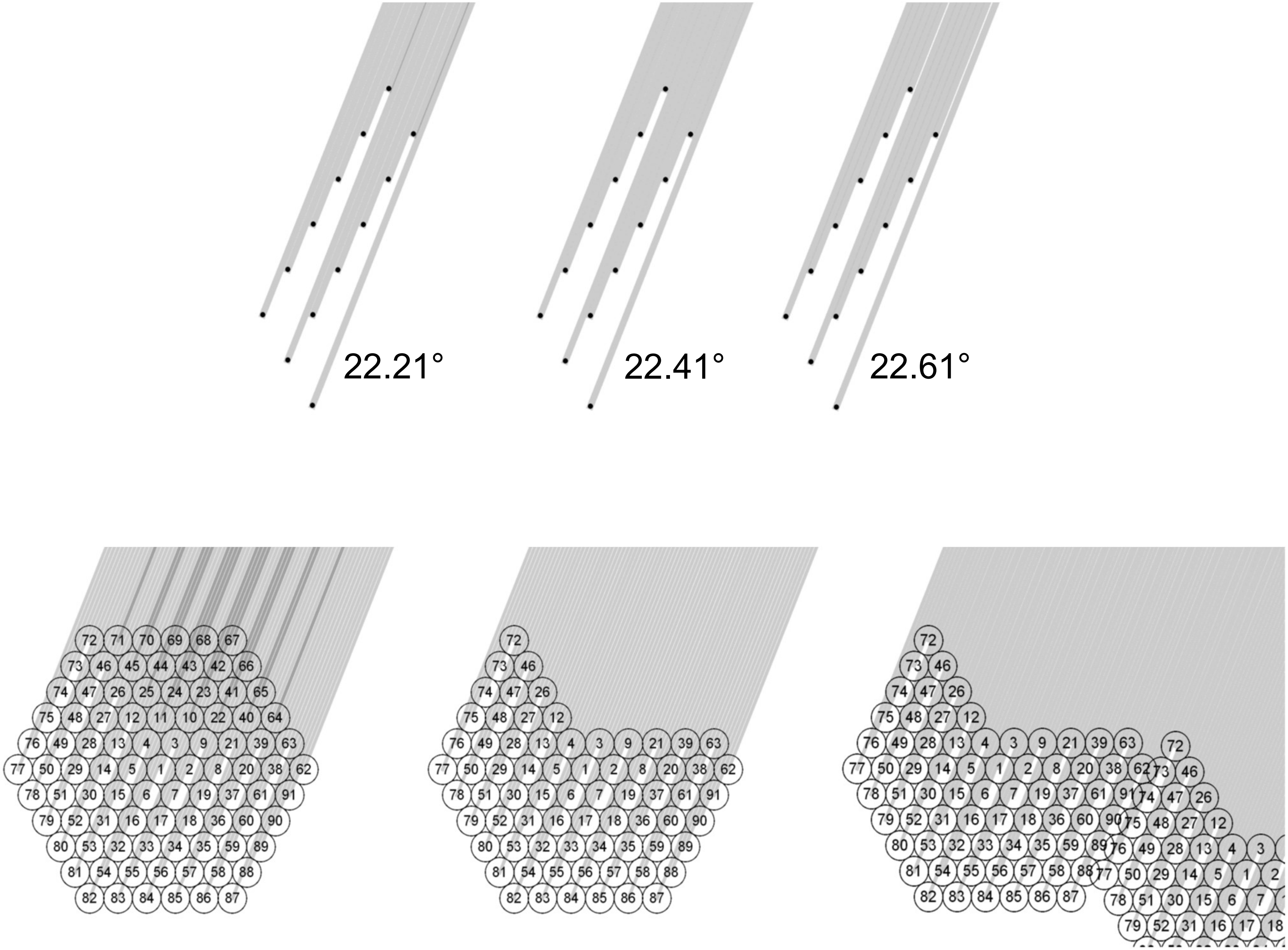
22.21°
22.41°
22.61°

1444
doi:10.1017/S1431927618007705

Microsc. Microanal. 24 (Suppl 1), 2018

Serial Thick Section Gas Cluster Ion Beam Scanning Electron Microscopy

Kenneth J. Hayworth[1], David Peale[1], Zhiyuan Lu[2], C. Shan Xu[1] and Harald F.Hess[1]

[1.] Janelia Research Campus, Howard Hughes Medical Institute, Ashburn, United States.
[2.] Department of Psychology and Neuroscience, Dalhousie University, Halifax, Canada.

Focused Ion Beam Scanning Electron Microscopy (FIB-SEM) is used to volume image heavy metal-stained, plastic-embedded biological samples with resolutions below 10 x 10 x 10nm, an ability that is especially important in connectomics [1]. FIB-SEM samples are typically restricted to be <50μm in the direction of the FIB beam because glancing angle milling results in artifacts over longer distances [1]. Removal rate is also restricted due to a current/spot size tradeoff. These limitations are especially problematic when one contemplates combining FIB with the increased speed offered by multibeam SEMs like the 91 beam Zeiss MultiSEM [2]. The MultiSEM's *minimum* field of view is ~180μm, and its imaging rate is approximately two orders of magnitude faster than FIB's milling rate. These considerations appear to preclude the integration of traditional FIB milling with MultiSEM imaging.

To overcome these limitations we chose to develop a broad ion beam milling approach using Gas Cluster Ion Beams (GCIB). GCIB delivers low-energy atoms to a surface and therefor does not require the use of a glancing angle. GCIB has been used for semiconductor polishing and for profiling in mass spectroscopy [3]. We attached a GCIB-10s gun from Ionoptika to a Zeiss Ultra SEM. Using a 10kV beam of Ar2000 (clusters of 2000 argon atoms), we verified that smooth, sub-10nm removal was possible from the surface of 100nm thick tissue sections. In order to obtain surfaces sufficiently smooth to produce quality secondary electron (SE) images (using 1.2kV landing energy and InLens detection

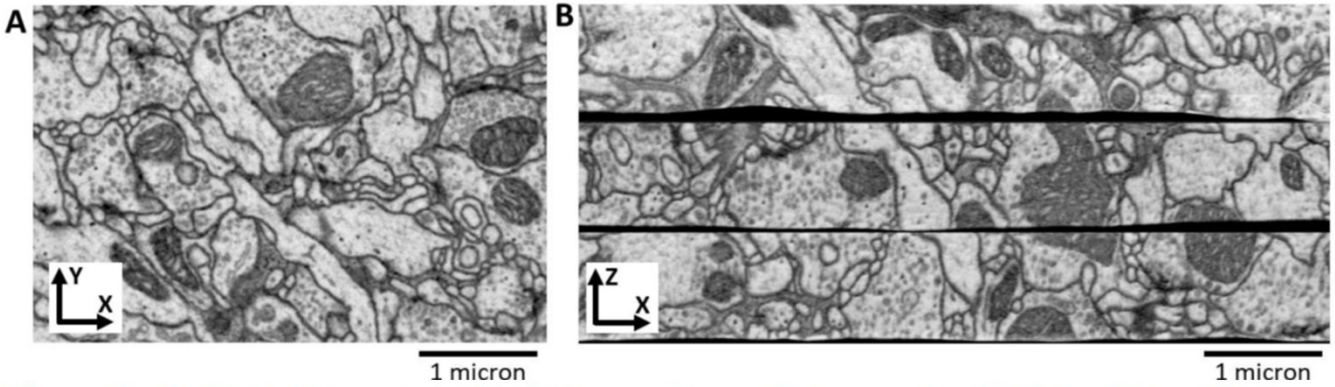

Figure 1. GCIB-SEM imaging. (**A**) SE image after multiple rounds of GCIB milling. (**B**) Cross section through dataset of three consecutive 1µm thick sections prior to computational flattening.

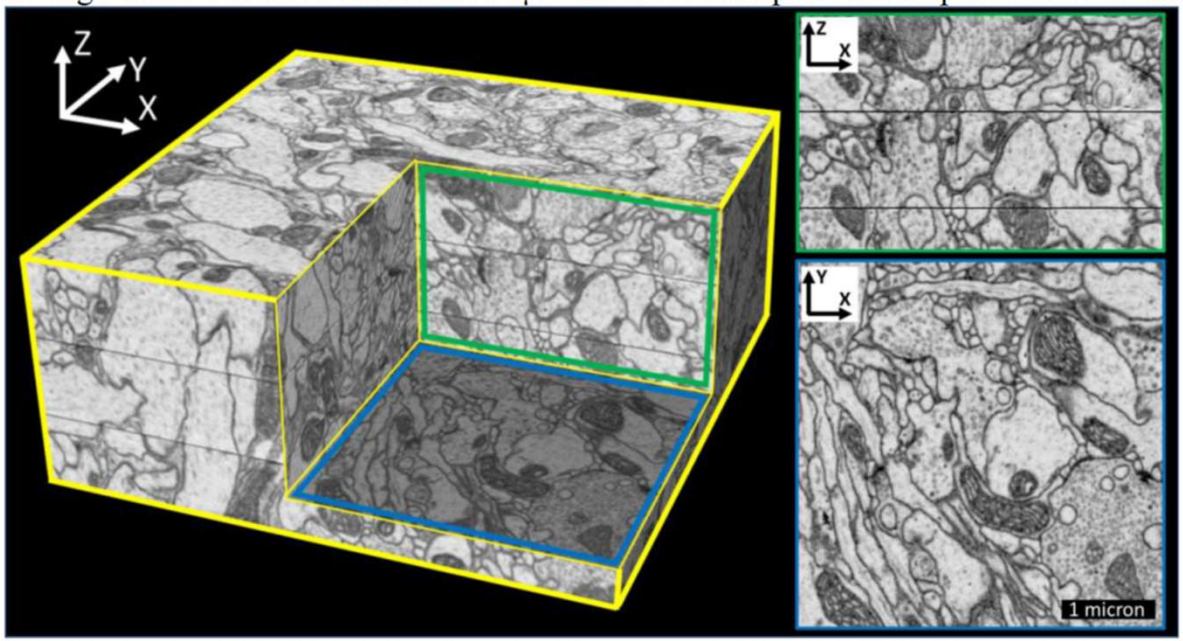

Figure 2. Final GCIB-SEM dataset after computationally flattening and volume-stitching the three consecutive 1µm thick sections together.

Hayworth e al. 2018

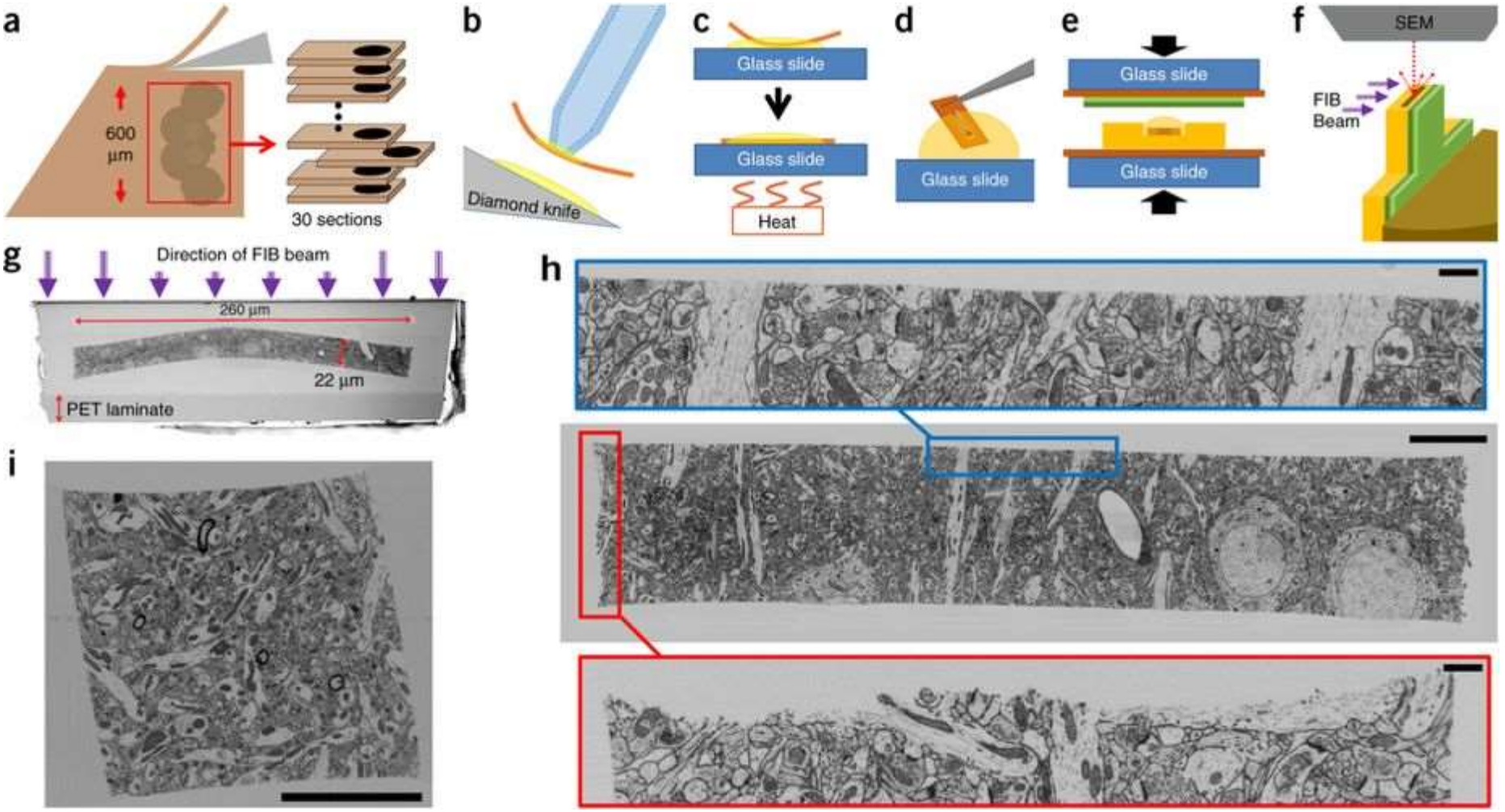

Hayworth, K. J., C. S. Xu, Z. Lu, G. W. Knott, R. D. Fetter, J. C. Tapia, J. W. Lichtman and H. F. Hess (2015). "Ultrastructurally smooth thick partitioning and volume stitching for large-scale connectomics." Nature Methods **12: 319.**

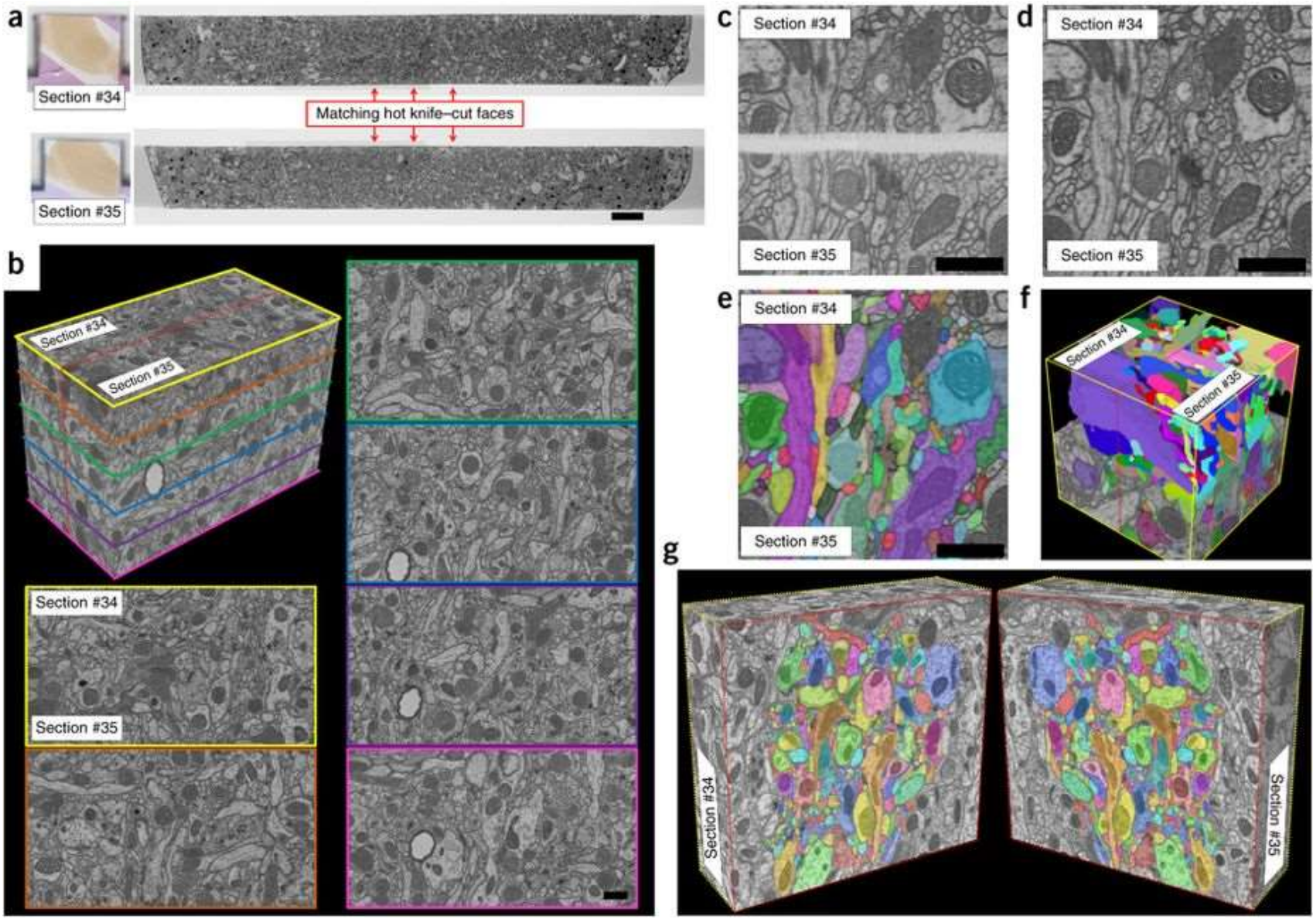

Hayworth, K. J., C. S. Xu, Z. Lu, G. W. Knott, R. D. Fetter, J. C. Tapia, J. W. Lichtman and H. F. Hess (2015). "Ultrastructurally smooth thick partitioning and volume stitching for large-scale connectomics." Nature Methods **12: 319.**

Maria Kormatcheva

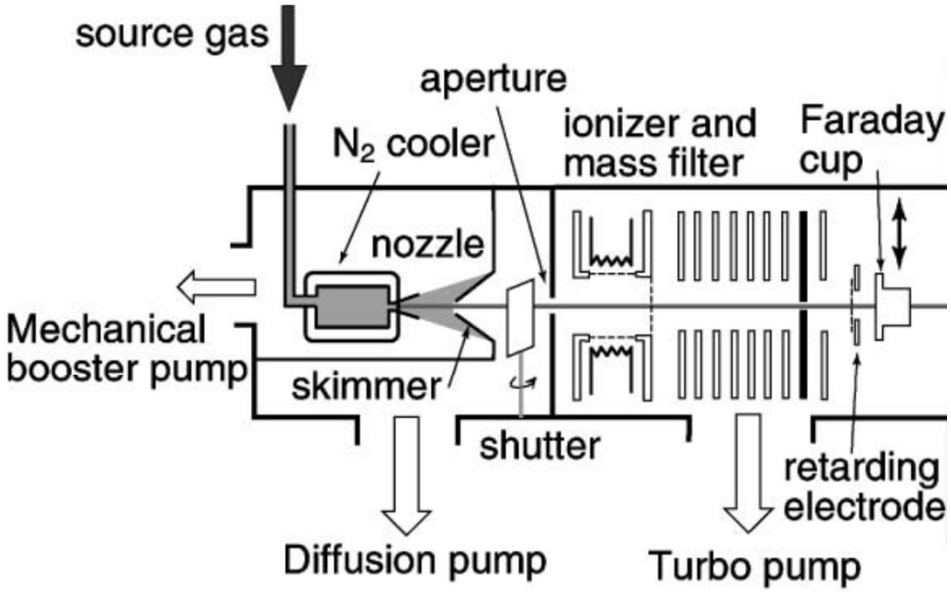

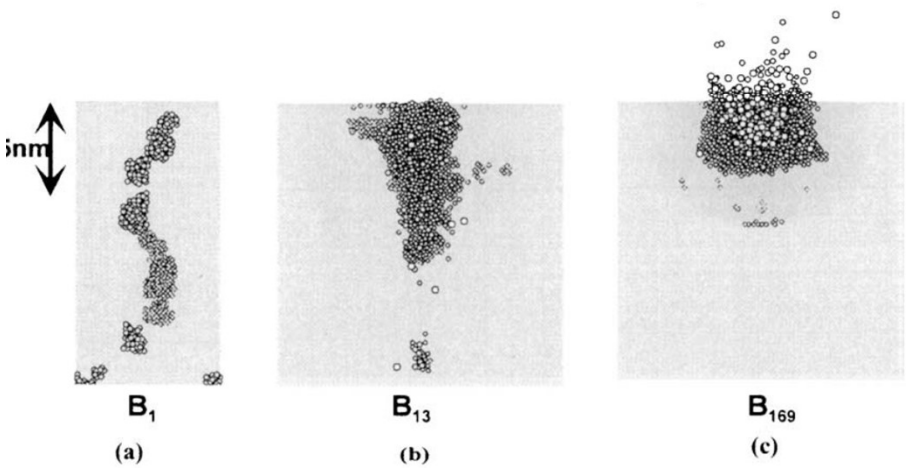

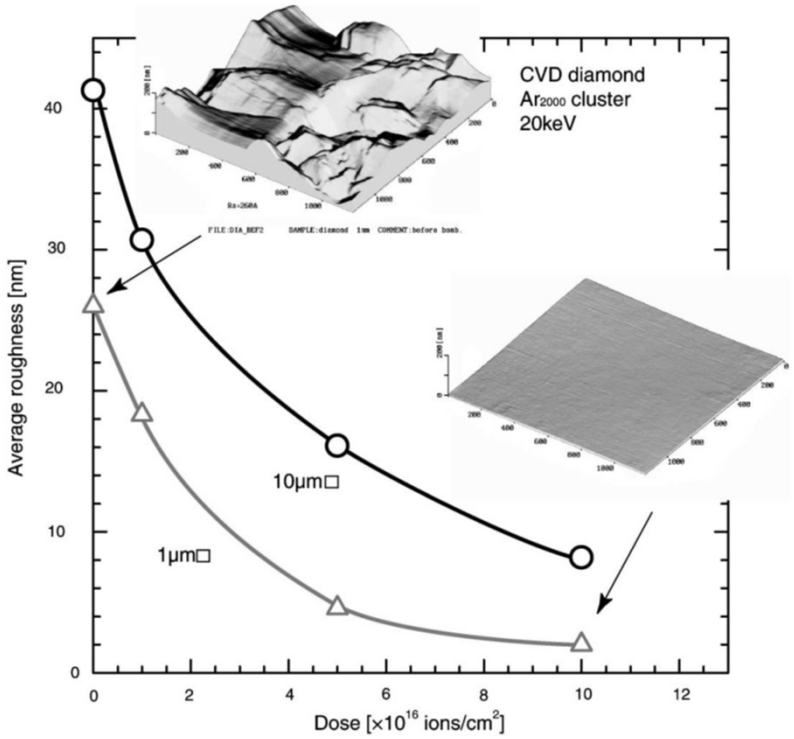

Illustration: Yamada et al., 2001

Illustration: Julia Kuhl

Stumbling Blocks, Pitfalls, Showstoppers, etc.:

Synapses (chemical), strength and other parameters

Synapses (electrical), existence etc.

Synapses (modulatory), etc.

Channel distributions

Variation between individuals

Isn't all that's interesting encoded in the genome?